PHOTOPLETHYSMOGRAPHY FOR NON-INVASIVE MEASUREMENT OF BONE HEMODYNAMIC RESPONSES TO CHANGES IN EXTERNAL PRESSURE

by

JAIME MATEUS

M.Eng. Aeronautical Engineering
Imperial College London, 2005

S.M. Aeronautics and Astronautics
Massachusetts Institute of Technology, 2008

Submitted to the Department of Aeronautics and Astronautics
in Partial Fulfillment of the Requirements for the Degree of

DOCTOR OF PHILOSOPHY IN AEROSPACE BIOMEDICAL ENGINEERING

at the

MASSACHUSETTS INSTITUTE OF TECHNOLOGY

June 2011

Author ……

Department of Aeronautics and Astronautics
May 12, 2011

Accepted by……

Eytan H. Modiano, Associate Professor of Aeronautics and Astronautics
Department of Aeronautics and Astronautics
Chair, Graduate Program Committee

PHOTOPLETHYSMOGRAPHY FOR NON-INVASIVE MEASUREMENT OF BONE HEMODYNAMIC RESPONSES TO CHANGES IN EXTERNAL PRESSURE

by

JAIME MATEUS

DOCTOR OF PHILOSOPHY IN AEROSPACE BIOMEDICAL ENGINEERING

at the

MASSACHUSETTS INSTITUTE OF TECHNOLOGY

Certified by……

Alan R. Hargens, Professor of Orthopaedic Surgery
Department of Orthopaedic Surgery
University of California – San Diego
Thesis co-advisor

Certified by……

Dava J. Newman, Professor of Aeronautics and Astronautics and Engineering Systems
Department of Aeronautics and Astronautics
Massachusetts Institute of Technology
Thesis co-advisor

Certified by……

Mary L. Cummings, Associate Professor of Aeronautics and Astronautics
Department of Aeronautics and Astronautics
Massachusetts Institute of Technology
Thesis Committee Chair

Certified by……

Roger D. Kamm, Germeshausen Professor of Mechanical and Biological Engineering
Department of Mechanical Engineering and Department of Biological Engineering
Massachusetts Institute of Technology
Thesis Committee Member

PHOTOPLETHYSMOGRAPHY FOR NON-INVASIVE MEASUREMENT OF BONE HEMODYNAMIC RESPONSES TO CHANGES IN EXTERNAL PRESSURE

by

JAIME MATEUS

Submitted to the Department of Aeronautics and Astronautics on
May 12, 2011 in Partial Fulfillment of the Requirements for the Degree of
Doctor of Philosophy in Aerospace Biomedical Engineering

Abstract

Adequate blood supply and circulation in bones is required to maintain a healthy skeleton, and inadequate blood perfusion is associated with numerous bone pathologies and a decrease in bone mineral density (BMD). Bone hemodynamics remains poorly understood and loss of BMD is still one of the limiting factors to long duration human spaceflight. Developments in photoplethysmography (PPG) hardware have made it a promising tool for non-invasive bone hemodynamic measurements. The aims of this thesis are to: 1) validate the use of PPG as a tool for non-invasive bone hemodynamic measurements, 2) characterize bone hemodynamic responses to changes in external pressure, and 3) identify the predominant mechanisms regulating bone hemodynamic responses to pressure changes.

A new PPG device capable of measuring bone hemodynamic responses was designed and tested. It represents the state-of-the-art in deep-tissue PPG instrumentation. Validation experiments including arterial occlusion, cold exposure, skin occlusion and nitroglycerin exposure were performed. Single-limb pressure chamber experiments were performed over a range of pressures from -50 to +50 mmHg to characterize the responses to changes in external pressure and to identify the predominant control mechanisms.

Our results support the use of PPG as a valid tool for measuring bone hemodynamic responses. Bone hemodynamic responses to changes in external pressure have been characterized for the first time. We also present the first report of a myogenic response in bone and show that the myogenic effect is the predominant control mechanism in bone over a wide range of pressure levels. Myogenic-induced vasoconstriction is observed at all negative pressure levels, with increasing vasoconstriction at the more extreme pressure differences. At positive pressures we observed an initial myogenic-induced vasodilation followed by activation of the intramuscular pressure receptors at +30 mmHg which overrides the initial response and causes vasoconstriction at the highest positive pressure. The availability of a new tool for non-invasive bone hemodynamic measurements opens the door to several new research opportunities with clinical, Earth-based as well as human spaceflight applications.

Thesis co-supervisors:

Alan R. Hargens
Professor of Orthopaedic Surgery

Dava J. Newman
Professor of Aeronautics and Astronautics and Engineering Systems

Acknowledgements

To all my advisers, mentors, colleagues, friends and family – thank you.

Thank you to all my committee members for their time and input into this dissertation: Alan Hargens for the enriching opportunity to work in your lab at UCSD and for all your support, Dava Newman for your support and enthusiasm throughout my years at the MVL, Missy Cummings for your mentorship in a variety of different roles from 16.400 to research, Roger Kamm for your expert and insightful advice. Thank you to my two readers for all of their valuable input: Scott Sheehan for the many unique conversations and medical perspective, and Thomas Heldt for always being willing to help me and for all the excellent feedback.

Thank you as well to James Waldie and Marlene Grenon who were extremely helpful in the initial stages of developing my PhD topic. A special thank you to George Kassabian, a truly superb electrical engineer, and Allen White from the Physics Electronics Workshop at UCSD for their expertise and flexibility in working with me in the development of the PPG. Thanks to Armando Rosales for enriching my Mexican and California experience and Chelsea Ellingson for all the help with my pilot studies.

I could not have hoped for a better place to work than the MVL. Thank you to all the current and former students who make it such a special place to be. Jessica Edmonds and Scott Sheehan, my two original officemates were the best introduction to MIT anyone could ask for. Thanks to the many more MVL friends including, but not limited to, Erika Wagner, Kevin Duda, Nic Granzella, Justin Kaderka, Torin Clark, Alex Stimpson, Roedolph Opperman, Ashley Wessendorf and Allie Anderson among many others. Thank you to the remaining MVL faculty and staff, Larry Young, Chuck Oman, Jeff Hoffman, Alan Natapoff, Andy Liu and Liz Zotos for all they bring to the MVL.

Thank you to the many other MIT faculty members who have contributed to my education at MIT in some form or another, in particular Ian Waitz, Dave Darmafol, and Karen Willcox.

To all my other non-MVL friends across Cambridge and the world, thank you for all the fun times and for making life outside the lab full of great experiences and memories. Thank you to the Muddy for keeping me sane and for all the Guinness. Finally, a special thank you to all my subjects, without whom, I would not have any data. And thank you to Chelsea and the Pi Beta Phi sorority for their endless supply of female subjects.

This work would not have been possible without the generous fellowship support from the Foundation for Science and Technology (FCT), Portugal. Thank you as well to the MIT Public Service Center, the UCSD Department of Orthopaedic Surgery and the UCSD Physics Electronics Workshop for their support.

Table of Contents

List of Acronyms

ANOVA	Analysis of variance
AG	Artificial gravity
BMD	Bone mineral density
BP	Blood pressure
BPM	Beats per minute
CO	Cardiac output
COUHES	Committee on the Use of Humans as Experimental Subjects
CVP	Central venous pressure
EPC	External pneumatic compression
GUI	Graphical user interface
HR	Heart rate
IPC	Intermittent pneumatic compression
IR	Infrared
IRB	Institutional review board
PAD	Peripheral arterial disease
PPG	Photoplethysmography
LBNP	Lower-body negative pressure
LBPP	Lower-body positive pressure
LED	Light-emitting diode
LDF	Laser Doppler flowmetry
MANOVA	Multivariate analysis of variance
MAP	Mean arterial pressure
MSNA	Muscle sympathetic nerve activity
NIRS	Near infrared spectroscopy
NPWT	Negative pressure wound therapy
SNS	Sympathetic nervous system

List of Figures

List of Tables

1.0 Introduction

As in any other tissue or organ in the human body, an adequate supply and circulation of blood is required to maintain a healthy skeleton. While we traditionally think of the circulatory system as being independent from the skeletal system, the two are intricately connected and a full understanding of one system cannot be had without consideration for the other.

1.1 Motivation

Much progress has been made in understanding the anatomy, function, and mechanisms regulating the circulatory physiology of the cardiovascular system as well as the microcirculation of skin, muscle and many other organs [88]. In contrast, however, much less progress has been made in understanding the physiology of bone blood flow [33, 120]. There is still some debate on the anatomical structure and function of the blood vessels in bones, and there is even more uncertainty about the mechanisms that regulate bone blood flow [70, 139].

The inherent technical difficulty associated with measuring bone blood flow is one of the reasons why our understanding of bone circulation has lagged behind our understanding of circulation in other tissues. Until recently, all available measurement techniques have required an invasive approach, and often require the use of radioactive particles [31, 139]. Recent advances in photoplethysmography (PPG) hardware have made it a suitable non-invasive measurement tool for hemodynamics of deeper tissues such as muscle and bone [150, 174]. While PPG has been widely used for measurements of circulation in the skin as well as in various muscles, measurement of bone hemodynamics with PPG is a novel application that has not yet been fully validated [3, 42, 219]. PPG is currently the only tool that allows for continuous, non-invasive measurement of hemodynamic responses in subcutaneous tissue such as muscle and bone. Validation of PPG as a tool for non-invasive bone hemodynamic measurements is necessary in order for it to become a more widely adopted and accepted method.

Bone circulation plays a crucial role in fracture repair, bone remodeling, and bone pathology [101, 120, 211]. For instance, chronic insufficient blood supply to the bone is a known precursor to osteoporosis, and an increase in bone blood flow is observed during fracture repair [139, 205, 211]. Reduced blood flow due to peripheral arterial disease (PAD) is also associated with an increased fracture risk due to lower bone mineral density (BMD) [52, 179]. Several studies have found a strong association between atherosclerosis and other cardiovascular diseases with osteoporosis [207], including several studies on postmenopausal women [102, 109, 136, 179].

The capability to non-invasively measure bone hemodynamic responses *in vivo* opens up several new research avenues that may enhance our understanding of how bone circulation is related to bone pathologies. By measuring the bone hemodynamic responses in a limb in response to changes in external pressure we can begin to understand the relative importance of different mechanisms in regulating bone circulation. An understanding of the key mechanisms may be important in developing new drugs and therapies to treat various bone disorders. Additionally, PPG may also be useful in testing the effectiveness of new drugs or drug delivery, by being able to specifically detect changes in bone hemodynamics in response to a new pharmaceutical agent.

One of the main limiting factors of long duration human spaceflight is the large BMD loss that is accrued by crewmembers. Despite the rigorous exercise countermeasures designed to mitigate bone loss, crewmembers still experience between 0.5% to 2.0% BMD loss per month in the weight bearing parts of the skeleton such as the lumbar spine, the hip and the lower extremities [37]. This rate of BMD loss is about an order of magnitude larger than what is observed in postmenopausal women [21]. Interestingly, small increases in BMD have been noted in other parts of the skeleton such as the skull and upper arms [37, 122, 159]. One hypothesis postulates that the cephalad fluid shift that occurs in weightlessness is, at least in part, responsible for the observed association between BMD loss and the weight-bearing parts of the skeleton [51, 140, 141, 215]. The exact mechanism of how the fluid shift affects bone health is not clear. Some data suggest that it may be related to the change in interstitial fluid flow due to changes in fluid pressure gradients in the bone [12, 101, 196], while other studies argue that the

pressure-induced fluid convection is not the main mechanism [126]. Several recent studies have provided additional data supporting the idea that bone circulation and BMD are tightly interconnected [20, 52]. A better understanding of the relationship between bone circulation and bone health is of obvious importance to human spaceflight. PPG may also become a useful tool in spaceflight experiments, by allowing astronauts to measure changes to bone hemodynamic parameters due to weightlessness.

1.2 Specific Aims and Hypotheses

The specific aims of this thesis are:

1. To validate the use of PPG as a non-invasive tool for *in vivo* bone hemodynamic measurements of the human tibia

   Hypothesis #1: *PPG is a valid method for obtaining measurements of bone hemodynamic responses in vivo.*

2. To characterize bone hemodynamic responses to single-limb exposure to hypobaric and hyperbaric external pressures

   Hypothesis #2: *Exposure to hypobaric pressures will result in vasoconstriction and exposure to hyperbaric pressures will result in vasodilation in the exposed limb.*

3. To investigate the relative contribution of systemic sympathetic and local myogenic mechanisms in the regulation of bone circulation

   Hypothesis #3: *At low to moderate pressure differences (up to 30mmHg above or below ambient pressure) the vasomotor tone will be predominantly controlled by the myogenic effect. At higher pressure differences (more than 30mmHg above or below ambient pressure) the sympathetic nervous system will also contribute to vasomotor regulation.*

1.3 Thesis Outline

Chapter 2 presents an overview of all the relevant background material as well as a comprehensive review of the relevant literature. This includes an overview of bone circulatory physiology, approaches to measuring bone blood circulation, and physiological responses to exposure to negative (hypobaric) and positive (hyperbaric) pressures.

Chapter 3 details the methods used for each experiment. An overview of the apparatus is described, including the PPG hardware development. Finally the data processing techniques together with the methods used in the statistical analysis are also presented.

Chapter 4 presents the results from all of the experiments including all parts of the validation study as well as the results from the pressure exposure experiments.

Chapter 5 is a comprehensive discussion of the results. It includes a discussion of the key findings as well as their applicability in different domains. The limitations of the work are also discussed together with suggested future research directions.

Chapter 6 presents a summary of the thesis, where the key findings and contributions are highlighted.

2.0 Background and Literature Review

2.1 Bone Circulatory Physiology

Bones are made up of two different layers, an outer layer made of compact bone (the cortex), and an inner spongy bone layer that encloses a network of trabeculae in a honeycomb-like structure. Long bones all have a similar structure: a long shaft or diaphysis and round ends, which typically have larger diameters than the shaft and are called epiphyses. Compact bone makes up the thick outer layer of the diaphysis, and at the center is the medullary cavity, which contains either yellow (fatty) or red (haemopoietic) bone marrow. The inside of the epiphyses are made of trabecular bone, and trabecular bone can also be found towards the ends of the diaphysis in the interior of the shaft. The outer layer of the epiphyses is made up of a layer of compact bone that is much thinner than the layer found around the diaphysis. The regions in between the diaphysis (shaft) and epiphyses (ends) of the bone are called the metaphyses. The metaphysis is separated from the epiphysis by a thin cartilage in growing bone, which gradually disappears as the bone matures. The outer surface of the bone is lined with a thin membrane called the periosteum [33, 137]. Figure 1 illustrates the different parts and layers of a typical long bone.

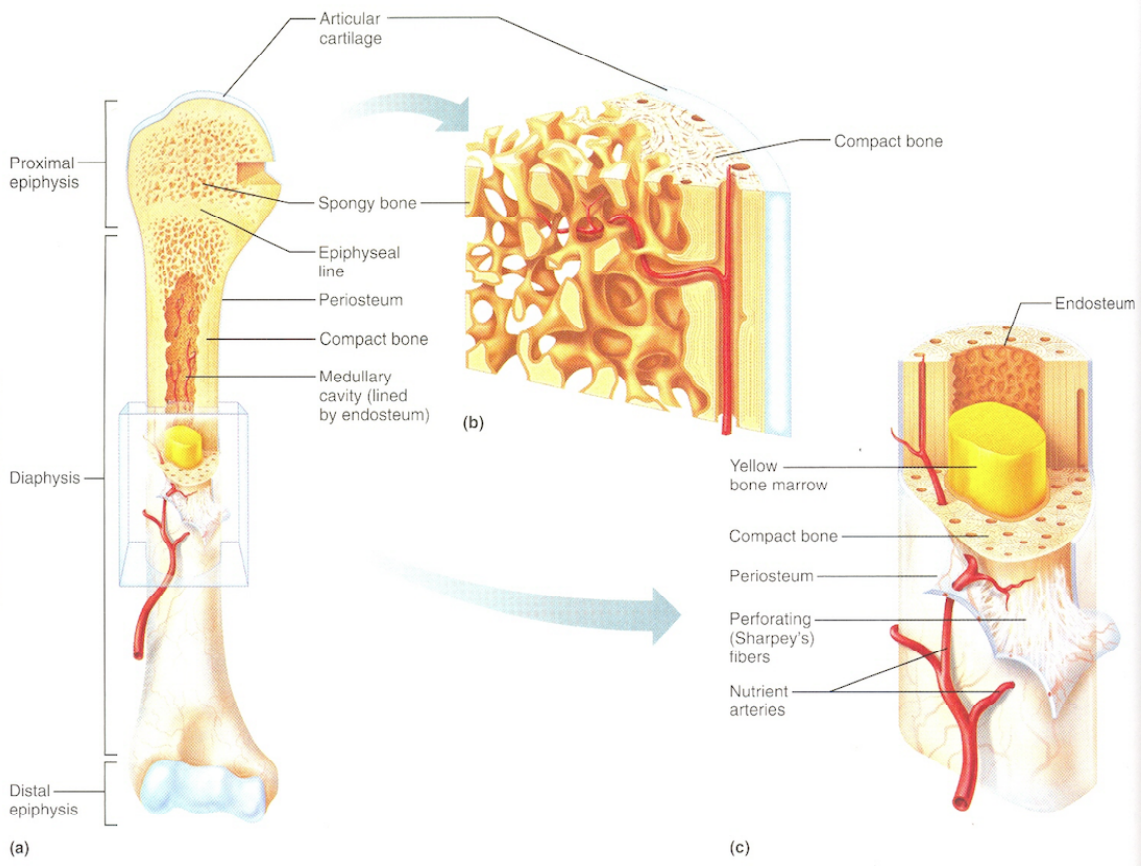

Figure 1 - Anatomy of a typical long bone [137]. (a) Typical structure of long bone. (b) close-up of the epiphysis showing both compact and spongy bone structure. (c) close-up view of diaphysis showing nutrient artery, compact bone and bone marrow.

2.1.1 Vascular Anatomy of the Long Bone

The vascular anatomy of a typical long bone can be divided into three separate systems: afferent vessels, the microvascular network, and efferent vessels. Blood supply to the bone comes from the afferent vessels, which include the nutrient artery, epiphyseal arteries, metaphyseal arteries, and periosteal arteries [33, 139]. Ionic exchange between the blood and bone marrow occurs only in the microvascular network [33], which is composed of medullary sinusoids, cortical capillaries and periosteal capillaries. The venous system includes the large central sinuses, as well as the epiphyseal, metaphyseal, periosteal, and nutrient veins [32, 120].

The nutrient artery is one of the main blood supplies to long bone, it typically enters the bone halfway along the diaphysis at a shallow angle [53, 139]. Once it reaches the medullary cavity it splits into central ascending and descending longitudinal arteries

that run parallel to the shaft, along the central longitudinal axis of the marrow, and alongside the central venous sinus, as depicted in Figure 2. Small branches come off the longitudinal artery and run radially outwards into both the marrow and into the encasing compact bone where they eventually branch off into small vessels that supply blood to the Haversian canals [129, 210]. Nutrient veins accompany the nutrient artery through the central sinus and into the smaller radial branches into the cortex [151].

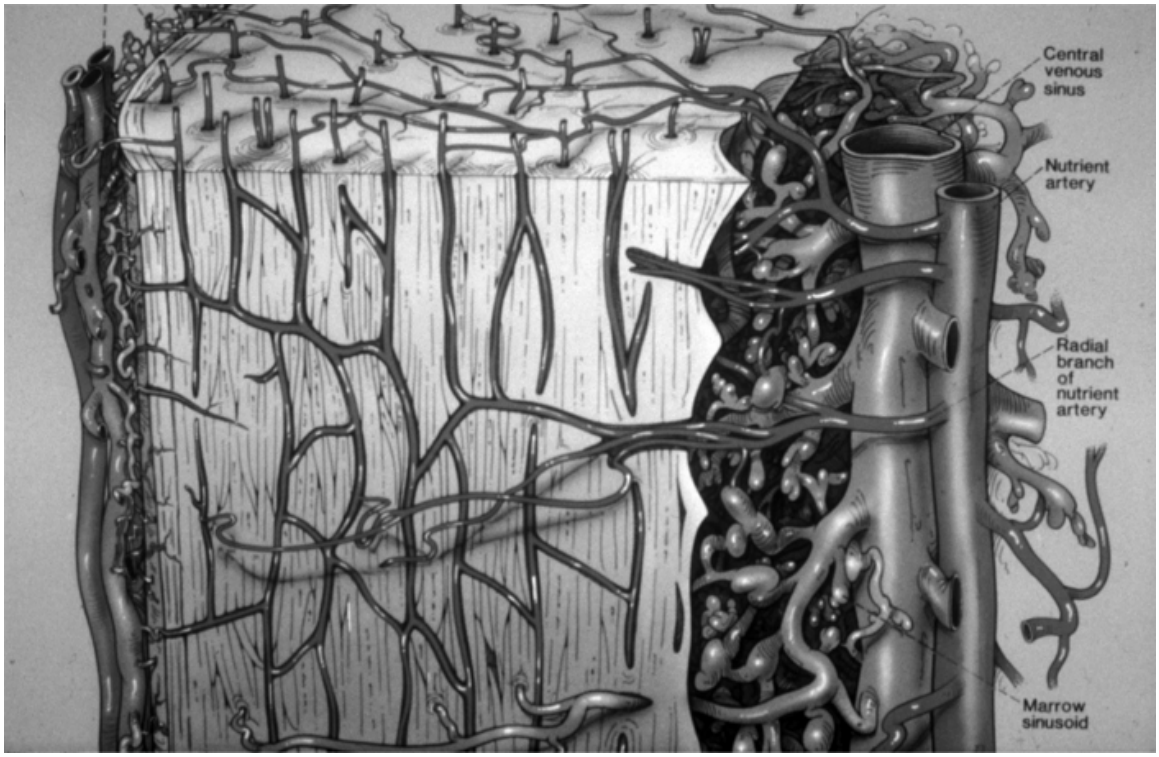

Figure 2 - Blood vessels in the diaphysis of a long bone showing the longitudinal branch of a nutrient artery (alongside the central venous sinus) and its radial projections into the cortex [139].

Compact bone is made up of many osteons, which are long cylindrical units that run parallel to the bone shaft. At the center of the osteon is the Haversian canal, which contains both arterial and venous blood vessels as well as nerve fibers. Capillaries have also been observed inside the Haversian canals, representing the exchange vessels within the cortical bone. Oriented roughly perpendicular to the Haversian canals are Volkmann's canals which connect the Haversian canals and the medullary cavity to the nerves and blood vessels outside of the bone [137], as shown in Figure 3. Arterial flow through healthy bone is centrifugal, coming from the nutrient arteries in the medullary cavity and going outwards through the cortex [32, 139].

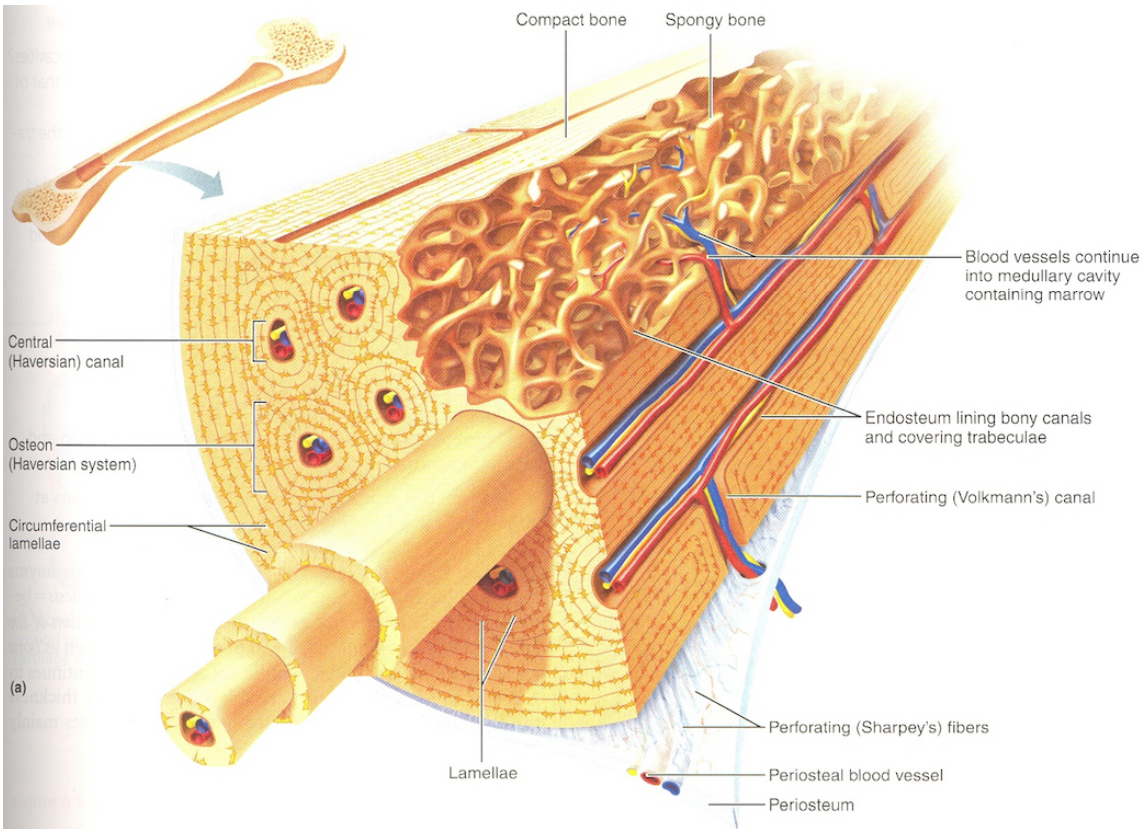

Figure 3 - Haversian canals in long bone showing the arteries (blue), veins (red) and nerves (yellow) [137].

In addition to the main nutrient artery, there are numerous smaller epiphyseal and metaphyseal arteries supplying blood to the ends of the bone [33, 53, 120]. On the periosteum a network of small periosteal vessels surround the bone. The extent to which the periosteal vessels supply blood to the bone is not clear; some have argued a "dual supply" theory where periosteal flow complements the centrifugal blood flow from medullary cavity, while others have argued against this. While the full extent of the function of the periosteal vessels is not fully understood, they appear to supply blood at least to the outer surface of the bone [151, 206]. Some evidence suggests that in certain diseases such as PAD, where arterial supply to the medulla may be impaired, the periosteal arterial supply may be enhanced. The increased periosteal blood supply acts as a compensatory mechanism and may effectively reverse the typical centrifugal blood flow direction [32].

The venous or vascular sinuses are thin vessels that connect to the central venous sinus, which runs parallel to the longitudinal artery in the marrow. The central venous

sinus collects the venous flow from the many smaller veins in the diaphyseal marrow [120]. It connects directly with the nutrient vein as well as numerous metaphyseal and epiphyseal veins, and it appears to also be connected to the periosteal veins [160]. It is thought that the cortical capillaries, on the other hand, connect with the periosteal capillaries, which drain to intramuscular veins [33].

While this classification of the vascular system in bone is helpful in understanding the overlying structure, it is important to realize that in reality the vascular network has numerous anastomoses that create interconnections between various branches of the vascular tree [33, 120, 139]. Additionally, there is still some debate as to the relative importance of the different vascular branches as well as to their functional anatomy [139].

2.1.2 Mechanisms Regulating Bone Blood Flow

Bone blood circulation is under the control of several different mechanisms including neural, humoral, and metabolic processes [107, 139, 188, 192]. Bone is highly innervated with sympathetic fibers, and while nerve fibers are found throughout they are more dense in the periosteum, metaphyses and epiphyses than in cortical bone [96, 139, 180]. Electrical stimulation of bone nerve fibers has been shown to result in vasoconstriction and reduced blood flow in different mammals such as cats, dogs [24, 25, 64, 65] and rabbits [189] as measured by decreased outflow from the bone or a decrease in intramedullary pressure. A drop in the intramedullary pressure is known to correlate with a decrease in blood flow through the bone, as the pressure difference that drives the centrifugal flow is decreased [188]. Additionally, increased bone flow has been observed after complete sciatic nerve section in rabbits [189].

Bone blood vessels have been shown to respond to a number of vasoactive substances. Early studies have shown a fall in blood flow and intramedullary pressure in response to injection of adrenaline [165, 178, 188]. More recent studies have demonstrated vasodilation in response to nitroglycerin and nitric oxide release, and vasoconstriction in response to endothelin. Overall, it appears that bone is more sensitive to vasoconstrictors than to vasodilators [29, 70, 139]. There are several metabolic factors such as blood pH, oxygen concentration, carbon dioxide concentration, and acid

metabolites that have been shown to affect bone blood flow [33, 188]. In general, decreasing the oxygen concentration or increasing the carbon dioxide content results in increased arterial flow. Reactive hyperemic responses have also been observed in bone, and these remained even after cutting the nerves, suggesting a strong metabolic control mechanism that does not depend on neural innervation [33, 188].

The myogenic response has been shown to be an important mechanism regulating blood flow in skin, muscle and many other organs [27, 28, 110, 177]. However, the exact mechanism is not yet fully understood [59, 100, 177], and to date no one has investigated if the myogenic effect also occurs in bone blood vessels. The myogenic effect was first reported by Bayliss in 1902, where he described the natural tendency of blood vessels to vasodilate in response to a decrease in transmural pressure, and to vasoconstrict in response to an increase in transmural pressure [10]. While the myogenic effect may be enhanced during sympathetic stimulation, it is a separate mechanism that can be seen even when all innervation has been cut [106, 163, 164, 177]. Changing the external pressure such as through lower-body negative pressure (LBNP) and lower-body positive pressure (LBPP) exposure are two ways to alter the transmural pressure, and hence elicit the myogenic effect [131, 134, 214]. Since the blood vessels inside the bone are encased inside the stiff bone structure, it is unclear how exposure to positive or negative pressure and the myogenic effect would affect the bone blood vessels.

2.2 Measurements of Bone Circulation

Methods for quantifying bone blood circulation have taken several different approaches, which can be broadly categorized into invasive and non-invasive methods. Since we are interested in non-invasive methods we provide a brief overview of the invasive approaches, followed by a more comprehensive review of non-invasive approaches including an in-depth discussion of PPG.

2.2.1 Invasive Methods

The use of radioactive microspheres, an evolution of earlier indicator dilution methods, is one of the most common invasive bone blood flow measurement techniques

and it is often considered the "gold standard" of bone blood flow measurements [5, 60, 139, 144]. This approach uses microspheres that are too large to pass through the capillary microcirculation, yet large enough to flow through the larger vessels in the arterial circulation. The microspheres are injected into the circulation, normally into the left ventricle, and they eventually get trapped in the capillaries and arterioles. Sites that are more perfused will end up with a higher concentration of microspheres than poorly perfused parts of the bone. A measure of blood inflow at one of the main peripheral arteries can be used together with the tissue radioactivity to obtain a quantitative measurement of blood flow through a limb [5, 31, 66, 139].

The main advantage of the radioactive microspheres technique is that it produces quantitative absolute blood flow data. A common limitation of non-invasive approaches is that they do not produce absolute measures of blood flow, instead the data they produce are relative to a baseline condition, with effects expressed as either change or percentage change from baseline. In either case, care must also be taken to specify which part of the tissue is being measured, as flow rates will be different in the different parts of the bone [30, 103]. Due to the radioactive nature of this approach, and the fact that it requires sampling of the osseous tissue, it is obviously not suitable for clinical use in humans or for repeated measurements.

2.2.2 Non-Invasive Methods

Non-invasive blood flow measurement techniques include laser Doppler flowmetry (LDF), Doppler ultrasound, near infrared spectroscopy (NIRS) and PPG. In LDF the tissue is illuminated with a laser light, which penetrates the skin and is scattered throughout the tissue. A small amount of the light is backscattered and is detected by a photodetector mounted on the probe. Light that is scattered as it hits moving red blood cells will be frequency shifted according to the Doppler effect, while light that is scattered in static tissue will not be frequency shifted. The red blood cell velocity can then be calculated from the power spectral density of the back-scattered light [128, 154]. While LDF has been successfully used in many experiments for measuring skin blood flow [138, 197] its penetration depth is shallow, typically around 1 mm, a factor that severely limits its applicability to bone blood flow measurements [104, 154].

Nevertheless, some studies have used LDF for bone blood flow measurements in cortical bone of rabbit tibiae with minimally invasive surgery. The experimenters surgically removed the skin and soft tissue surrounding the bone in order to be able to place the probe directly on the bone [43, 161, 191]. Another approach that uses the Doppler principle is Doppler ultrasound, which has been shown to be a reliable and repeatable measure and has been used in many experiments [7, 132, 146, 155, 190]. However, since ultrasound imaging does not penetrate bone tissue it cannot be used for measuring blood flow inside the bone, yet blood flow measurements of the nutrient artery to a bone may be a useful indicator of blood flow through the bone.

Some recent studies have applied a NIRS technique for non-invasive measurements of bone blood flow in the tibia [15]. After some complex signal processing and spectral analysis of the backscattered light, this method gives estimates of changes in oxyhemoglobin and deoxyhemoglobin, from which tissue O_2 saturation can be estimated [16, 17, 55, 56, 142]. Although the penetration depth of this NIRS technique has been reported at depths up to 15mm [17], which would be enough to reach the bone marrow, this figure has not been experimentally validated. Furthermore, since light from different wavelengths will have different depths of penetration [44, 157], it is not clear how the authors are capable of distinguishing bone blood flow from flow in the skin between the probe and the bone surface. Furthermore, it is worth noting that the term blood flow is often loosely used in the NIRS literature. While changes in blood oxygen levels and tissue oxygen saturation are in some situations associated with changes in blood flow, the two metrics are not necessarily correlated. NIRS can reliably measure changes in tissue oxygen saturation, but, in general, conclusions about the vasomotor tone and blood flow in the tissue cannot be made solely based on NIRS measurements.

2.2.3 Photoplethysmography

Although PPG has been used for many years, at least as far back as 1937 [97-99, 183, 209], only much more recently has it been widely adopted in clinical settings [3]. PPG is currently used for several different applications including pulse oxymetry, and microvascular skin and muscle hemodynamic measurements [63, 72, 73, 77, 172, 173, 216-220]. Recently, PPG has been used to measure bone circulation in the patella and

this new application has been partially validated [150]. We expect to be able to replicate these bone circulation measurements in any part of the skeleton that is close to the skin. Only a thin layer of skin covers the medial surface of the tibia, making it a good site for PPG measurements of bone circulation. This site is particularly desirable, as it also allows us to look at the changes in limb hemodynamics resulting from exposure to different pressures.

There are two main parts to the PPG system: a light source, typically from a light-emitting diode (LED) and a photodetector. The light source illuminates an area of the skin and the photodetector detects the attenuated light that is reflected after being absorbed and scattered by the underlying tissue. By using near-infrared (IR) light the attenuation by the skin is relatively small and constant; more attenuation occurs if there is more blood and vice-versa [3, 115]. Note that while the physical principles underlying PPG and NIRS are similar, the two approaches differ predominantly in the way that the signal received by the photodetector is processed and in the choice of LED wavelengths, leading to different physiological measures. Since blood oxygen content affects its absorption spectrum, the LEDs in PPG typically operate at about 560 and/or 800nm, which are isobestic points in which oxygenated and deoxygenated hemoglobin have the same absorption spectra [79]. The penetration depth increases with wavelength, at 560nm the penetration depth is typically about 1-2mm and at a wavelength of 800nm it can be as high as 13mm [11, 147, 174]. Since studies of the optical properties of bone have shown that it is nearly transparent to light of wavelengths within the "biological window" of 800 to 1100nm [4, 9, 127, 162, 202], application of PPG to bone blood measurements should also be possible by using LEDs with an 800nm wavelength. However, actual measurements of the penetration depth through bone tissue have not been performed.

The recorded signal from a PPG contains a pulsatile component that is synchronous with the heartbeat and a quasi-static component representative of the total blood volume, referred to as the "AC" and "DC" components, respectively [3, 42, 115]. While the DC component of the PPG signal is generally indicative of the total blood volume in the tissue, there has been considerable debate as to the reliability of this measurement parameter. In practice, the DC component of the PPG signal has been

shown to be an unreliable measure of blood volume, possibly due to several confounding factors such as sensitivity to changes in ambient light and changes in the absorption characteristics of blood with varying oxygenation levels [41].

The AC signal of the PPG waveform is often described as being a direct representation of the volume changes in the blood vessel in response to a pulse wave. The peak-to-peak amplitude of the AC signal is directly related to the vessel distensibility, and it is therefore also an indicator of the vasomotor tone [184]. For a given pressure waveform, if the smooth muscle surrounding a blood vessel is relaxed the vessel will distend more than if the smooth muscle is contracted. Several studies have shown a strong correlation between the AC signal and cutaneous blood flow in the fingertips [41, 61], however, this correlation has not been generalized to other tissue types and anatomical locations [3]. There is still some debate as to exactly what is measured by the AC signal, since it has been shown that several factors such as the orientation of the red blood cells and movement of the vessel wall also affect the signal.

Several experiments have demonstrated a change in the AC signal in situations where volume changes are not possible. Data from PPG recordings of the dental pulp and experimental set-ups involving blood flowing through glass tubes has demonstrated a pulsatile PPG component in the absence of volumetric blood changes [41, 150]. Under these conditions, the AC signal is thought to originate from changes in the orientation of the red blood cells in the microcirculation [41] and we would expect the AC signal to be highly correlated with the pressure difference in these situations, as has been experimentally demonstrated [150]. This type of flow through a rigid pipe can be approximated by Poiseuille's law, which would imply that the flow rate is directly proportional to the pressure difference. Note that applying Poiseuille's law to circulation through blood vessels needs to be done with caution, since several of the assumptions are violated, namely: 1) the flow is pulsatile and not constant which would not lead to a parabolic flow velocity profile, 2) blood viscosity is not constant, it is a function of the flow velocity, 3) and blood vessels are not straight pipes. Despite these violations, we may be able to use Poiseuille's law to obtain a gross characterization of the microcirculatory flow. In an experiment that varied the pulsatile blood pressure in a glass tube, the pulsatile pressure was shown to be highly correlated with the PPG AC signal

(r=0.82) and also highly correlated with the flow rate (correlation coefficient not reported), as shown in Figure 4 and Figure 5, respectively.

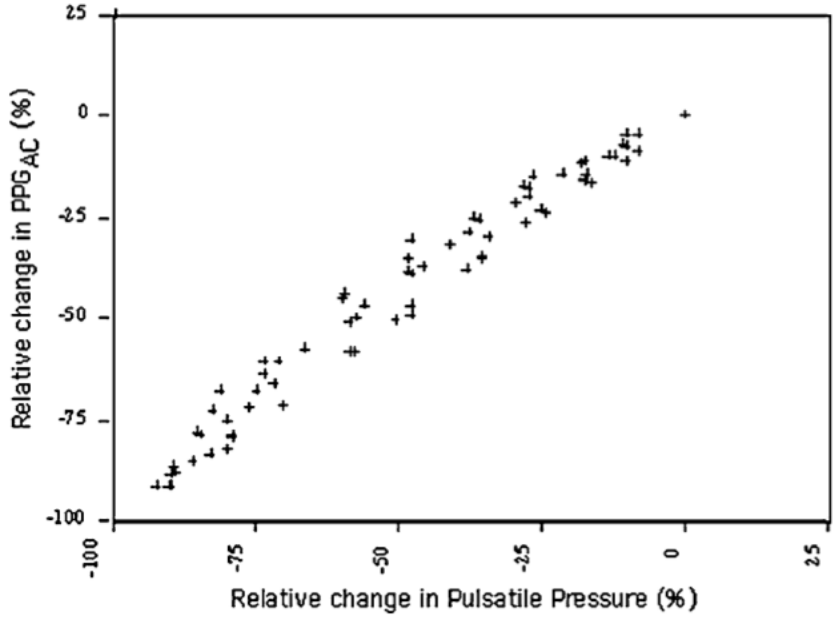

Figure 4 - Change in PPG AC signal as a function of pulsatile blood pressure in a rigid glass tube [150].

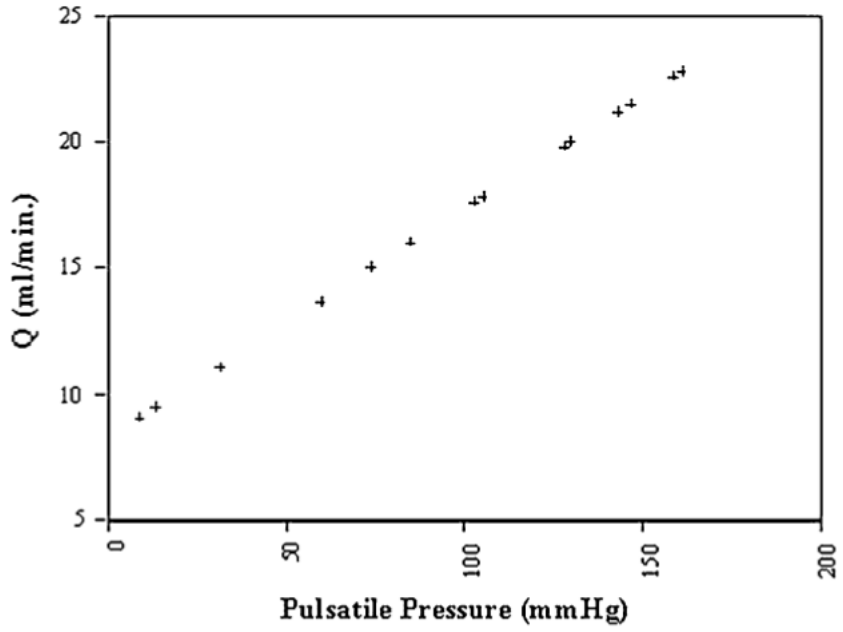

Figure 5 - Blood flow rate, Q, as a function of pulsatile pressure in a rigid glass tube [150].

These results agree with the prediction based on Poiseuille's law. This same experiment was performed with both normal and hemolyzed blood from the same donors,

and while the results in Figure 4 and Figure 5 represent the data from whole blood, in the case of hemolyzed blood no AC signal was present [150]. This supports the concept that light absorption by the red blood cells is responsible for the changes in the PPG signal.

In many PPG measurements the changes in the AC signal are likely to be representative of both changes in the blood flow velocity as well as changes in the pulsatile blood volume. With our current techniques, it is not generally possible to quantify what percentage of the signal originates from each of these two factors. When measuring PPG responses to various stimuli, knowledge of the stimulus itself may help in further understanding which factor is predominant in the measured AC responses. For example, during arterial occlusion we know that the blood flow velocity goes to zero, while during exposure to cold we would expect local cold-induced vasoconstriction to affect the pulsatile signal.

Both an increase in the blood flow velocity as well as an increase in blood volume due to arteriolar vasodilation would represent an increase in nutrient supply to the tissue and an increase in perfusion. Similarly, a decrease in the AC signal would represent a combination of vasoconstriction and a reduction of blood flow velocity, both of which would be detrimental to tissue perfusion. We can therefore consider changes in the AC signal to be generally representative of changes in the relative perfusion of the tissue [3, 42, 61, 153, 184, 186, 222]. Since all PPG measurements are relative and not in absolute units, applications of PPG typically represent the data as a relative change from a baseline level.

By looking at the frequency domain, the AC signal can be further decomposed [185]. The AC component will normally have a fundamental frequency at about 1 Hz. The exact location of the fundamental frequency depends on the heart rate, such that a frequency of 1 Hz would correspond to a heart rate of 60 beats per minute (BPM) [3, 115]. In the frequency range from 0.01 to 0.5 Hz, the signal reflects the activity of the sympathetic nervous system (SNS). Since changes in SNS also affect heart rate (HR), the fundamental frequency range around 1 Hz is also modulated by the frequencies below 0.5 Hz. Changes in the power spectral density at the different parts of the spectrum can be used to infer changes in SNS tone from a baseline measurement [89, 115].

Some studies have used probes that combine LDF and PPG in a single instrument to measure blood flow at different depths, by using the LDF for skin blood flow measurements and the PPG for measurements of deeper muscle tissue [11, 90, 91, 128]. However, measurements at different depths can also be achieved with a single PPG probe by adjusting distance between the LEDs and the photodetector as well as choosing suitable LED wavelengths [171-174, 195, 201].

2.3 Physiological Response to Externally Applied Pressure

The second specific aim of this thesis is to characterize bone hemodynamic responses to single-limb exposure to changes in external pressure. Single-limb exposure to changes in external pressure is a useful way to study the mechanisms that regulate blood circulation for several reasons. Firstly, there is a vast body of literature on skin and muscle blood flow that suggests which mechanisms are likely to be active and dominant when the tissue is exposed to different pressure levels above and below atmospheric pressure, and from which we can build our hypotheses. Secondly, exposing only a single limb to the pressure change while taking measurements on both limbs gives us an extra piece of information that allows us to separate systemic SNS reflexes from local myogenic effects, since we expect SNS reflexes to affect both limbs while the myogenic effect should only be present in the limb that is exposed to the change in pressure [131].

There are many different ways to alter the external pressure to the body. Pressure chambers have been used to expose the entire body as well as smaller circumscribed parts to both negative and positive pressures. Negative pressure wound therapy (NPWT), in which suction is applied to an open wound, is an even more localized application of negative pressure that has been shown to aid in wound healing [1, 22, 117]. Application of positive pressure has been even more varied with methods including lower body positive pressure (LBPP), compression stockings, and inflation of pressure cuffs [2, 23, 57, 62, 105, 114, 118]. Local pressure cuff inflation has been done both continuously, to block arterial and/or venous flow, and intermittently up to various pressure levels. These approaches are more commonly known as external or intermittent pneumatic compression (EPC or IPC) [58, 116, 143].

While there are important relationships between all of these methods, this current study is concerned with the application of negative and positive pressure to a single limb. All these methods can be categorized based on two characteristics, 1) the size of the area being exposed to pressure changes, and 2) the duration of exposure to pressure changes. The first category varies from whole body exposures to local exposures of a small open wound. We are interested in exposing a large enough body part to a change in pressure so as to cause a significant change in the local blood flow while not overly provoking whole-body systemic responses. Therefore, the literature most relevant to the current work falls in the middle of this category, ranging from exposures of part of a single limb such as a hand or foot to exposure of the entire lower body such as in lower body negative pressure (LBNP). The second category can vary from long duration exposure in the order of hours, to intermittent and cyclical exposures of just a few seconds. The time ranges relevant to this study are those with continuous, non-cyclical pressure exposures of a few minutes to less than an hour. These time frames are long enough to evoke different mechanisms that regulate blood circulation, yet they are shorter than the time constants associated with interstitial fluid shifts resulting from changes in external pressure. Therefore, the review here presented is focused on the most relevant parts of a very wide body of literature, which does not include IPC, compression stockings, pressure cuffs, or NPWT.

2.3.1 Hypobaric (Negative) Pressure

The effects of locally applied external pressure on human physiology have been extensively studied in several different applications. Much of the focus has been on the hemodynamic response to an increase or decrease to the externally applied pressure. Many studies have looked at the effect of decreasing the external pressure by means of hypobaric chambers or suction applied locally and directly onto the skin, and the cardiovascular and local microvascular blood flow changes in response to decreases in external pressure have been heavily researched [1, 6, 10, 81, 92, 108, 124, 134, 148, 166, 213]. LBNP has been proposed as a countermeasure to orthostatic intolerance for astronauts [71, 93, 95, 121]. Additionally, LBNP while exercising may result in added health benefits in helping to prevent musculoskeletal de-conditioning and maintaining

exercise capacity and spine function [123, 124, 135, 193, 194]. Although many aspects of LBNP have been examined, no study has looked at the effect of negative pressure on bone hemodynamics.

Wolthuis et al. performed a comprehensive literature review on lower body pressure in 1974 [213]. Much of the review covered here is a summary of some of his main findings together with more recent developments in the field. The first studies of application of reduced pressure to parts of the human body were reportedly performed by Junod in 1834, who looked at hyperemia in various anatomical regions [14, 112, 113]. After the initial work in mid 1800s, not much was done until interest in the field re-emerged in the 1950s. Numerous studies looked at the effect of reduced pressure on blood flow in the forearm [8, 18, 35, 38-40, 54, 82-87], hand [46, 50, 82], calf [47-49] and foot [45]. The initial response in the upper limbs is generally characterized by a transient vasodilation leading to increased flow, which is quickly followed by vasoconstriction. At large pressure differences of -130 mm Hg or greater, the vasoconstriction stops and vasodilation at levels similar to the initial transient are seen. At high enough pressures the smooth muscle along the vessel walls is no longer able to compensate the large increase in transmural pressure and eventually gives way, resulting in vasodilation. Similar results are observed in the lower limbs. However, the resulting dilation only occurs at much higher pressure differences around -250 mm Hg. This larger resistance to an increase in transmural pressure is likely associated with the fact that the lower limbs are accustomed to sharp increases in transmural pressure during orthostatic stress [213].

LBNP results in fluid shift from the upper to the lower body and can be a strong stimulus to the cardiovascular system, evoking many reflexes. The fluid shift leads to blood pooling in the veins of the lower body and, to a lesser extent, fluid shifts into the extravascular interstitial space [6, 213]. LBNP has been used as a tool for modeling and studying orthostatic stress and has been of particular interest in the aerospace community because of its relevance to space physiology and potential use as a countermeasure in human spaceflight [71]. LBNP results in a drop in central venous pressure (CVP) since venous return is reduced due to the blood pooling. This is accompanied by a reduction in stroke volume and cardiac output (CO) of 50% and 30%, respectively, at -50 mm Hg. In

response to LBNP, systolic blood pressure (BP) consistently drops but no consistent trends are seen in diastolic BP, with some studies reporting an increase and others a decrease [213]. Mean arterial pressure (MAP) is also generally decreased. The drop in BP is compensated by a marked increase in HR of about 20% at -40 mm Hg [149], and increase in total peripheral vascular resistance [108, 208]. The loss of systolic BP sensed by the high-pressure arterial baroreceptors [169] triggers an increase in SNS tone to the sinoatrial node of the heart, which results in an increase in HR and a large increase in peripheral vascular resistance. However, forearm vascular resistance increases even for levels of LBNP as low as -5 mm Hg. At such low LBNP levels, the high-pressure baroreceptor reflexes are not yet activated, since systolic BP and MAP are not affected. The increase in forearm vascular resistance is due to other mechanisms such as increased SNS tone triggered by cardiopulmonary low-pressure baroreceptors and the myogenic effect [108, 131, 221].

Several mechanisms including the myogenic effect and SNS reflexes affect the peripheral vasoregulation response to LBNP, and one study has quantified the relative contributions of each mechanism, noting that they contribute in different proportions in the arms and legs [131]. In all of these studies it has been assumed that pressure applied to the surface of the skin is equally transmitted to all parts of the underlying tissues, and this has been validated to some extent by Lundvall [133, 134]. The pressure seal design is also important, the seal should be tight enough to maintain the pressure difference between the inside and outside of the chamber, but at the same time not so tight that it would significantly interfere with venous outflow [80, 81, 198]. There are no published studies on the effect of LBNP on bone hemodynamics.

2.3.2 Hyperbaric (Positive) Pressure

Different methods have been used to increase the external pressure, including hyperbaric chambers, pneumatic compression cuffs, compression stockings, or direct mechanical application of pressure to the skin [19, 57, 76, 118, 125, 130, 152, 155, 156, 175, 187, 212]. Although many cardiovascular and hemodynamic effects of lower-body positive pressure (LBPP) have also been studied, little is known about the effect on bone circulation [94]. In fact, regardless of the method used to change the applied pressure,

almost nothing is known about the effect of changes in external pressure on bone hemodynamics [20, 145].

LBPP has not been studied as extensively as LBNP, but has recently received some renewed interest due, in part, to its potential application as an aid in rehabilitation of patients recovering from orthopaedic surgery [57, 67, 170]. In one of the first LBPP studies, Bevegård looked at some of the cardiovascular and peripheral vascular effects of quickly changing the pressure in a lower-body chamber to 40 mm Hg above or below ambient pressure [13]. In accordance with previous results, LBNP resulted in a decrease in CVP and CO, MAP remained unchanged, and the calculated peripheral vascular resistance as well as forearm vascular resistance and HR all increased significantly [13, 213]. LBPP resulted in significant increases to MAP and CVP, but no changes were noted in HR or peripheral vascular resistance, although forearm vascular resistance was decreased [13]. Many researchers have expanded this work and shown similar general trends in their results [75, 175, 187].

In another LBPP experiment, Shi et al. increased the pressure gradually from 0 to +40 mm Hg in order to observe the thresholds of activation for the baroreceptors, and concluded that they are not as sensitive to loading as to unloading, and they also suggested that intramuscular pressure receptors are activated at pressures between +20 to +40 mm Hg [74, 75, 187]. Interactions between the SNS and the intramuscular pressure receptors have been further studied and it has been suggested that the decrease in SNS tone observed at low LBPP pressures is countered at higher pressures due, at least in part, to the activation of the intramuscular pressure receptors [74, 76].

The effects of posture (supine vs. standing) and exercise have also been shown to significantly affect the cardiovascular response; larger changes in BP are generally observed in the supine position [68, 78, 156, 168]. Research has also more recently focused on the myogenic response to changes in transmural pressure [130], which plays a major role in local control of vasoregulation [177]. However, no study has yet looked at the effect of LBPP on bone blood circulation, or at the relative contribution of the SNS and myogenic effects in bone vasomotor responses to LBPP.

2.3.3 Summary of Response to Changes in External Pressure

The main mechanisms responsible for the physiological responses to changes in external pressure are illustrated in Figure 6. Since the information in this figure is based on the current literature, these mechanisms represent primarily the response of muscle and skin to changes in external pressure. Note that we do not know what mechanisms are involved in regulating bone circulation in response to changes in external pressure, but the information in Figure 6 serves as a starting point from where we can develop our initial hypotheses.

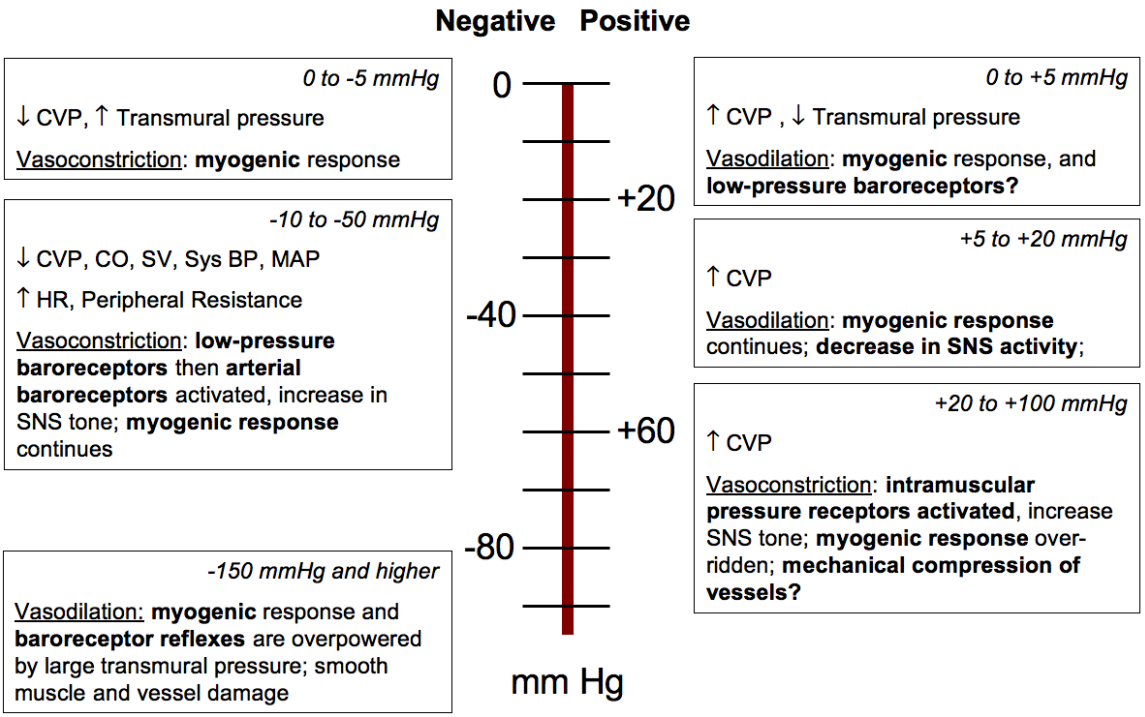

Figure 6 - Summary of mechanisms involved in the physiological hemodynamic response in skin and muscle to changes in external pressure

For negative pressures we expect to see vasoconstriction starting at pressure levels as mild as -5 mmHg, and a progressive increase in vasoconstriction as the pressure difference increases. The myogenic response is thought to be the only mechanism in effect at -5 mmHg. At some point below -10 mmHg the low pressure baroreceptors sense the drop in CVP and peripheral resistance is increased. At low enough pressures, around -50 mmHg, the high pressure baroreceptors are also activated and these result in further vasoconstriction through the increase in SNS tone, which is also accompanied by an

increase in HR. Throughout this pressure range both the myogenic and sympathetic mechanisms are contributing towards vasoconstriction. Eventually, at a high enough pressure difference of -150 mmHg or more, we expect to see vasodilation. However, this is due to the fact that there is a limit to the pressure difference that the smooth muscle tissue can sustain. At high enough pressures this limit can be surpassed, leading to smooth muscle and vessel damage and the physical appearance of petechiae, which are small local hemorrhages due to burst capillaries. In all of our experiments we will not be using such high pressure differences, and thus expect to only see vasoconstrictive response at all the negative pressures.

For positive pressures as mild at +5 mmHg, we expect that the change in transmural pressure will evoke myogenic vasodilation. More vasodilation is expected at higher pressures up to about +20 mmHg as the myogenic effect is further activated and the low-pressure cardiopulmonary baroreceptors may also respond to an increase in CVP by decreasing the SNS tone. At some point between +20 to +40 mmHg, the intramuscular pressure receptors are activated resulting in vasoconstriction and countering the vasodilation from the myogenic effect. At higher positive pressures we expect to see further vasoconstriction due to the intramuscular pressure receptors as well as mechanical compression of the leg. The mechanical compression of the limb may eventually lead to venous collapse and can have an important effect on the physiological response by changing the amount of blood that can be pooled in the venous system of the limb.

2.4 Identified Research Gaps

Throughout the literature review and background section we have covered the relevant aspects of several different bodies of literature, including the physiology of bone blood flow, non-invasive measurements of blood circulation, and the effects of changes in external pressure on blood circulation. There are several salient gaps in the literature that this thesis is designed to address.

Firstly, while PPG is a promising non-invasive approach for bone hemodynamic studies, there is only one study that has used PPG on bones [150]. There is a need to

replicate this approach and produce further validation data that supports our claim that the PPG can actually be used to measure bone hemodynamics (specific aim #1).

Secondly, while there have been numerous studies characterizing the response of the systemic cardiovascular system as well as muscle and skin tissue to changes in external pressure, very little is known about the hemodynamic response in bone to changes in external pressure. By using PPG we can for the first time characterize the physiological response to changes in external pressure in bone (specific aim #2).

Finally, the mechanisms responsible for the bone hemodynamic response have also not been described. An understanding of the relative importance of myogenic and sympathetic mechanisms in the regulation of blood circulation in bones is an important yet missing step in our understanding. The myogenic effect in bone has also never been studied or documented (specific aim #3).

3.0 Methods

This chapter presents a detailed overview of all the experimental set-up. This includes the development of the required hardware and instrumentation, as well as all the experiment protocols and procedures. A description of the data reduction and processing are also presented.

3.1 Experiment Apparatus

3.1.1 Pressure Chamber Set-up

A picture of the pressure chamber set-up together with the pressure seal and the sealing ring that attaches the pressure seal to the chamber is shown in Figure 7.

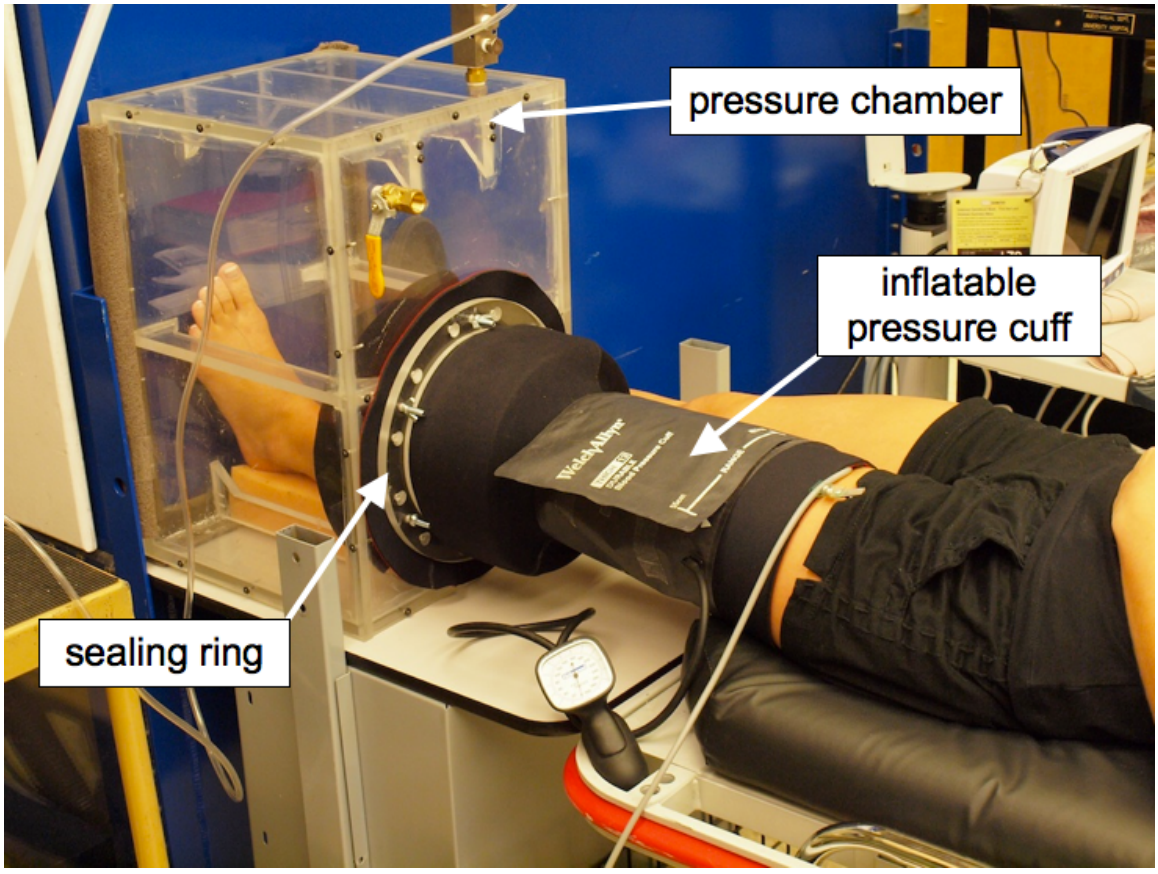

Figure 7 - Pressure chamber with neoprene pressure seal and sealing ring

A small rectangular pressure chamber approximately 50 by 30 by 30cm (19 by 12 by 12in) was used for the pressure experiments. A 20 cm (8in) diameter circular cutout on the top panel allowed subject's limbs to be inserted into the chamber. The chamber was made from 1.27cm (0.5in) thick impact resistant clear acrylic sheets. The structure was reinforced by adding a series of "ribs" along the walls. The chamber was designed to withstand pressure differences as large as 100 mmHg above and below ambient pressure, though the operating pressure of the chamber during all experiments did not exceed 50 mmHg above or below ambient pressure. An emergency pressure valve was also installed on the top of the chamber. The valve could be opened by either the experimenter or the subject in case of an emergency where rapid pressure equalization was needed.

In order to seal the chamber, a flexible seal that would form an airtight connection between the chamber and the subject's limb was designed and fabricated (Surf 'n Sea®, San Diego, CA). A neoprene seal was designed in the shape of a leg, with a large opening at the bottom that would attach to the chamber. The closed cell neoprene is air tight and strong enough to sustain the expected pressure differences. The inherent elasticity of the neoprene allowed subjects with a wide variety of leg diameters to fit comfortably into the pressure seal. During exposure to negative pressures the friction between the neoprene seal and the limb is large enough to keep the seal in place. However, during high positive pressures the pressure seal tends to "balloon" outwards and shift upwards along the leg. In order to minimize any movement of the seal, an inflatable wide thigh pressure cuff (Welch Allyn® Thigh 13 Blood Pressure Cuff, Skaneateles Falls, NY) was placed on the outside and upper part of the pressure seal. The pressure cuff was inflated to the same pressure as the pressure inside the chamber, as this was shown to be sufficient to prevent any slippage of the pressure seal and also minimized any air leakage through the top of the seal.

The neoprene seal was designed with a wide "lip" at the bottom of the leg that would fit over the top of the chamber. This neoprene flange is placed between the chamber and an acrylic ring that is mounted on top of the seal and secured into place by tightening 6 wing nuts that screw onto bolts that are fixed to the chamber.

3.1.2 PPG Hardware

A custom PPG device was designed and built for this study. A prototype probe was first designed and used in some of the preliminary experiments. A second-generation PPG probe was subsequently developed and used for some of the validation experiments and for all of the pressure experiments.

Regardless of the version of the hardware, the underlying principles in the PPG instrumentation remain the same. Figure 8 presents a schematic of the typical components of a PPG instrument. This particular schematic includes two different light sources, a green LED and a near IR LED. These two light sources can be arranged to provide information at different tissue penetration depths. The user is allowed to adjust the intensity of the LEDs by manually rotating a control knob for each LED. Light from the LEDs is absorbed and scattered throughout the tissue. A small amount of that light is reflected back onto the PPG probe and this is sensed by the photodetector, which generates a certain amount of current as a result. The signal then goes through a current-to-voltage converter that changes the signal from the photodetector into a voltage.

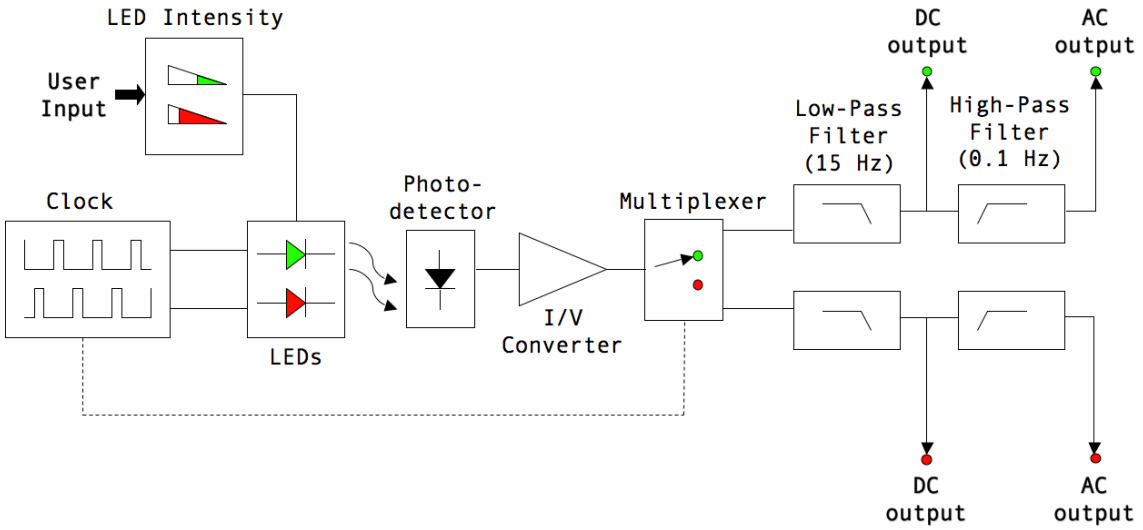

Figure 8 - Schematic of the PPG Circuit

The LEDs are not continuously emitting light, instead they are alternately cycled at a very high frequency. The clock is set to cycle at a high frequency between switching one LED on, having both LEDs off, switching the other LED on, switching both off, and so on in a continuous loop. As shown in Figure 8, the "clock" item in the schematic is

connected to both the LEDs and the multiplexer, which allows the multiplexer to divide the signal into two parts, one corresponding to each of the LEDs. Each of the signals is then low pass filtered with cut-off frequency of 15Hz, which eliminates some of the high-frequency noise and from which the DC component of the signal is extracted. The signal is then high-pass filtered at 0.1Hz in order to extract the AC component. The PPG signal is further processed using our data analysis software as described in section 3.1.3.

The penetration depth of the PPG signal depends primarily on three things: 1) the separation between the LED and the photodetector, 2) the intensity of the LED and 3) the wavelength of the LED [3]. Penetration depth increases with increased separation distance between the LED and the photodetector, increased LED intensity and with longer wavelengths (assuming we are operating within the biological window of 800-1100nm). Previous studies have shown that the penetration depth of an LED operating at a wavelength of 880nm (near IR) with a separation of 20mm from the photodetector is at least 13mm, and therefore suitable for measurements of deeper tissues. For skin measurements penetration depths of 1-2mm have been achieved by using LED with 560nm wavelength (green light) that are placed very close (~3.5mm) to the photodetector [171]. Note that the thickness of the skin that covers the medial surface of the tibia is typically about 4.0 ± 1.8mm (mean ± standard deviation, based on pilot measurement data), and a rough estimate of the diameter of the tibia at the level of the nutrient foramen is about 20mm [36], therefore the 13mm penetration depth of the IR signal is appropriate for our objectives.

Besides the effect on penetration depth, there is another factor that influences our choice of LED wavelength. Light absorption by blood varies as a function of wavelength and is different for oxygenated and deoxygenated hemoglobin, as can be seen in Figure 9. At certain wavelengths, known as isobestic points, the absorption coefficient for oxygenated and deoxygenated hemoglobin are the same, and within the biological window there is an isobestic point at 805nm. By choosing wavelength at or close to isobestic points, the PPG device will be equally sensitive to changes in oxygenated and deoxygenated hemoglobin. In all of our applications, we have used green LEDs with a wavelength of 526nm placed 3mm away from the photodetector for skin measurements,

and IR LEDs with wavelengths close to the 805nm isobestic point and positioned 20mm away from the photodetector for measurements of deeper tissue.

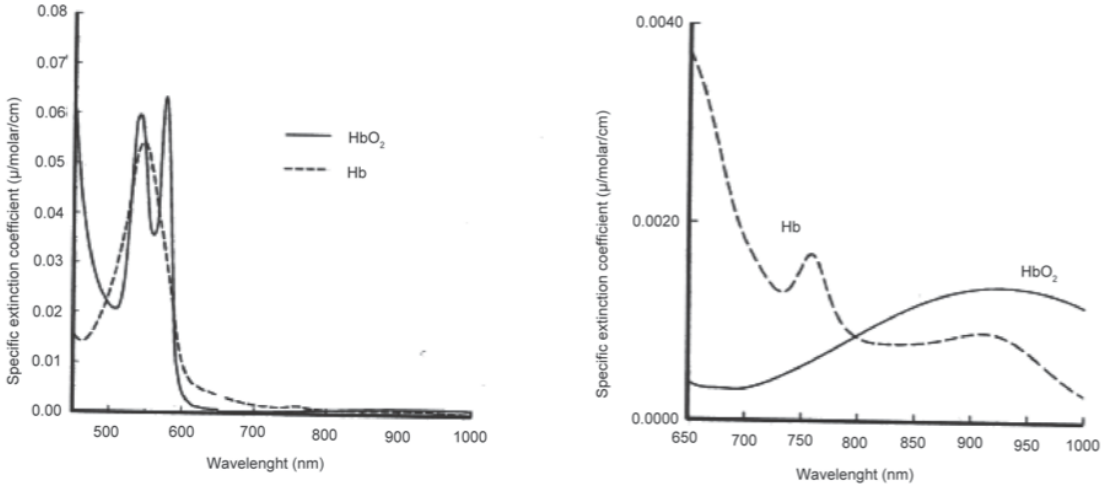

Figure 9 - Absorption coefficient for oxygenated and deoxygenated hemoglobin as a function of wavelength showing the isobestic point at 805nm [26]

Prototype PPG

The head stage of the prototype PPG is shown in Figure 10. The head stage connects to a control box that powers the PPG and allows for the individual adjustment of the LED intensities. The control box includes an output channel for the AC and DC components of the green and IR signal, which are connected to a data acquisition board (National Instruments BNC-2090, Austin, TX) that is in turn connected to a desktop computer. The PPG control box also has an output channel that is directly connected to a digital oscilloscope (LeCroy® 9400, Chestnut Ridge, NY) and is used for adjusting the LED intensities to within the desired operating range. This equipment set-up is shown in Figure 11. The oscilloscope allows the LEDs to be adequately powered – below a minimum threshold voltage the LEDs will not turn on, and if they are too bright the light can saturate the photodetector. By looking at the waveform on the oscilloscope we can ensure that the LED intensity is below the saturation point of the photodetector.

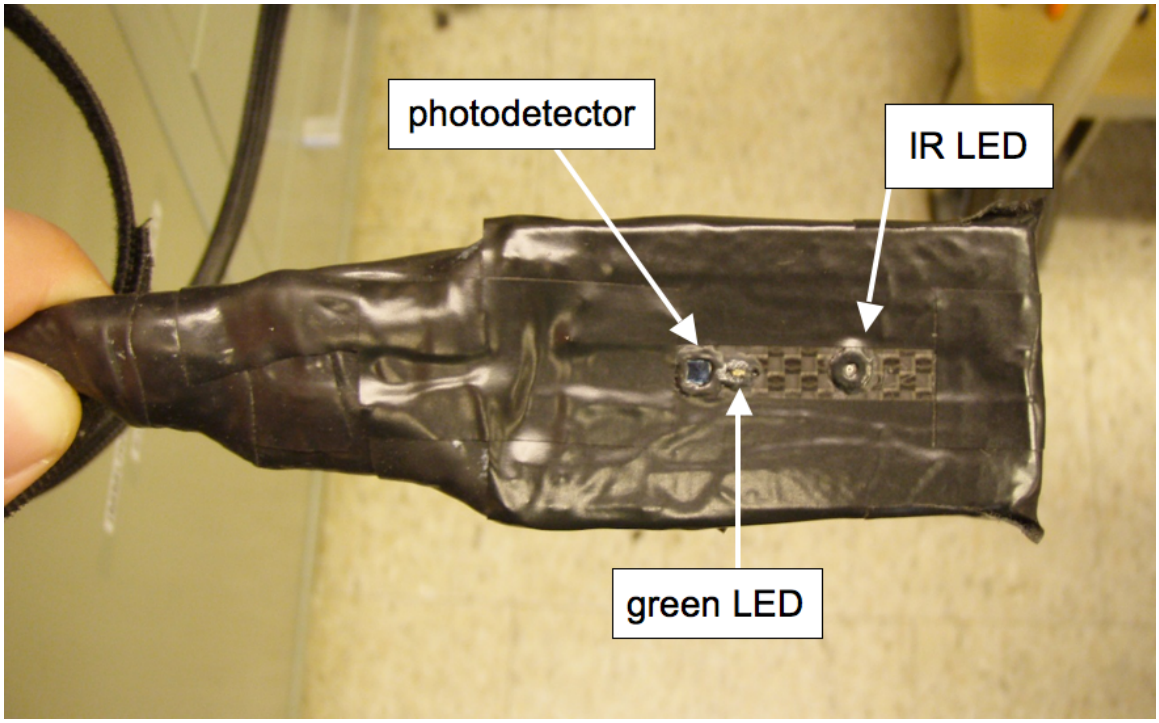

Figure 10 - Prototype PPG head stage showing the two LEDs and the photodetector

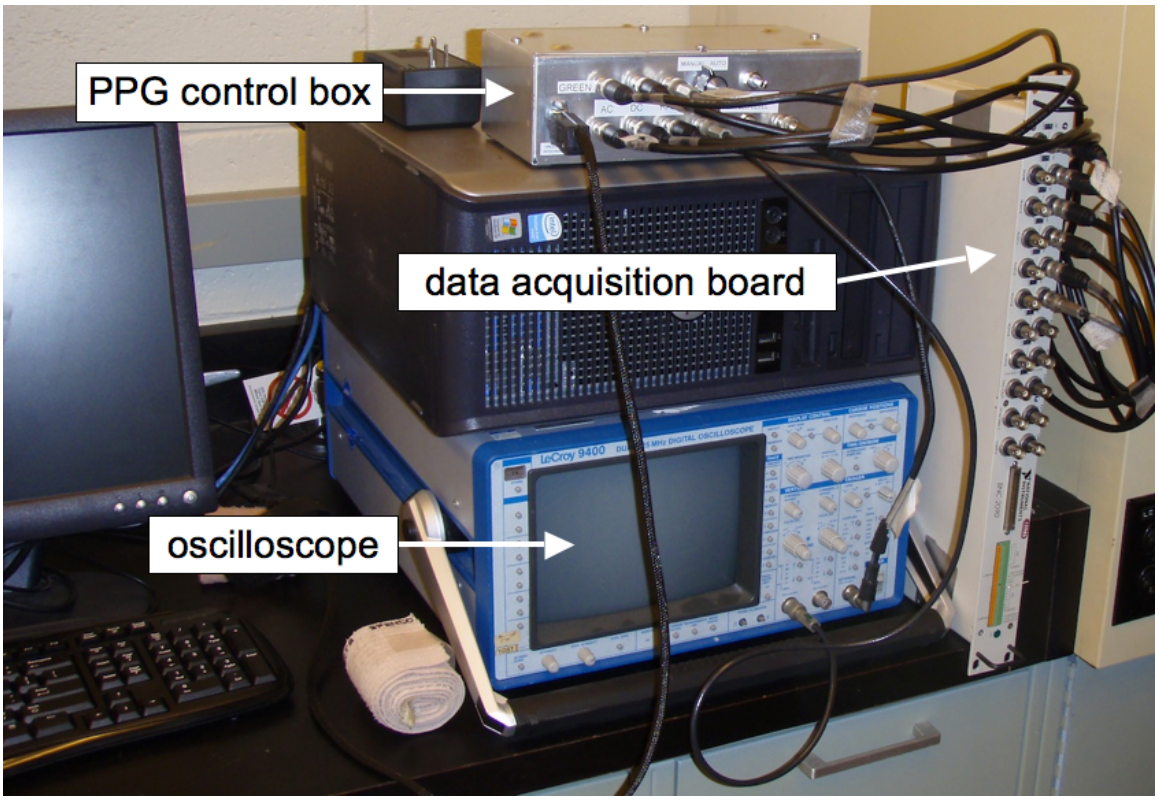

Figure 11 - Set-up of the prototype PPG system

Second Generation PPG

The prototype PPG system was used in the initial validation experiments, and this is further described in experimental protocols in section 3.2. The second-generation PPG probe incorporated several improvements including:

- Temperature sensor added to PPG probe allowing for monitoring of temperature changes throughout a recording session
- Longer, more flexible and durable medical grade cable with Lemo® connectors for the PPG probes
- Two separate PPG units, allowing for simultaneous measurements at two different sites
- Thin ribbon cable between the PPG head stage and the PPG cable, facilitating passing the cable between the neoprene pressure seal and the skin
- Rigid casing for the PPG head stage, allowing direct application of pressure through the probe
- Custom built PPG head stage casing with small ridges preventing any leakage of light from the LEDs directly to the photodetector

The photodetector, green LED, IR LED, and temperature sensor can be seen in Figure 12, which shows the head stage of the second generation PPG probe. The control box was also redesigned, as can be seen in Figure 13.

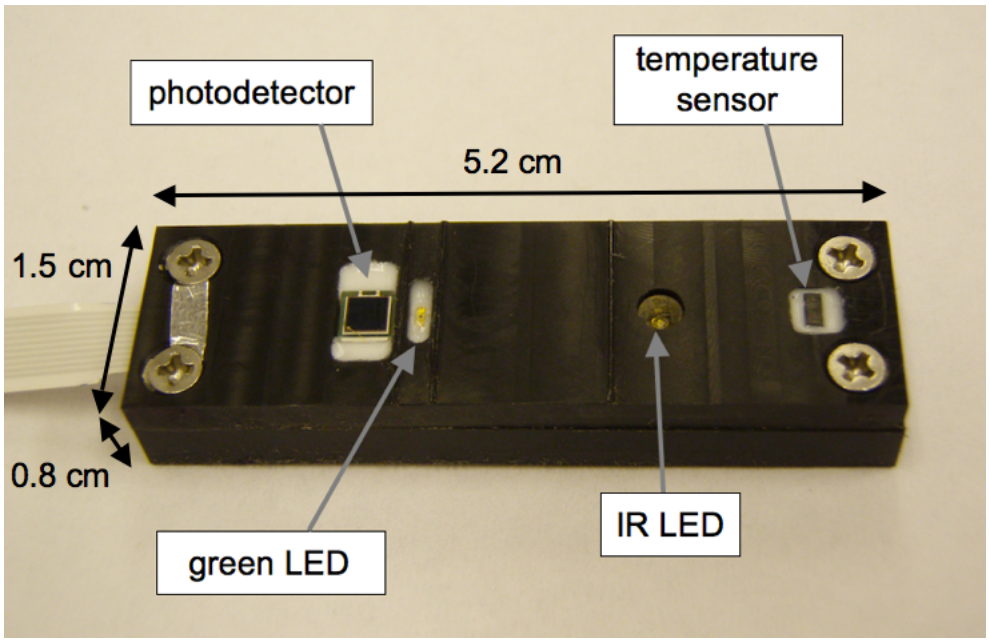

Figure 12 - Second generation PPG probe head stage

Figure 13 - Control box for second generation PPG

3.1.3 PPG Software

The PPG signal data recording and processing was done using National Instruments® LabView 7 Express 2003 (National Instruments®, Austin, TX). Two different LabView interfaces were designed: one for recording the data and one for post-recording data processing.

There are 10 different outputs from the PPG hardware that are of interest. Each probe has 5 output channels: 2 AC signals and 2 DC signals (one for the green LED, and one for the IR LED), and one output for the temperature sensor. The PPG interface allows the user to specify a file recording location on the attached computer, and lets the user start and stop the data recording via the pressing of a button on the graphical user interface (GUI). The GUI also displays 4 line charts that show the rolling 60s history of all the AC and DC channels. The data are recorded at a sampling frequency of 300Hz, and are stored in text files.

A separate LabView interface is used to process the data and extract the relevant parameters. The GUI displays the AC and DC traces for both PPG sensors at the same time, and the user is allowed to select a portion of the signal to analyze. For example, the data file may contain data recorded over several minutes, but the user may be interested in getting information from only the first minute to serve as a baseline measurement. There are also a lot of factors that can introduce artefacts into the PPG data. For instance, if the subject were to move excessively, contract a leg muscle, or sneeze, we would see large disturbances in the PPG signal. The GUI allows the user to only select the parts of the signal that are of interest, so the computed parameters originate solely from high-quality parts of the signal and do not contain any unwanted artefacts that could significantly skew the data. Figure 14 shows the data acquisition GUI, however, note that only half of the screen is shown here for legibility purposes. The other half of the screen is essentially a mirror image of the graphs where data from the second PPG probe are displayed.

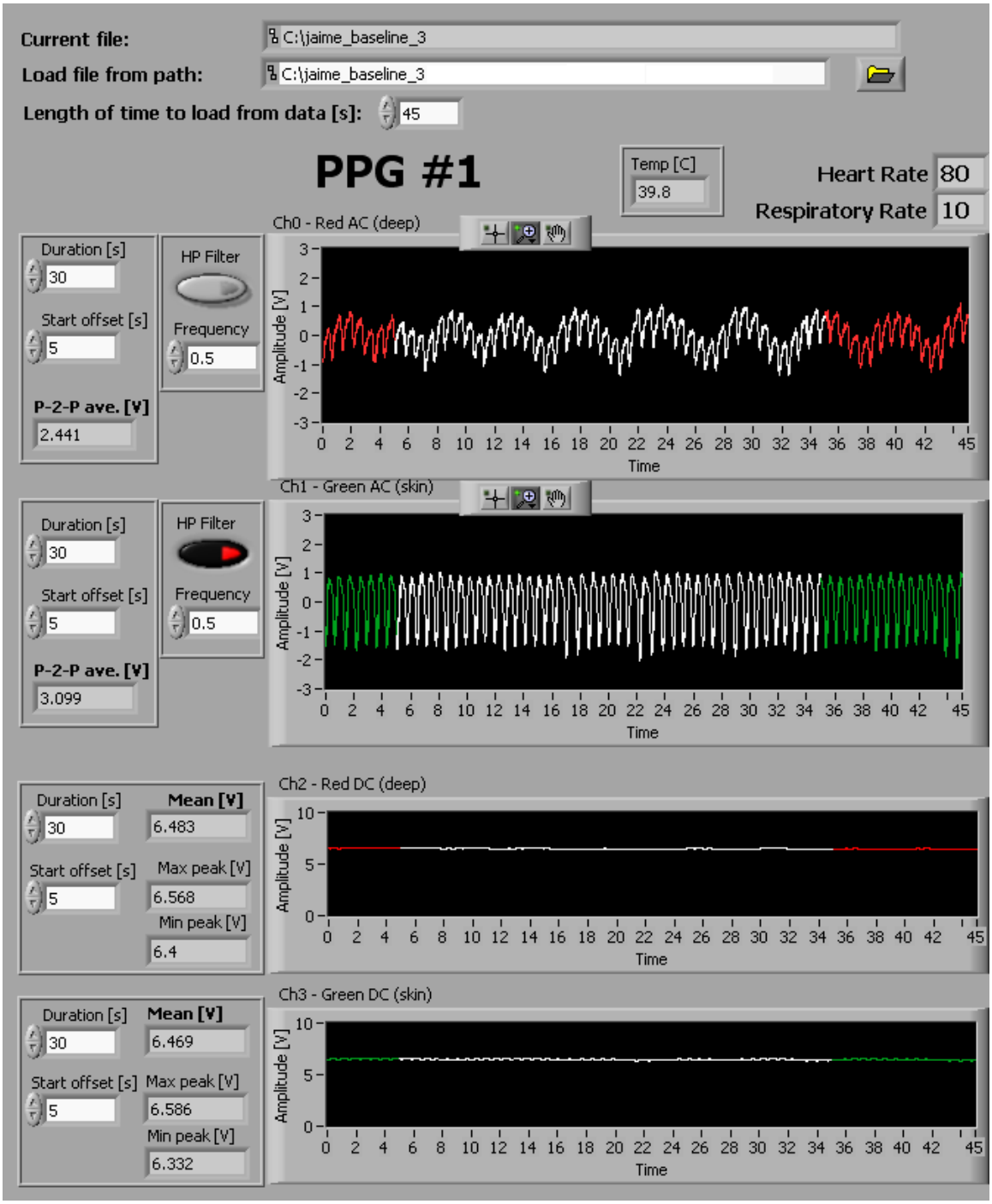

Figure 14 - LabView GUI for analyzing the PPG signal (only half of the screen is shown here for one probe). The bone (red) and skin (green) signals are displayed; the part of the signal that has been selected for analysis is shown in white.

All the parameters that are analyzed are calculated based on only the time-span of the signal that has been selected (shown in white in the graphs). The red signal corresponds to the bone signal (IR LED) and the green to the skin signal (green LED). The software extracts the HR and respiratory rate of the PPG signal by finding the corresponding peaks in the frequency spectrum of the signal, since we know that the HR should be around 1 Hz and the respiratory rate will normally have a peak between 0.1 to 0.2 Hz. The temperature from each sensor is also displayed at the top of the screen.

The AC component of the PPG signal is synchronous with HR, but it also displays a lower frequency oscillation that corresponds to the respiratory rate. This can be clearly seen in the bone (red) AC plot in Figure 14, however, this oscillation has been eliminated in the skin signal (green). There is an optional high-pass filter, set to a default frequency of 0.5 Hz, which can be used to eliminate this oscillation. All of the AC data we analyzed was first high-pass filtered at 0.5 Hz before the peak-to-peak amplitudes of the AC signal were calculated. The difference between the green and red AC traces in Figure 14 clearly shows the effect of the high-pass filter in removing the respiration-induced oscillations. The main parameter that we are interested in is the AC peak-to-peak amplitude, which is displayed on the left of the screen separately for both the green and red signals.

3.1.4 Other Equipment

The pressure inside the chamber was monitored by using a digital pressure monitor (World Precision Instruments, Sarasota, FL) that was connected to the chamber via a flexible hollow plastic tube. Blood pressure and HR measurement were also taken throughout the various experiments using an automated blood pressure monitor (HEM-775, Omron® Healthcare Inc., Bannockburn, Il) with the pressure cuff placed around the left upper arm. The thickness of the layer of skin above the medial surface of the tibia was also measured using skin-fold calipers (Slim Guide - Creative Health Products Inc., Plymouth, MI).

3.2 General Experimental Methods

All of the experiments were performed with subjects lying supine. Before beginning any of the experiments, subjects were asked to remain resting in the supine position for at least five minutes. Prior to exposure to any of the stimuli, baseline BP and HR were measured using the automated blood pressure monitor, which was always placed on the left arm. Measurements of the tibia skin thickness were taken on the limb(s) that was used for the experiment by using the skin-fold caliper. Additional demographic information such as age, gender, height and weight were recorded. Only one limb per subject was used for the validation experiments. The left leg was used for half of the subjects and the right leg for the remaining half; subjects were randomly assigned to each group. For the pressure experiments, one PPG probe was placed on each limb. The PPG probe was placed on the skin on the medial surface of the tibia at a distance (measured from the proximal end of the PPG probe) of about 4-9cm distal to the tibial tuberosity. Once the probe was placed on the skin, a marker was used to draw around the four corners of the probe, and the probe was then covered with a loosely wrapped bandage. By marking the location of the probe we could check if the probe had shifted between the beginning and the end of the experiment. The bandage was used to block the ambient light from reaching the probe, and thus prevent any leakage of light into the photodetector, which would affect the PPG signal.

Healthy male and female subjects were recruited for all experiments. Even though we were not expecting any gender differences, we attempted to keep an approximately equal number of male and female subjects in each experiment. All subjects gave informed written consent prior to participating, and this study was approved by the institutional review board (IRB) at the University of California – San Diego, as well as the Committee on the Use of Humans as Experimental Subjects at MIT, which serves as the Institute's IRB. A copy of the consent forms can be found in Appendix A. Detailed demographic information on the subjects is given in subsequent sections for the corresponding set of experiments.

3.3 PPG Validation Experiments

3.3.1 Introduction

The first set of experiments was designed to address the first specific aim, which is to validate the use of PPG for bone hemodynamic measurements on the human tibia. In order to do this we devised a series of experiments using PPG to record the response to various stimuli including: 1) arterial occlusion, 2) exposure to cold, 3) skin occlusion via mechanical pressure, and 4) exposure to nitroglycerin.

A full validation of the PPG technique on bone would require comparisons to a "gold standard". Unfortunately, any of the techniques that could be considered a gold standard for bone blood flow are invasive and not suitable for *in vivo* measurement in humans. The use of animal models would allow us to compare PPG to invasive techniques and would be a valuable contribution to our validation efforts. Unfortunately, as described in the literature review, there is an inherent ambiguity in interpreting the PPG AC signal as the contributions to the signal from changes in vasomotor tone and blood flow velocity cannot be readily separated. While we may be able to correlate the PPG signal to one of these parameters in a given tissue, the correlation and relationship between these measures would not be easily generalizable to any stimulus or to any anatomical measurement location. The microvascular structure in different tissues can vary widely and different stimulus may evoke different responses that may be captured by the PPG but not necessarily by the other measurement technique. For example, during cold-induced vasoconstriction the blood flow velocity may not necessarily change much even thought the local flow resistance is increased. In this situation the PPG and blood velocity measure would not be highly correlated. However, for a different stimulus such as arterial occlusion, we would expect the PPG signal to be highly correlated to the blood flow velocity.

Our goal is to provide some preliminary data in the validation process. A full validation of the PPG technique has not been completed in other tissues and has barely been explored in bone tissue. While these experiments are designed to verify that our instrument works as expected, we acknowledge that there is room for more extensive validation work, as is further discussed in section 5.6.

3.3.2 Arterial Occlusion and Cold Exposure

The arterial occlusion and the cold exposure parts of the validation study were all performed in the same experimental session. The prototype PPG probe was used in both of these experiments.

Arterial Occlusion

An inflatable wide thigh pressure cuff (Welch Allyn® Thigh 13 Blood Pressure Cuff, Skaneateles Falls, NY) was placed around the mid thigh and inflated in order to block the arterial and venous flow to the limb. Prior to inflating the pressure cuff, baseline PPG data were recorded for 1 minute. The cuff was then inflated to 180 mmHg and kept at that pressure for 1 minute. The subjects were told that they might experience some pain when the cuff is inflated, and that they should report this to the experimenter. If any pain was reported, the experimenter reduced the pressure to 170 mmHg and, if the pain persisted, to 160 mmHg. PPG data were recorded continuously throughout and the recording continued for about 2.5 minutes after the deflation of the pressure cuff.

We hypothesized that the peak-to-peak amplitude of the AC component of the PPG signal for both bone and skin would drop to zero during the arterial occlusion. Since we are fully blocking the pulsatile arterial flow to the limb, the pulsatile component of the PPG signal should also disappear. After releasing the pressure in the cuff, we expect the AC signal to stabilize at a similar level to what was observed in the baseline condition. The initial response after releasing the pressure may exhibit a transient hyperemic response, which should subside after a few seconds.

Cold Exposure

We used an ice pack filled with ice-cubes to expose the measurement site to cold. Baseline PPG data were recorded for 1 minute, and then the probe was removed so that the ice pack could be placed on the same location on the limb. The ice pack was left in place for 5 minutes, after which it was removed and the PPG probes placed back on the same spot (by aligning them with the drawn marker lines) and data were recorded for one minute. The PPG probe was then removed and the limb was left exposed to the room temperature for 5 minutes, in order to allow it to begin warming up. The PPG probe was placed back on the skin and data were again recorded for an additional minute. We therefore ended up with 3 separate 1-minute recordings: before the cold exposure, right

after the cold exposure, and a third recording about 5 minutes after removal of the ice pack.

Since exposing the limb to the ice pack required the removal of the PPG probe, we also had to address the question of the effect of removing and replacing the probe on the PPG measurements. In order to investigate this, we replicated the exact same protocol as in the cold exposure condition, except that instead of using the icepack we just left the limb exposed to the room temperature. This serves as a control condition for the replicability of the PPG measurements when a probe is removed and then later placed back onto the same location. In other words we took a 1-minute baseline recording, removed the probe for 5 minutes, took another 1-minute recording, removed the probe for another 5 minutes, and finally replaced the probe for a final 1-minute recording.

We hypothesized that the cold exposure would result in cold-induced vasoconstriction, and that the PPG signal should slowly return to levels close to the baseline after the limb has been exposed to room temperature for a few minutes. We also hypothesized that there would not be a significant difference between the three measurements in the control condition, in other words, if the PPG probe is removed and placed back in the same location within a short time period the PPG signal will not be significantly different.

Treatment Order

The order in which we applied the three treatments was fixed: first the control condition, followed by the cold exposure and finally arterial occlusion. Since the arterial occlusion was the most provocative stimulus, it was the last treatment that the subjects experienced. Subjects also took a 5-minute break, where they were allowed to move and talk as long as they remained in the supine position, in between each of the treatment conditions.

Subjects

A total of 9 subjects (5 male, 4 female) participated in this experiment with an average (± standard deviation) age of 26 ± 4 years, weight of 73 ± 13 kg, height of 1.72 ± 0.06 m, resting systolic BP of 118 ± 14 mmHg, diastolic BP of 74 ± 9 mmHg and tibial skin thickness of 4.2 ± 2.1 mm. No adverse effects were reported, and all subjects completed the experiment.

3.3.3 Nitroglycerin Patch and Skin Occlusion

Since the IR PPG signal has to pass through the skin as it penetrates the deeper tissue and then the backscattered light has to pass through the skin again before it is sensed by the photodetector, it is possible that the IR PPG signal responds not only to changes in the circulation in the deep tissue but also to changes in the skin circulation. However, based on our knowledge of how light scatters through the tissue, in the typical "banana" shape, we expect that the thin layer of skin does not significantly contribute to the IR PPG signal [69, 200, 204]. In order to assess the effect of changes in the skin circulation on the IR signal, we devised two experiments that would selectively alter the skin circulation without affecting the circulation in the bone. In the skin occlusion experiment our goal was to selectively reduce the skin PPG signal to zero while not affecting the bone signal, and in our nitroglycerin patch experiment we aimed to selectively increase the skin signal without affecting the bone circulation. Both of these experiments were performed with the second generation PPG probes.

Skin Occlusion

The occlusion of the skin circulation was done by applying pressure directly thought the PPG probe. Since the head stage of the second-generation PPG probe is encased in a rigid plastic container, pressure could be applied directly through the probe without damaging the internal electronics. (This was not possible with the prototype probe, since the back of the probe was not protected with a rigid casing). Based on some pilot testing and previously published studies in which similar methods were used [150], a pressure of 150 mmHg[1] through the probe was determined to effectively block the microvascular circulation in the skin.

The PPG signal was continuously recorded throughout this experiment. A baseline period of one minute was recorded followed by 60-90s of skin occlusion, and then another minute of post-occlusion data after removing the applied pressure.

We hypothesized that the pulsatile flow would be eliminated and decrease to zero in the skin, but would not be affected in the bone during the occlusion. We also

[1] The back casing of the head stage of the PPG probe has an area of $7.95 \times 10^{-4} m^2$, therefore by applying approximately 15.8N of force, a pressure of approximately 2.0×10^4 Pa or about 150 mmHg can be applied to the skin through the probe.

hypothesized that the PPG signal would return to baseline levels in the 1 minute post-occlusion period.

Nitroglycerin Patch

Nitroglycerin is a known potent vasodilator, and it is commonly used in the treatment of angina [158, 176]. A small 4cm^2 nitroglycerin patch with a 0.1mg/hr dosage (Nitroglycerin Transdermal System, Mylan®, Canonsburg, PA) was used to administer the drug to the skin. In the treatment of angina, nitroglycerin patches are placed on the chest area for long period of time of 12-14 hours over a 24-hour period. Such long duration exposures result in a widespread dispersion of nitroglycerin through the systemic circulation [34, 111]. In our experiments, we are only applying the nitroglycerin patch for 15 minutes, and with such a short exposure we only expect to see local changes in tissue perfusion and no changes in systemic cardiovascular parameters such as BP or HR.

Baseline PPG data was recorded for 1 minute, then the PPG probes were removed and the nitroglycerin patch was placed at the center of the recording site for 15 minutes. Afterwards, the patch was removed and discarded and PPG data were recorded for 3 minutes. Blood pressure measurements were also taken before and after the nitroglycerin administration.

We hypothesized that the nitroglycerin exposure would increase the skin circulation with little or no effect on the bone signal.

Treatment Order

Since the effects of the nitroglycerin patch can be long lasting, the order of the treatments was fixed; subjects first did the skin occlusion part of the experiment followed by the nitroglycerin patch experiment. Subjects had a 5-minute break between the two experiments, where they were free to move on the bed, but remained resting in the supine position.

Subjects

A total of 6 subjects (3 male, 3 female) participated in the skin occlusion experiment and all of these except for one of the female subjects also participated in the nitroglycerin patch experiment. The 6 subjects had an average (± standard deviation) age of 24 ± 12 years, weight of 71 ± 43 kg, height of 1.70 ± 0.08 m, resting systolic BP of

115 ± 15 mmHg, diastolic BP of 72 ± 12 mmHg and tibial skin thickness of 4.7 ± 3.0 mm. No adverse effects were reported, and all subjects completed the experiment.

3.3.4 Data Collection and Processing

The PPG signal was recorded continuously throughout the arterial occlusion and skin occlusion experiments. The data file was split into three parts representing the pre-, per- and post-occlusion segments. For each segment, the average peak-to-peak amplitude of the AC component of the PPG signal for both skin and muscle was computed over at least 30 seconds of a clean PPG signal. There are several factors that can introduce artefacts into the PPG signal such as if the subjects were to move, sneeze, or be otherwise surprised or affected by an external disturbance. These situations often introduce spikes in the AC data, which need to be eliminated prior to computing the average of the peak-to-peak amplitudes. By looking at each data segment individually, these spikes can be selectively removed from the time span of data that is used in computing the 30-second average. Each data segment is at least 1 minute long, which gives the experimenter plenty of data to work with in the case that there are disturbances in the signal that need to be removed. The same approach is used in treating the data from the cold exposure and control experiments as well as the nitroglycerin.

3.4 Pressure Experiment

3.4.1 Introduction

The second and third aims of this thesis were to characterize the bone hemodynamic response to changes in external pressure by taking PPG measurements on the tibia, and to quantify the relative contributions of the sympathetic reflexes and myogenic effect to the response. In this experiment we alter the external pressure by placing one limb inside a pressure chamber and then increasing and decreasing the pressure difference between the inside and the outside of the chamber. In order to distinguish between the myogenic effect and sympathetic reflexes, PPG measurements are taken on both limbs, even though only one of the limbs is inside the pressure chamber. Any myogenic response should only be present in the limb that is exposed to

the pressure difference, whereas any large sympathetic reflex, if evoked, should be present in both limbs [131].

3.4.2 Experiment Protocol

The general methods described in section 3.2, were also used for the pressure experiment. Note, that unlike in the validation experiments, one PPG probe was placed on each limb; however, only one limb from each subject was placed in the pressure chamber. Based on some preliminary testing and a power analysis, we recruited 12 subjects, 6 male and 6 female to participate in this experiment. For each gender, the left leg was placed inside the chamber for 3 subjects, and the right leg was used for the other 3 subjects. Subjects were randomly selected for the left/right limb groups. The experiment took less than 2 hours per subject including the time needed to explain the experiment, obtain informed consent and experiment set-up and execution.

Once subjects were lying on the bed, the neoprene pressure seal was placed around their leg and pulled up towards the upper thigh. The seal remained in contact with the subject's limb from the top of the knee to the top or middle of the thigh for a distance of about 25cm. (How far up the thigh the pressure seal reached is a function of the length of the subject's limb). The PPG probes were passed underneath the pressure seal, and the sealing ring was used to attach the pressure seal to the chamber and securely tightened to prevent air leakage. A second PPG probe was then placed on the limb outside the chamber. Additionally the wide pressure cuff was placed around the thigh on top of the neoprene seal, as this would be inflated during the positive pressure parts of the experiment. The blood pressure cuff was also placed around the subject's left arm over the brachial artery. Subjects were made as comfortable as possible by placing a small pillow underneath their heads and also ensuring that there was a small natural bend in their knees by placing a soft pillow at an adjustable height to prevent the knees from being locked. Once all the set-up was completed, the subjects were asked to relax and lay down for 5 minutes before commencing the experiment. Throughout all phases of the experiment subjects were asked not to talk (unless there was a problem or some discomfort) and also to remain relatively still in order to not adversely affect the PPG recordings.

Nine different pressure levels were used in the experiment: -50, -30, -15, -5, 0, +5, +15, +30, and +50 mmHg below and above ambient pressure. The order of the pressure levels was randomized for each subject, but consecutive pressure levels were always alternated between negative and positive pressure levels. Each pressure level was maintained for 4 minutes, and after exposure to a non-zero pressure level the pressure in the chamber was brought back to 0 mmHg for a period of 4 minutes prior to going to the next pressure level. Additionally, subjects were exposed to two 4-minute baseline periods at 0 mmHg, one before the first non-zero pressure exposure and one after the final non-zero pressure exposure. A sample of the pressure protocol is shown in Table 1. Note that the actual order of the pressure levels was randomized for each subject. Some subjects were randomly selected to start at a negative pressure levels and others at a positive level. All the PPG data for any given pressure level is expressed as a change from the baseline recording immediately preceding the pressure level. By referencing the data to the preceding baseline level as opposed to referencing all pressure levels to the first baseline segment at the beginning of the experiment, we can control for effects with longer time-constant, such as fluid shifts to or from the extravascular space.

Table 1 - Sample experimental pressure exposure protocol

Order	Pressure *mmHg (kPa)*		Duration [min]
1	0	(0.0)	4
2	-15	(-2.0)	4
3	0	(0.0)	4
4	50	(6.7)	4
5	0	(0.0)	4
6	-30	(-4.0)	4
7	0	(0.0)	4
8	5	(.67)	4
9	0	(0.0)	4
10	-50	(-6.7)	4
11	0	(0.0)	4
12	30	(4.0)	4
13	0	(0.0)	4
14	-5	(-.67)	4
15	0	(0.0)	4
16	15	(2.0)	4
17	0	(0.0)	4

Several factors contributed to the choice of pressure levels. Firstly, we were limited to +50 and -50 mmHg at the extremes due to the limitations of the vacuum pump used to pressurize the chamber. Additionally, at more extreme pressures, mechanical compression of the vessels in the leg is likely to become predominant factors affecting the hemodynamic response. While these effects may also be of interest, they fall outside the scope and aims of this thesis. There are several examples in the literature where the myogenic effect can be seen at pressure levels as low as 5 mmHg above or below ambient pressure, hence our choice of 5 mmHg as our lowest pressure increment. It has also been suggested that intramuscular pressure receptors are activated between 20-40 mmHg [76, 187], hence we might expect a different response at a pressure below and above the activation of the intra-muscular pressure receptors which explains our choice of 15 and 30 mmHg above ambient pressure; the -15 and -30 mmHg pressure levels were kept for symmetry between the positive and negative pressure levels.

The physiological effects that we investigated, such as the myogenic effect and sympathetic reflexes, are all quickly activated in response to a change in pressure and the response can be seen to reach a steady state within about 1 minute. However, prolonged exposure to positive or negative pressures will evoke other physiological responses such as fluid shift to or from the extravascular space. We emphasized the short-term response to the pressure changes, and in order to prevent prolonged exposures to negative or positive pressures, we always alternated from a negative to a positive pressure level. The pressure exposure at each level lasted for 4 minutes, which is long enough for the response to reach a steady state. In preliminary testing we looked at the time needed for the PPG signal to reach a steady state after a change in pressure. We considered the most extreme possible changes from +50 to -50 mmHg and vice-versa as well as the subtlest changes from 0 to +5 and -5 mmHg and vice-versa. In all cases the PPG signal reached a steady-state value after about 1 minute of the pressure change. Therefore, pressure exposures of 4 minutes were selected, as this should be enough time to obtain reliable data points representing each pressure level.

In addition to the PPG measurements, we also measured the pressure that is applied to the skin in the upper thigh where the pressure seal wraps around the leg. The pressure seal needs to be tight enough to maintain the pressure difference between the

inside and outside of the chamber. However if it is too tight it will significantly interfere with the leg circulation by compressing the large veins and inhibiting venous outflow from the limb. In order to quantify the amount of pressure that is applied to the leg at each chamber pressure level we performed a small pilot study using a Tekscan® pressure measuring system (Tekscan®, Inc., Boston, MA). A detailed explanation of this pilot experiment and its results are presented in Appendix B.

3.4.3 Subjects

A total of 12 subjects (6 male, 6 female) participated in the pressure experiments. All subjects gave informed written consent prior to participation and all completed the protocol with no adverse effects. Subjects had an average (± standard deviation) age of 24 ± 5 years, weight of 71 ± 15 kg, height of 1.73 ± 0.08 m, and tibial skin thickness of 4.0 ± 1.9 mm.

3.4.4 Data Collection and Processing

The PPG signals were continuously recorded throughout the entire pressure protocol, beginning with the first 4-minute 0 mmHg baseline period and ending in the final 4-minute baseline period after all of the pressure exposures. The data file was split into 17 segments corresponding to each of the 4-minute baseline and pressure levels, as listed in Table 1. The blood pressure cuff was used to obtain BP and HR measurements at each of the 17 segments, and this was always done in the third minute of each 4-minute segment. The PPG data was analyzed minute-by-minute, such that an average AC peak-to-peak amplitude was obtained for both the skin and bone channels for each limb for each minute in each of the 17 segments. In processing the PPG data, each average was computed over a period of at least 30 seconds, and care was taken to ensure that no external disturbances in the PPG signal were used in the 30-second average calculation. In all cases the PPG data were either expressed as the raw data or as a change from baseline, both in Volts, as discussed in section 3.3.4.

4.0 Results

All of the PPG data are expressed as raw values or changes from baseline. While it is common practice to treat this type of data as percentage changes from baseline [203], this is not an appropriate technique for the PPG data. First, the PPG data are not absolute and are always in reference to a baseline level. However, the baseline level for different people in the same experimental condition will vary due to several factors such as their skin color and skin thickness. Using percentage changes will tend to skew the data towards the data points with smaller baseline values (i.e. a 1V increase in a signal that has a baseline of 1V represents a 100% increase, while it only represents a 33% increase if the baseline signal were 3V). Furthermore, studies have shown that greater statistical power is achieved when analyzing data expressed as either a raw value or a change from baseline, rather than as a percentage change form baseline [199, 203]. All of our PPG data are expressed as either a change from baseline or as a raw value in all of our statistical analyses.

4.1 Validation Experiments

The same procedure is used throughout the statistical analysis of all of the validation experiments. First, the data are checked for normality at each treatment level using the Shapiro-Wilk test. The null hypothesis is that the data are normally distributed, $\alpha = 0.05$. Comparisons are then made between all factor levels for the skin and bone PPG signals independently. The treatment level comparisons are all within subjects, since in all of these experiments we had repeated measurements on the same subject at different points in time. In all cases, the comparisons are performed by using two-tailed paired t-tests. Additionally, in the cases where the data are not normally distributed, as determined by the Shapiro-Wilk test, the Wilcoxon signed ranks tests was also used and reported in addition to the paired t-test. The family-wise alpha was set at 0.05, and Bonferroni adjusted alpha levels were used for multiple comparisons performed on the same dependent variable. The detailed results of the normality tests can be found in

Appendix C, and the detailed output from the t-tests can be found in Appendix D. Unless otherwise noted, the data in all of the graphs are expressed as means and their 95% confidence intervals.

4.1.1 Arterial Occlusion

The PPG AC peak-to-peak amplitudes for the skin and bone data are shown in Figure 15 for the three phases of the experiment: baseline, arterial occlusion, and post-occlusion. The results of the comparisons between the three phases are given in Table 2.

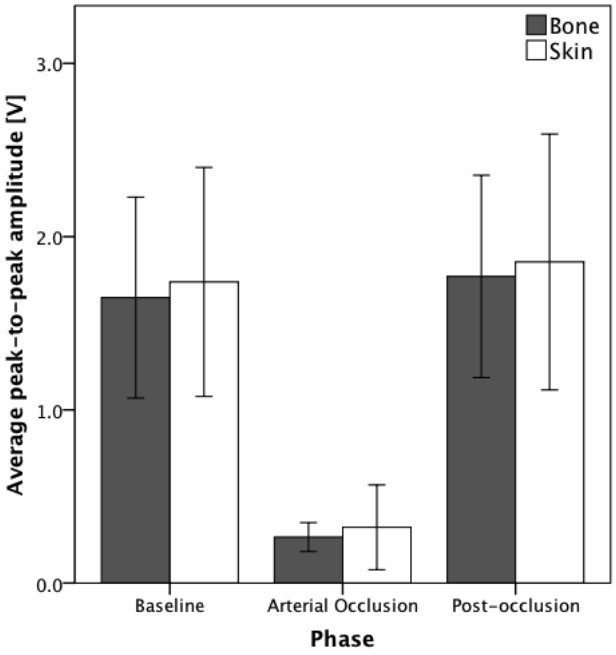

Figure 15 - PPG AC data from arterial occlusion experiment for both skin (white bars) and bone (dark bars) signals. Data are expressed as means ± 95% confidence intervals.

Table 2 - Treatment level comparisons for arterial occlusion experiment

Channel	Comparison	p-value		Bonferroni adjusted α
		t-test	*Wilcoxon signed ranks*	
Bone	baseline – arterial occlusion	<0.001	**0.008**	0.017
	arterial occlusion – post-occlusion	<0.001	**0.008**	0.017
	baseline – post-occlusion	0.516	0.779	0.017
Skin	baseline – arterial occlusion	**<0.001**	.	0.017
	arterial occlusion – post-occlusion	**<0.001**	.	0.017
	baseline – post-occlusion	0.367	.	0.017

During the arterial occlusion the PPG waveform disappeared, and the AC signal essentially dropped to zero. The algorithm used in the data processing is designed to measure the peak-to-peak amplitudes of any signal, even if the signal is just noise. The non-zero AC averages shown in Figure 15 represent a measure of the noise amplitude in the PPG signal during the arterial occlusion; this data is not representative of any significant physiological signal. During the arterial occlusion the PPG signal was not synchronous with HR and the typical PPG waveform was absent. While the data in this phase in Figure 15 could have been represented as zero, we have chosen to leave it in its original form.

As seen in Figure 15, there is a significant difference between the baseline and occlusion phases and between the occlusion and post-occlusion phases for both bone and skin, as shown in Table 2. The PPG data from the bone were not found to be normally distributed, however, both the t-test and the non-parametric analyses are in agreement and yield similar results. There was no significant difference between the baseline and post-occlusion phases in either signal.

4.1.2 Cold Exposure and Control

The results from the cold exposure experiment are shown in Figure 16 for all three phases of the experiment: baseline, cold exposure, and 5-min post-cold. The results of the comparisons between each phase are given in Table 3. The cold exposure significantly reduced the skin and bone PPG signals right after the removal of the ice pack (post-cold). Both the skin and bone signal remained noticeably reduced 5 minutes after removal of the ice pack (5-min post-cold), but the reduction only remained significant for the skin signal. There was no significant difference in either PPG signal between the post-cold and 5-min post cold phases.

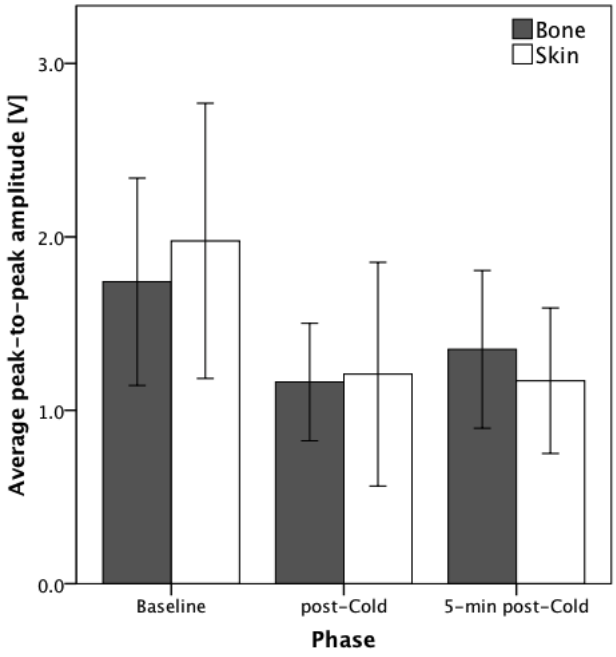

Figure 16 - PPG AC data from cold exposure experiment for both skin (white bars) and bone (dark bars) signals. Data are expressed as means ± 95% confidence intervals.

Table 3 - Treatment level comparisons for cold exposure experiment

Channel	Comparison	p-value		Bonferroni adjusted α
		t-test	*Wilcoxon signed ranks*	
Bone	baseline – cold	**0.005**	.	0.017
	cold – 5min post	0.299	.	0.017
	baseline – 5min post	0.037	.	0.017
Skin	baseline – cold	0.003	**0.011**	0.017
	cold – 5min post	0.901	0.953	0.017
	baseline – 5min post	**0.017**	.	0.017

The results from the control experiment are shown in Figure 17 for all three phases of the control experiment. Comparisons between the three phases are presented in Table 4. As can be seen in Figure 17, the PPG signals are similar throughout the three treatment levels and there are no significant differences in either PPG signal between any of the phases.

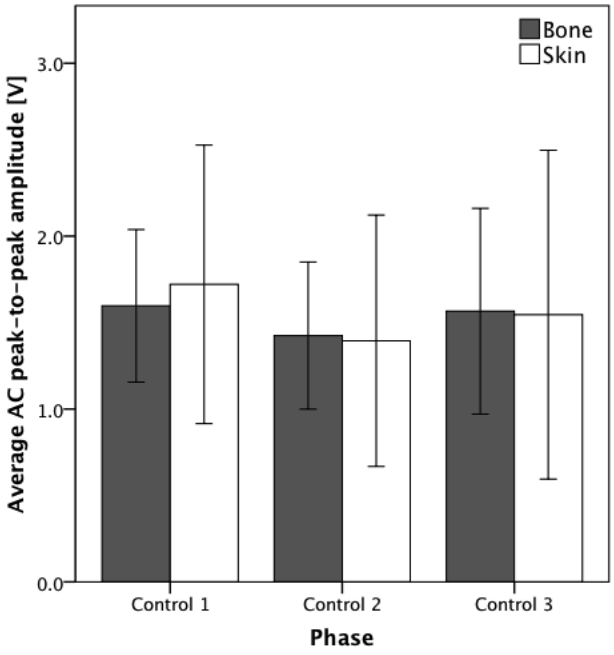

Figure 17 - PPG AC data from control experiment for both skin (white bars) and bone (dark bars) signals. Data are expressed as means ± 95% confidence intervals.

Table 4 - Treatment level comparisons for control experiment

Channel	Comparison	p-value		Bonferroni adjusted α
		t-test	*Wilcoxon signed ranks*	
Bone	control_1 – control_2	0.085	.	0.017
	control_2 – control_3	0.284	0.441	0.017
	control_1 – control_3	0.839	0.260	0.017
Skin	control_1 – control_2	0.045	0.038	0.017
	control_2 – control_3	0.242	0.441	0.017
	control_1 – control_3	0.348	0.374	0.017

4.1.3 Nitroglycerin Patch

The results from the nitroglycerin patch experiment are shown in Figure 18, expressed as changes from baseline. The results of comparisons between pre- and post-nitro exposure are shown in Table 5. The bone signal was not significantly different from baseline, but the skin signal showed a significant increase from baseline.

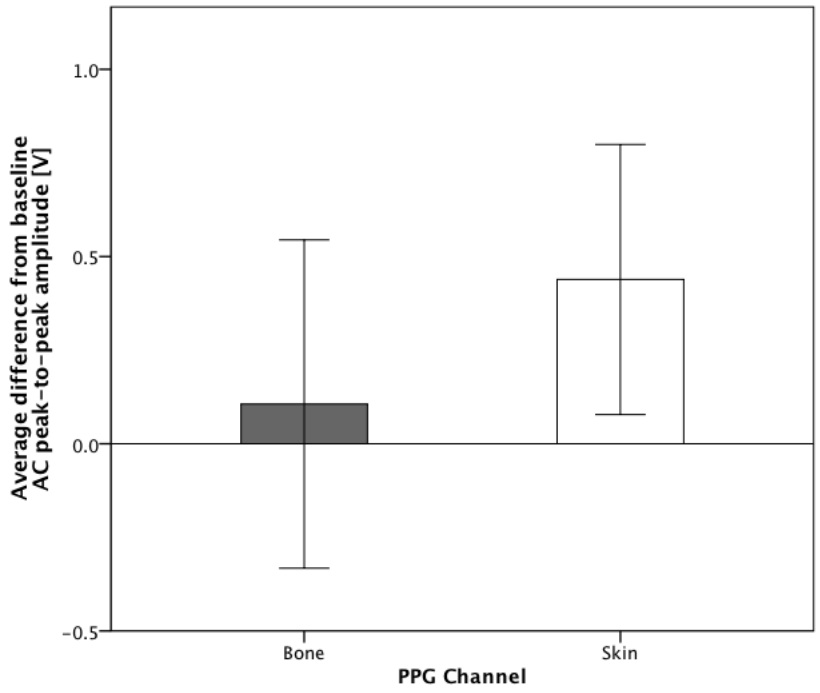

Figure 18 - PPG AC data from nitroglycerin patch experiment, data is shown as difference from baseline for both skin (white bar) and bone (dark bar) signals. Data are expressed as means ± 95% confidence intervals.

Table 5 - Treatment level comparisons for nitroglycerin patch experiment

Channel	Comparison	p-value		Bonferroni adjusted α
		t-test	*Wilcoxon signed ranks*	
Bone	pre – post	0.627	.	0.025
Skin	pre – post	**0.003**	.	0.025

4.1.4 Skin Occlusion

The results from the skin occlusion experiment are shown in Figure 19, for all three phases of the experiment: baseline, skin occlusion, and post-occlusion. The results of comparisons between the treatment levels are shown in Table 6. The skin signal was significantly different from both the baseline and post-occlusion phases. No other comparisons were significantly different.

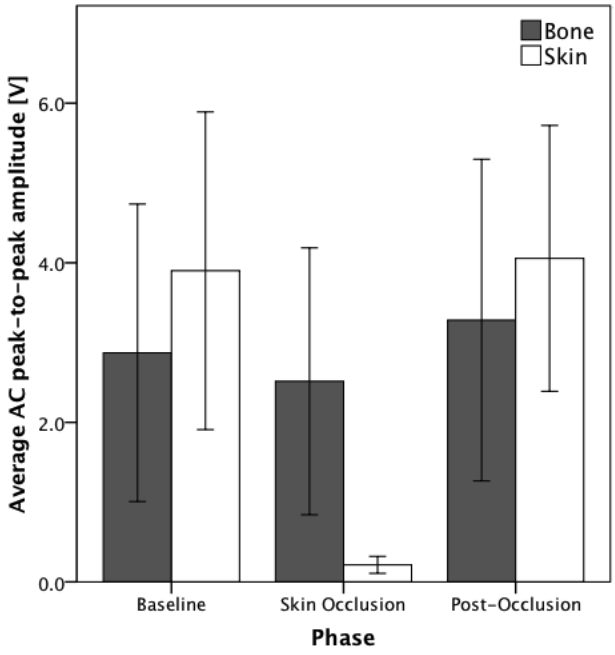

Figure 19 - PPG AC data from skin occlusion experiment for both skin (white bars) and bone (dark bars) signals. Data are expressed as means ± 95% confidence intervals.

Table 6 - Treatment level comparisons for skin occlusion experiment.

Channel	Comparison	p-value		Bonferroni adjusted α
		t-test	*Wilcoxon signed ranks*	
Bone	baseline – occlusion	0.161	0.173	0.017
	occlusion – post-occlusion	0.035	0.058	0.017
	baseline – post-occlusion	0.066	0.075	0.017
Skin	baseline – occlusion	**0.005**	.	0.017
	occlusion – post-occlusion	**0.002**	.	0.017
	baseline – post-occlusion	0.487	.	0.017

4.2 Pressure Experiments

Repeated measures analysis of variance (ANOVA) models were used to analyze the bone and skin PPG data separately. The only factor in the model was the pressure level (pressure difference between the inside and outside of the chamber), with 8 levels corresponding to each of the tested pressures (-50, -30, -15, -5, +5, +15, +30 and +50 mmHg). The dependant variable was either the skin or bone average AC peak-to-peak

amplitude, which was repeatedly measured on the same subject at each pressure level. All the data for each factor level was expressed as a difference from baseline as previously explained in section 3.4.4.

We did not expect to see changes in BP and HR at most pressure levels as the pressure differences and fluid shifts are not likely to be large enough to evoke these responses, except maybe at the more extreme pressures of +50 and -50 mmHg. The data sets at these two pressure levels were tested for normality using the Shapiro-Wilk test, and two-tailed paired t-tests were used to compare see if HR and BP were significantly different from baseline at either +50 and -50 mmHg.

4.2.1 PPG Data from Limb Inside the Chamber

The skin and bone PPG data for the leg inside the chamber are given in Figure 20. Both the skin and bone signals decrease at all the negative pressures, with greater decreases noted at the larger pressure differences. An increase in the bone signal is seen at positive pressures ranging from +5 to +30 mmHg and with a larger increase at the higher pressures. This trend is reversed at +50 mmHg, where the bone signal is markedly reduced and falls to levels below baseline. The skin signal follows a similar pattern at the positive pressures; it increases at the +5 and +15 mmHg levels, but begins to decrease at +30 mmHg and falls below baseline levels at +50 mmHg.

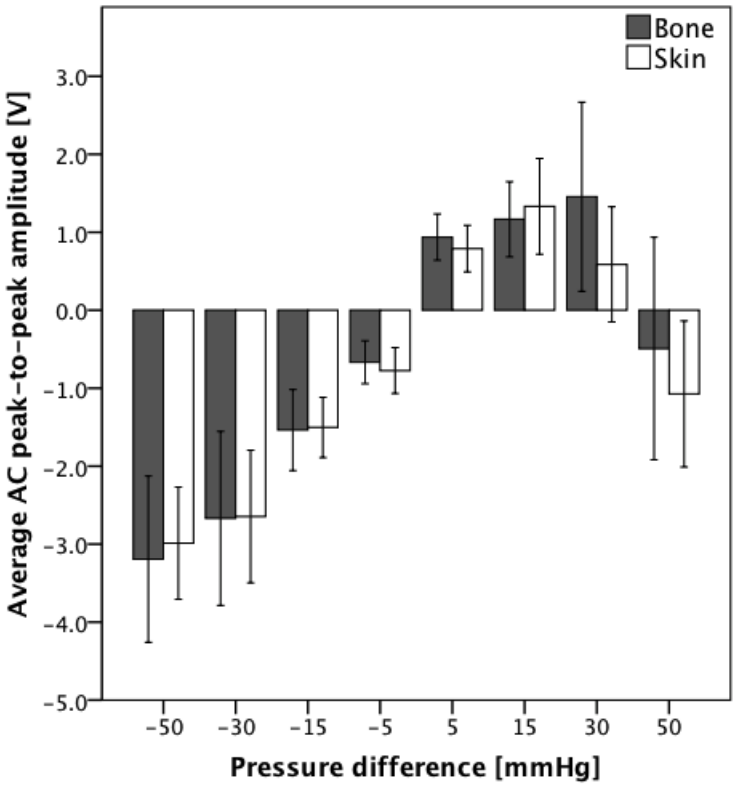

Figure 20 - PPG AC data from the pressure experiment for the leg inside the chamber for both skin (white bars) and bone (dark bars) signals. Data expressed as means and 95% confidence intervals.

A repeated measures ANOVA with a Greenhouse-Geisser correction indicates a significant difference in the bone PPG data between difference pressure levels ($F(2.59,28.03)=21.73$, $p<0.0005$). For the skin PPG data, a repeated measures ANOVA with a Greenhouse-Geisser correction also indicates a significant difference between the pressure levels ($F(2.97,71.89)=37.35$, $p<0.0005$). Both the skin and bone PPG signals vary significantly across the different pressure levels. Given the large differences from baseline illustrated by the means and confidence intervals in Figure 20, this is not surprising. A more comprehensive overview of the ANOVA model and results, including validity of required assumptions and analysis of residuals can be found in Appendix E.

4.2.2 PPG Data from Limb Outside the Chamber

The skin and bone PPG data for the leg outside the chamber are given in Figure 21. Both the bone and skin PPG signals in the limb outside the chamber are largely unaffected by the pressure inside the chamber. There is a trend that shows a decrease in

the bone and skin signal at +50 mmHg, however this is not a significant difference from baseline.

A repeated measures ANOVA with a Greenhouse-Geisser correction does not indicate a significant difference in the bone PPG data between difference pressure levels for the leg outside the chamber ($F(2.77,30.50)=0.96$, $p=0.418$). For the skin PPG data, a repeated measures ANOVA with a Greenhouse-Geisser correction also does not indicate a significant difference between the pressure levels ($F(2.97,32.65)=0.74$, $p=0.532$). Both the skin and bone PPG signals on the limb outside of the chamber are not significantly affected by the pressure changes inside the chamber at any of the pressure levels tested.

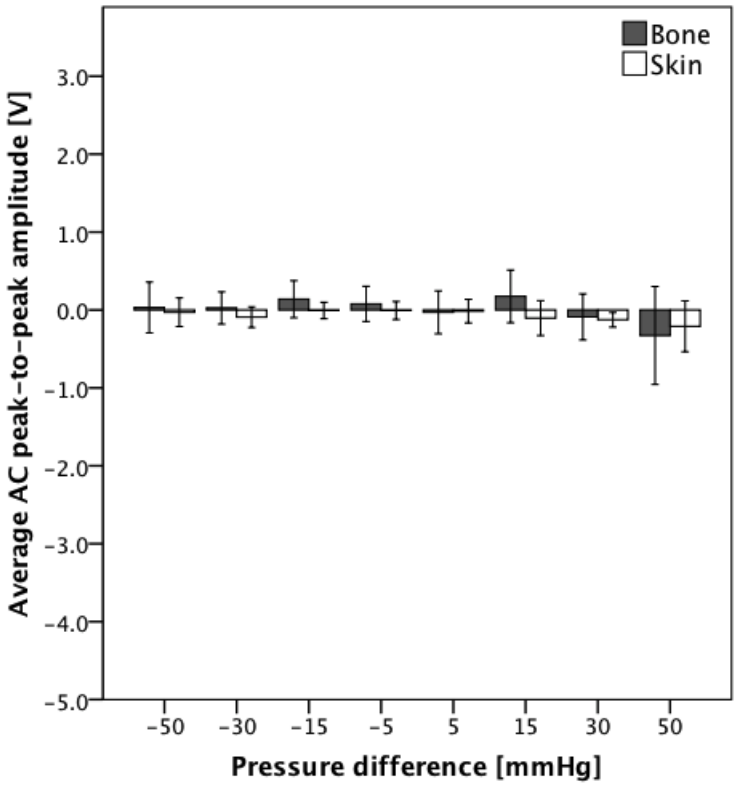

Figure 21 - PPG AC data from the pressure experiment for the leg inside the chamber for both skin (white bars) and bone (dark bars) signals. Data expressed as means and 95% confidence intervals.

4.2.3 Heart Rate and Blood Pressure Data

The BP data for the pressure experiment are shown in Figure 22, and the HR data are given in Figure 23. T-tests were used to compare the HR and BP data at +50 and -50 mmHg to the baseline levels. These results are summarized in Table 7 and Table 8 for

the BP and HR data, respectively. Detailed output from the normality tests and t-tests can be found in Appendix F.

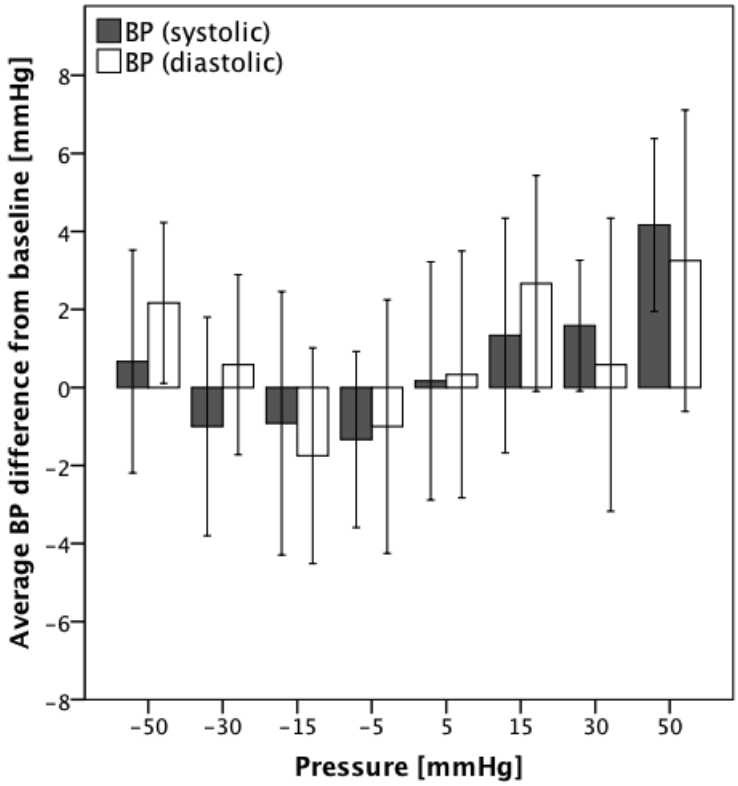

Figure 22 - Systolic (dark bars) and diastolic (white bars) BP data from the pressure experiment. Data expressed as means and 95% confidence intervals of differences from baseline.

Systolic blood pressure at +50 mmHg was significantly increased from baseline. There were no other significant differences in systolic or diastolic BP from baseline at any pressure level. However, as can be seen in Figure 22, there appears to be a trend of increased BP at the extreme pressures of +50 and -50 mmHg. Although the differences were not significant, diastolic BP appears to be elevated at these two extreme pressure levels.

Table 7 - BP comparisons between +50 and -50mmHg and baseline

BP	Comparison	p-value *t-test*	Bonferroni adjusted α
Systolic	-50mmHg – baseline	0.751	0.025
	+50mmHg – baseline	**0.007**	0.025
Diastolic	-50mmHg – baseline	0.041	0.025
	+50mmHg – baseline	0.194	0.025

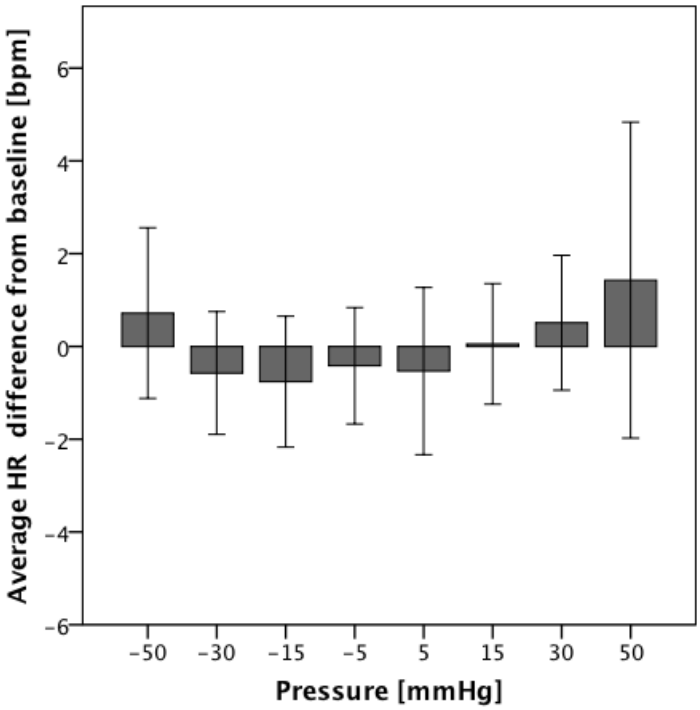

Figure 23 - HR data from the pressure experiment. Data expressed as means and 95% confidence intervals of differences from baseline.

The HR data were not significantly different from baseline at any of the pressure levels. However, similarly to the BP data, there is a trend that can be seen in Figure 23. At the extreme pressure levels of +50 and -50 mmHg, HR is higher than at the milder pressure differences, though these differences are not significantly different from baseline.

Table 8 - HR comparisons between +50 and -50mmHg and baseline

HR Comparison	p-value *t-test*	Bonferroni adjusted α
-50mmHg – baseline	0.408	0.025
+50mmHg – baseline	0.376	0.025

5.0 Discussion

5.1 Validating PPG for Bone Hemodynamic Measurements

The first aim of this thesis was to validate the use of PPG as a non-invasive bone hemodynamic measurement tool in the human tibia, and our hypothesis was that PPG is a valid method of measuring bone hemodynamic responses. The results from the various validation experiments are discussed below. They represent a strong argument for the validity of PPG as a method for bone hemodynamic measurements, supporting our original hypothesis.

5.1.1 Arterial Occlusion and Cold Exposure

In the arterial occlusion experiment, the pressure cuff around the thigh was inflated to 180 mmHg, which, in the supine position, should be enough to completely block the arterial inflow to the limb, and hence eliminate the AC component in the PPG signal in both skin and bone. As illustrated in Figure 15, both the skin and bone PPG signals decreased to effectively zero during the arterial occlusion and recovered to a level similar to baseline shortly after releasing the pressure in the cuff. This is in agreement with what we would expect, and indicates that reduction of blood flow to zero velocity is directly related to eliminating the pulsatile AC PPG signal and decreasing the peak-to-peak amplitude to essentially zero.

Another way to affect the local circulation is by exposure to cold, which causes vasoconstriction. While cold-induced vasoconstriction can reduce local blood flow and tissue perfusion, this stimulus is not as strong as arterial occlusion and is not likely to result in a complete cessation of blood flow. As shown in Figure 16, both skin and bone responded to the cold exposure with a reduction in their PPG signals. This decrease in the PPG signal was mostly maintained even after waiting 5 minutes post-cold exposure. However, at the 5 minutes post-cold exposure phase the bone signal was no longer significantly different from baseline. This likely represents the fact that the deeper tissue is capable of recovering from the cold exposure faster than the skin, which was in direct

contact with the ice-pack and thus was likely to have experienced a larger drop in temperature.

The mechanism causing this reduction in the PPG signal is different than in the arterial occlusion experiment. With arterial occlusion the PPG signal is reduced because the blood flow velocity is zero. In the cold exposure experiment we do not know how the local blood flow is being affected. We know that cold-induced vasoconstriction, which occurs primarily at the arteriole level, will reduce the local perfusion and increase the local resistance to flow. Hence, the PPG signal responds to both a decrease in blood flow velocity as well as to vasoconstriction.

5.1.2 PPG Measurement Repeatability (Control Experiment)

In order to perform the cold exposure experiment, the PPG probe had to be removed from the surface of the leg to allow for placing the ice pack on the surface of the limb. The probe had to then be placed back onto the same location to take the post-exposure measurements. This experimental set-up raises the question of the repeatability of the PPG measurements when the probe has to be removed and replaced. In our control experiment we tested the repeatability of the PPG measurements by removing the probe for short periods of time and then placing them back on the limb for subsequent measurements. The trends in Figure 17 show that the measurements across all three recordings are similar, and there are no significant differences between any of the recordings in either PPG signal as reported in Table 4. Nevertheless, we can expect that by removing and replacing the probes we will likely always introduce some added variability to the data. If the sample size and effect size of the stimulus that we are testing are large enough, we may still be able to obtain the desired results in spite of an increase in variability in the data. However, any experimental set-up that requires the PPG probes to be removed and replaced for a subsequent measurement is unlikely to be suitable for studying small effect sizes, in particular if the probe is removed for a long period of time.

5.1.3 Nitroglycerin Patch and Skin Occlusion

While the first few parts of the validation studies have shown that the PPG seems to respond as expected to various stimuli, in all of these experiments the bone and skin signal have followed similar trends. Since the PPG bone signal has to first penetrate through the skin layer in order to reach the deeper tissue, it is possible that the bone signal is also affected by changes in the skin circulation. In order to be able to claim that our device can independently and selectively respond to changes in skin and bone, further validation is required.

The purpose of the nitroglycerin experiment was to selectively stimulate the skin circulation without significantly affecting the bone response. Nitroglycerin is a known potent vasodilator, and a short exposure through a transdermal patch should affect the skin signal significantly. Arguably, prolonged exposure to the transdermal nitroglycerin patch (or exposure to much higher concentrations) would also eventually affect the bone signal. However, since the mode of drug delivery is through a transdermal patch, and since the exposure time is fairly short, we would expect the skin signal to be selectively more affected than the bone signal. Our results support this notion, as can be seen by the significant increase in the skin signal in response to the nitroglycerin exposure shown in Figure 18.

We have already shown that PPG can selectively respond to a change in the skin signal without registering a change in the bone signal. The purpose of the skin occlusion experiment was to measure the opposite response, a decrease in the skin signal without affecting the bone. Since there is only a thin layer of skin between the PPG probe and the tibia (and no muscle tissue), the blood in the skin circulation can effectively be squeezed out and blocked by applying sufficient pressure to the skin. By applying a pressure of 150 mmHg directly through the PPG probe head stage, we expect to eliminate the skin signal without significantly affecting the bone signal. Our results match our expectations as can been seen by the data in Figure 19, where the skin signal is almost entirely eliminated, yet the bone signal remains unaffected.

The results from the nitroglycerin and skin occlusion experiments show that changes in the skin circulation are appropriately detected by the skin channel and do not simultaneously affect the bone signal. This capability is essential in allowing us to

investigate the bone circulation and be able to claim that the bone response is not a byproduct of artefacts introduced by changes in the skin signal.

5.2 Response to Changes in External Pressure

The second aim of this thesis was to characterize the bone hemodynamic responses to single-limb exposure to changes in external pressure. We had hypothesized that exposure to negative pressures would result in vasoconstriction and positive pressures would result in vasodilation. The third aim was to investigate the contribution of various physiological mechanisms to the observed responses. We hypothesized that the myogenic effect was the predominant mechanism at pressures up to 30 mmHg above or below ambient, and that at larger pressure differences sympathetic mechanisms would also contribute to the vasomotor response.

The PPG data from both limbs together with the BP and HR data allow us to attribute the responses we have observed to various physiological mechanisms and to characterize the response at the different pressure levels.

5.2.1 Vasoconstrictive Response to Negative Pressures

At all of the negative pressure levels, we observed significant vasoconstriction in both the skin and bone signals for the leg inside the chamber. Even for levels as low as 5mm Hg below ambient pressure, vasoconstriction can be noted in both the skin and bone. At such low pressure differences it is likely that the sole mechanism responsible for this response is the myogenic effect. The decreased chamber pressure is transmitted through the tissue into the skin and down into the surface of the bone [133, 134]. This effectively increases the transmural pressure, which results in myogenic vasoconstriction [177]. The response at this pressure level is not likely to be due to changes in SNS tone or to mechanical compression of the limb. We can see from Figure 22 and Figure 23 that BP and HR, respectively, are unchanged from their baseline levels at this pressure difference. Similarly, the pressure applied to the limb through the pressure seal is not different from the pressure that the seal applies at baseline as explained and illustrated in Figure 27 in Appendix B, and therefore it is unlikely to be affecting the PPG data.

As the pressure difference increases and we progress to more negative pressures the myogenic effect is likely to be enhanced as the transmural pressure is further increased. However, at the more extreme negative pressures of -30 and -50 mmHg, other factors may also affect the PPG response. If the high-pressure baroreceptors were activated, we would expect to see a drop in systolic BP, increase in HR and vasoconstriction in the limb outside the chamber [81, 149]. The absence of all these other effects suggests that the high-pressure baroreceptors have not been activated.

Activation of low-pressure baroreceptors is not necessarily correlated with decreases in MAP or with changes in HR. However, we would expect them to be associated with increased vasoconstriction in the limb outside the chamber [221], which did not occur. At a pressure of -50 mmHg, the diastolic BP is noticeably, though not significantly, increased as can be seen in Figure 22. This trend of increased diastolic BP may represent the activation threshold for the low-pressure baroreceptors. The low-pressure baroreceptors reflex can affect the peripheral resistance and the venous tone. Based on the PPG data from the limb outside the chamber, we do not see any evidence that the peripheral resistance has been affected by any of the sympathetic reflexes. However, in response to the decreased CVP due to blood pooling in the limb at -50 mmHg, the low-pressure baroreceptor reflex may have responded by increasing the venous tone. An increase in venous tone would tend to sustain the filling pressure of the right heart, which would mitigate any drop in CO. Since HR remains relatively unchanged, the small drop in CO would be reflected in a reduced pulse pressure, which is evidenced by the unaltered systolic BP and increased diastolic BP. The increased diastolic BP is due, at least in part, to the myogenic-induced peripheral vasoconstriction in the limb inside the chamber.

In summary, the myogenic response is activated at the lowest negative pressure differences and appears to be the dominant mechanism that is causing the vasoconstrictive response. We hypothesized that vasoconstriction would be observed at all the negative pressures, and our data confirms this hypothesis. We had also hypothesized that there would be a larger contribution of sympathetic mechanisms at -50 mmHg, however, our data suggests that even at this pressure the myogenic effect is the

predominant mechanism and no large sympathetic reflexes have yet been activated, though the low-pressure baroreceptors appear to be just at their activation threshold.

5.2.2 Responses to Positive Pressures

The response to positive pressure can be characterized by an initial vasodilation at pressure levels up to +30 mmHg for bone and up to +15 mmHg for skin, followed by a reversal of the response that ends with skin and bone vasoconstriction at +50 mmHg. The myogenic response is likely the dominant mechanism responsible for the observed vasodilation. The increased pressure inside the chamber is also transmitted to the leg tissues, effectively decreasing the transmural pressure. The decrease in transmural pressure will trigger a myogenic response that will result in dilation of the blood vessels. At the pressure levels where vasodilation is observed, the systolic and diastolic BP, and HR as well as PPG signals from the limb outside the chamber remain unchanged from their baseline levels. This indicates that the high-pressure baroreceptors are not activated. The low-pressure baroreceptors are not necessarily correlated to changes in the BP and HR, but, if they were activated, we would also expect them to affect the PPG signal from the limb outside the chamber. The myogenic response appears to be the predominant mechanism responsible for the vasodilatory response seen at pressure levels up to +30 mmHg. (Note that while the SNS reflexes could contribute to an increase in SNS tone (vasoconstriction) during exposures to negative pressure as a result of the decreased CVP, they would be associated with decreases in SNS tone (vasodilation) during exposure to positive pressures due to the increase in CVP).

There is a noticeable change in the trend of the PPG data from the leg inside the chamber at +30 mmHg. Even though the PPG signals are, on average, above the baseline levels, the PPG skin signal is no longer significantly larger than the baseline value. As we move to the highest positive pressure level of +50 mmHg the skin signal decreases significantly from baseline, indicating vasoconstriction. The bone signal also indicates vasoconstriction, yet this is not a significant difference from baseline. The pattern of the response changes at the higher pressure levels of +30 and +50 mmHg, overriding the myogenic effect and resulting in vasoconstriction. At +50 mmHg we also observe a significant increase in the systolic BP, and a noticeable (yet not significant) increase in

HR. At this pressure, the PPG signal from the limb outside the chamber shows a trend of vasoconstriction, though this is not significantly different from baseline. If the baroreceptor reflexes were activated, we would expect to see vasodilation in the PPG signal and decreases in the HR and BP data, which is the opposite of what is observed at a pressure of +50 mmHg.

Several studies have suggested that the intramuscular pressure receptors are activated at pressures of about +30 mmHg [74, 76, 187]. The reversal in the PPG trend that is observed at +30 mmHg could be, at least in part, explained by the activation of the intramuscular pressure receptors. It has also previously been suggested that the intramuscular pressure receptors would increase the sympathetic tone and could override the baroreceptor reflexes, which would tend to inhibit the SNS tone at positive pressures. The activation of the intramuscular pressure receptors could also explain the increase in systolic BP, increase in HR and vasoconstriction in the PPG signals from both legs.

However, the magnitude of the vasoconstriction seen in the PPG signal from the limb inside the chamber is noticeably larger than the changes seen in the leg outside the chamber, as can be seen in Figure 20 and Figure 21. This result suggests that there may be another factor affecting the PPG data from the limb inside the chamber. At a chamber pressure level of +50 mmHg, the pressure seal exerts a pressure of between 21 to 46 mmHg onto the upper thigh (95% confidence interval based on the results from the Tekscan® experiment presented in Appendix B). At these pressure levels it is likely that the venous outflow is being compromised which would reduce the PPG signal in that leg. The greater levels of vasoconstriction observed in the limb inside the chamber at +50 mmHg is likely due to mechanical compression of the veins in the limb due to the high chamber pressure as well as the pressure of the seal around the thigh.

The confidence intervals at the +30 and +50 mmHg pressure levels are noticeably wider than at the other pressure levels as can be seen in Figure 20. Two factors likely contribute to this: 1) there may be some variability in the activation threshold of the intra-muscular pressure receptors across different individuals due to inherent physiological differences, and 2) at the high positive pressures some air was able to continuously leak past the pressure seal, and this leakage tended to be greater in subjects with skinnier legs.

Both of these factors may have contributed to an increased variance in the data at those pressure levels, as is evidenced by the larger confidence intervals.

The vasodilation seen at pressures up to +30 mmHg matches our original hypothesis. However, our hypothesis did not predict the trend towards vasoconstriction at +50 mmHg. We had also correctly hypothesized that the myogenic response would be dominant at pressure levels up to +30 mmHg, but we expected SNS reflexes to be an important mechanism at +50 mmHg. Instead, our data shows that at +50 mmHg the intramuscular pressure receptors and the possible mechanical compression of the limb through the pressure seal are two important mechanisms that appear to be more important than the SNS reflexes we anticipated.

Vasodilation and increased blood flow at mild positive pressures have been previously reported by several studies. In one study, increased forearm perfusion was observed at positive pressures, and blood flow increase was greatest at about +20 mmHg of compression [23]. Another study has reported improved sensitivity using Semmes-Weinstein monofilaments in the feet of both healthy and diabetic patients after 3 minutes of single-limb exposure to +30 mmHg of pressure [167]. The clinical benefits of positive pressure exposure have not yet been fully exploited, however, prior research on skin and muscle tissue has suggested that positive pressure exposure may have various clinical applications in the treatment of diabetic foot ulcers, venous insufficiency, deep-vein thrombosis, diabetic neuropathy among other pathologies [167]. Our results have shown that vasodilation also occurs in bone tissue in response to positive pressure exposure. This may have important clinical applications as a new therapy for aiding in fracture repair, osteoporosis and mitigating BMD loss both on Earth as well as during long-duration spaceflight.

5.2.3 Myogenic Effect in Bone

We have claimed that the myogenic effect is the predominant mechanism that is causing vasoconstriction at negative pressures and vasodilation at the positive pressures in both the skin and bone tissues. In skin and other soft tissues in which the external pressure changes are directly transmitted, the myogenic response can be readily evoked by altering the external pressure. However, the bone vasculature is encased in a bone

matrix that is mostly rigid. It seems unlikely that changes in external pressure are fully and directly altering the transmural pressure of the blood vessels inside the bone. Yet, it is possible that at least some of the pressure may be transmitted through the bone casing and to the vessels inside the bone, in particular through the trabecular parts of the skeleton, which are less rigid than cortical bone. However, the transmission of pressure through the bone to the inner bone tissue has not yet been measured.

We propose that the myogenic response in bone is a secondary effect to myogenic responses in the surrounding soft tissue. The following sequence of events, as described below and illustrated by the flowchart in Figure 24, is proposed as a possible explanation for the myogenic response observed in the bone:

1) Changes in external pressure (P_{out}) are transmitted through the soft tissues in the limb, thus reducing the transmural pressure and wall tension for the blood vessels in the skin and muscle tissue surrounding the tibia.
2) In response to the changes in transmural pressure and wall tension, the myogenic effect is triggered resulting in vasodilation of the blood vessels in the skin and muscle tissue but not in the osseous circulation.
3) The myogenic vasodilation results in a decrease in the blood pressure inside the skin and muscle blood vessels (P_v) that surround the bone, causing a drop in pressure in the arterial supply to the bone including the nutrient, epiphyseal and metaphyseal arteries.
4) The drop in pressure in the arterial supply to the bone (P_v) results in a decrease in the transmural pressure for the blood vessels inside the bone.
5) Finally, the drop in transmural pressure in the vessels inside the bone triggers a secondary myogenic response, which results in vasodilation of the blood vessels inside the bone.

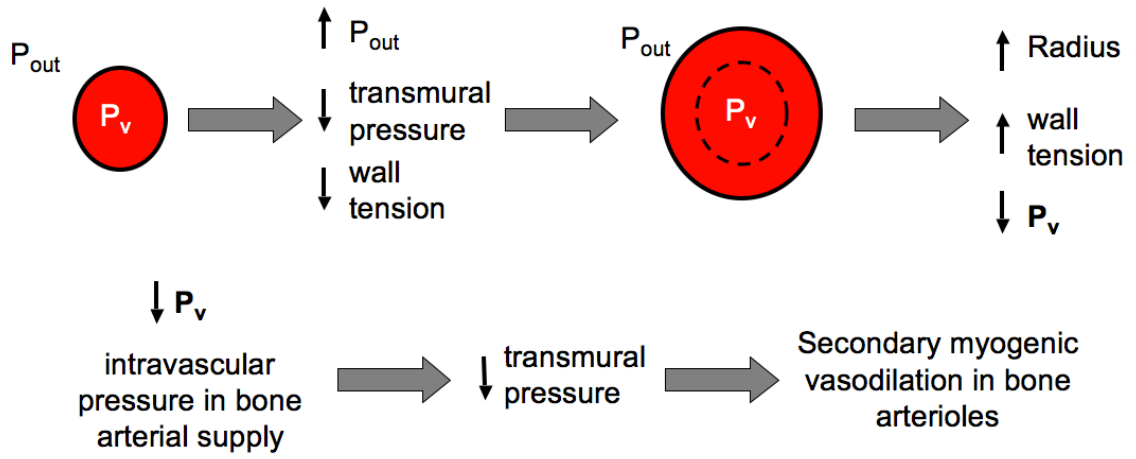

Figure 24 - Flowchart showing the hypothesized activation mechanism of the myogenic effect inside the bone

5.3 Interpreting the PPG Signal

We have previously noted that there is some inherent ambiguity in interpreting the PPG signal [3, 41]. The PPG AC signal responds to both a change in blood flow velocity (through changes in the red blood cell orientation) as well as to pulsatile blood volume changes as the blood vessel walls expand and contract. This means that a decrease in the PPG AC signal can be due to a decrease in the red blood cell velocity or to a contraction of the smooth muscle around the blood vessels which reduces the volumetric changes that it experiences throughout the cardiac cycle. While this ambiguity may seem like a severe limitation on the interpretability and usefulness of the PPG device, we propose a broader interpretation of the PPG signal that is clinically relevant and practical.

Microvascular perfusion of any tissue is dependant on both the amount of blood flow through the capillary bed, as well as the vasomotor tone of the blood vessels. If the blood vessels are fully dilated but the blood flow velocity is very low, the nutritional supply of the tissue may be compromised. Similarly, if the blood vessels are fully constricted but there is a moderate or high blood flow velocity (through arterial-venous anastomoses, or other paths) the nutritional supply of the tissue will again be compromised in the areas where there is no blood supply. If an increase in the PPG signal is noted it represents either an increase in the blood flow velocity or vasodilation of the tissue being sampled. In either case, the tissue perfusion is increased. The reverse

argument holds true, if the PPG signal decreases this may represent either vasoconstriction or a decrease in the blood flow velocity – both of which would represent a decrease in tissue perfusion. The distinction between these two effects is represented in our arterial occlusion and cold exposure experiments. In reality, for most practical situations, changes in the PPG signal are likely representative of simultaneous changes in blood flow velocity and in vasomotor tone. The main point is that the PPG signal can be thought of as a relative measure of changes in tissue perfusion.

5.4 Limitations

There are a few important limitations related to the PPG hardware that should be acknowledged. The biggest limitation of the PPG is that the data it produces are not expressed in a unit of measurement that is physiologically tangible, making direct interpretation of the data difficult, unless the data are expressed in relative terms. The only reliable data that can be obtained from the PPG, at least at the moment, are always expressed with reference to some baseline condition. In essence we can take a measurement, provide a stimulus and then take a subsequent measurement during or after the stimulus, and compare how the PPG signal changed from the reference condition. We cannot, however, provide a stimulus while taking a PPG measurement and then report those values as representative of the effect of that stimulus. The PPG hardware has to be calibrated before use by adjusting the intensity of the LED lights. This is necessary since people will have different skin and tissue properties, and there is not necessarily a single setting that will work all the subjects. These factors combined make it difficult to compare PPG data across groups of different subjects and also to compare PPG data from different experiments, in particular if there are differences in the PPG hardware such as the separation distance between the LED and photodetector, LED wavelengths, probe geometry, etc.

Long-term PPG studies are also difficult to perform reliably, since the baseline condition will change within the same subject over the course of a few hours or less. Therefore, the PPG device is unlikely to be useful if repeated measurements on the same subject are to be performed days or months apart. One possibility, however, is to develop

a stimulus that is representative of a characteristic that is being measured, and apply the same stimulus at each of the repeated measurements. For example, the degree of reactive hyperemia may be different in patients with diabetic neuropathy than in healthy controls. If a treatment was being tested on the diabetic patients the same stimulus could be applied to the patient at each of the measurement sessions (which could be months or years apart). There would be a PPG baseline and post-stimulus recording at each of the measurements sessions and long-term data could be compared by looking at the magnitudes of the changes from baseline across all the measurement sessions.

One further limitation is that PPG measurements cannot be performed when subjects are exercising or during muscular contraction. The PPG signal is sensitive to movement and vibrations, making most non-stationary measurements not reliable.

When considering the use of PPG for measurement of bone hemodynamics, it is important to understand that not all parts of the skeleton are suitable for PPG measurements. The penetration depth of the bone channel in our PPG probe is of about 13mm. This allows us to measure bone hemodynamics in certain areas such as the tibia, patella, calcaneus, and other bones that are close to the surface and have little or no muscle tissue in between the skin and the surface of the bone. Measurement of deeper tissues will always be limited to the penetration depth of the PPG signal. Furthermore, accurate estimation of penetration depth will likely require *in vivo* measurements of the signal penetration depth, which increases the cost and complexity of testing new probe designs.

We have described the mechanisms that are responsible for the hemodynamic responses that we have observed at the different pressure levels. However, it is important to note that even if separate experiments use the same pressure levels, these may not correspond directly to our pressure levels. The activation of the SNS reflexes is triggered by changing the CVP or the MAP enough for the baroreceptors to sense the change in pressure. Both the pressure difference that a subject is exposed to and the amount of tissue that is exposed to this pressure difference will determine how much fluid shift occurs and hence at what pressure level these reflexes are activated. For example, exposure of the entire lower body to LBNP is likely to evoke SNS reflexes at pressure differences that are much lower than the pressure required to evoke the same reflexes if

only a single limb or part of a limb is exposed to the pressure change. Yet it appears that some other mechanisms, such as the intramuscular pressure receptors, may be activated at the same pressure regardless of the surface area of the body that is exposed to the pressure difference. While this mechanism may be activated at the same pressure level, it may still produce effects of different magnitude that are a function of how much body tissue is exposed to the pressure difference.

Finally, there are a few other variables that would have been desirable to measure, which would help corroborate some of our findings. Muscle sympathetic nerve activity (MSNA) would have been a useful measurement that should be correlated to activation of the intramuscular pressure receptors as well as baroreceptor-induced SNS reflexes. Changes in CVP should also be associated with activation of the SNS reflexes, and would have been useful in confirming or denying the activation of these mechanisms. However, these measurements are invasive and often painful and thus may affect the results in themselves.

5.5 Summary of Contributions

The contributions from this thesis can be categorized into two groups: 1) engineering contributions and 2) physiological mechanisms and basic science. The main contributions in each category are listed below.

5.5.1 Engineering Contributions

- The further development and validation of the PPG device represents the state-of-the-art in deep tissue PPG measurement devices. It is a significant improvement over earlier implementations of deep-tissue PPG instrumentation [150, 174, 219].
- The validation studies have provided further evidence supporting the claim that PPG can be reliably used for bone measurements. Three specific contributions are particularly important:
    - The independence of the skin and bone signals has been demonstrated with the skin occlusion and nitroglycerin experiments.

- The skin occlusion experiment not only serves to illustrate the independence of the two signals, but it also shows that we are in fact measuring a PPG signal from the bone tissue.
- This is the first use of PPG for measurements on the human tibia; it builds upon and expands on previous bone PPG validation work in the patella [150].

- The flexible pressure seal has proven to be a reliable means of maintaining the pressure difference while little interference on the venous circulation at pressure differences from -50 mmHg to +30 mmHg.

5.5.2 Basic Science and Physiology Contributions

- The myogenic response has been shown to exist in the bone for the first time, adding to our understanding of the importance and relevance of the myogenic effect [10, 110].
- The bone hemodynamic response to changes in external pressure has also been characterized for the first time.
- The myogenic response has been shown to be the dominant effect regulating both bone and skin vasoconstriction at pressures up to -50 mmHg, and also regulating bone and skin vasodilation at pressures up to about +30 mmHg.
- The results provide further evidence that the intramuscular pressure receptors are activated at around +30 mmHg [74, 76, 187].

5.6 Future Research Directions

Understanding the mechanisms that regulate bone circulation is an important missing piece in our knowledge of integrated physiology. There are numerous pathologies where being able to increase or decrease bone perfusion may be beneficial. By understanding the mechanisms that regulate bone perfusion, we may be able to better develop the tools and approaches that can improve bone perfusion.

One potential application of PPG is in being able to measure the bone hemodynamic response to various pharmacological agents. A recent study has shown

that nitroglycerin may be beneficial to maintaining BMD in post-menopausal women [109]. By using the PPG, this area of research could be expanded by demonstrating the short-term influence of nitroglycerin on bone perfusion, which is thought to translate into long-term changes in BMD. While the current literature suggests that bone blood flow is responsible for the observed BMD changes, bone perfusion has not been directly measured in this context. PPG may be a valuable tool in better understanding the relationship between bone perfusion and long-term bone health and BMD changes.

The PPG hardware could be improved by incorporating several instruments together. Both NIRS and Doppler velocimetry instruments are based on very similar hardware components. The differences between these three techniques are primarily in the signal processing techniques. A new instrument could be developed that merges these three technologies and produces an output that contains the relative tissue O_2 saturation, the blood flow velocity (based on Doppler shifts) as well as the raw PPG signal from which the peak-to-peak amplitude, among other parameters, could be obtained. One of the advantages of this approach would be the simultaneous acquisition of multiple pieces of information from the same tissue. Among other things, the availability of blood flow information would allow for a better interpretation of the PPG AC signal as the contributions to the change in the peak-to-peak amplitudes from changes in vasomotor tone and from changes in red blood cell velocity could be quantified. This would result in much more specific information regarding the changes in tissue perfusion which may be of greater clinical utility. Furthermore, this instrument would facilitate the validation of the PPG signal, as it would be easier to compare the multiple facets of the data to data from other invasive and non-invasive hemodynamic measurements. A more comprehensive validation of the PPG signal is important if this technique is to be more widely adopted.

The cephalad fluid-shift and adaptive fluid volume changes that occur as a result of exposure to weightlessness has been hypothesized to be associated with the pattern of BMD loss in that is observed in human spaceflight. The large BMD losses in the weight-bearing parts of the skeleton and the lack of changes, or even slight increases, in BMD in the upper body and skull could be explained by the observed fluid shifts. Changes in bone perfusion could be measured at different locations throughout the upper and lower

body in weightlessness with PPG. If the pattern of changes in bone perfusion were to match the pattern of observed BMD losses, this would be an important piece of evidence that would allow us to better understand the relationship between fluid shift, bone perfusion and BMD changes. If the fluid shifts were indeed negatively affecting BMD, this would have strong implications in terms of suitable countermeasures to bone loss in long-duration human spaceflight. In particular, it would suggest that LBNP, artificial gravity (AG), or another countermeasure that directly affects the fluid distribution would be necessary.

6.0 Conclusion

The data from our validation studies support our original hypothesis that PPG can be used for bone hemodynamic measurements. Specifically, our skin occlusion experiment has provided us with compelling evidence that the deep tissue PPG signal is in fact representative of the bone circulation. The skin occlusion experiment together with the nitroglycerin study, have demonstrated the independence of the skin and bone signals. The bone signal is not significantly affected by changes in the skin circulation and each channel is representative of hemodynamic changes at different penetration depths.

While the response of muscle, skin and other tissues to changes in external pressure have been previously studied, we have provided the first description of the changes that occur in bone circulation in response to changes in external pressure. Furthermore, a basic understanding of the predominant control mechanisms affecting skin and bone circulation has also been reported. The myogenic response has, for the first time, been observed and measured in bone tissue. In our experimental set-up it has been the predominant mechanism responsible for vasoconstriction at negative pressures and also the predominant mechanism responsible for vasodilation at moderate positive pressures. Our data also support the hypothesis that intramuscular pressure receptors are activated at about +30 mmHg, as has previously been suggested by other studies [76, 187].

The availability of a novel and non-invasive tool to measure bone hemodynamic responses *in vivo* opens the door to many possible research opportunities. The bone response to new therapies and pharmacological agents can be tested, and new experiments may use this device to gain a better understanding of bone circulatory physiology. All of these research questions may lead to novel Earth-based applications. There are also possible spaceflight applications of this technology, as it may help to better understand the relationship between weightlessness-induced fluid shifts and BMD loss.

Appendix A: Consent Forms

Contents:

#100363: Non-Invasive Measurements of Bone Blood Flow (3 pages)

#100741: Bone Blood Flow Responses to Changes in External Pressure (3 pages)

UNIVERSITY OF CALIFORNIA, SAN DIEGO
CONSENT TO ACT AS A RESEARCH SUBJECT

NON-INVASIVE MEASUREMENTS OF BONE BLOOD FLOW

Alan R. Hargens, PhD and co-workers are conducting a research study to investigate the use of non-invasive blood flow measurement techniques to measure blood flow in bones. This research project is being done at the University of California – San Diego, in collaboration with the Massachusetts Institute of Technology – Cambridge, MA. Adequate bone blood flow is important for maintaining bone health, and inadequate blood supply to the bones is associated with numerous bone pathologies such as osteoporosis. The capability to non-invasively measure bone blood flow may have important clinical applications in the assessment of bone health, and in facilitating bone blood flow research.

You have been asked to participate in this study because you are a healthy volunteer above the age of 18. There will be approximately 20 subjects, both male and female, participating in the study. The purpose of this study is to assess the use of non-invasive optical techniques to measure blood flow in the bones.

If you agree to be in this study, the following will happen to you:

1. Non-invasive skin and deep tissue blood flow measurements will be taken with either a photoplethysmography (PPG) or near-infrared spectroscopy (NIRS) measurement system. This requires the placement of small flat probes along the surface of your skin. These probes are completely external and placed only on the surface of your skin in either your arms or legs. The probes may be attached to your skin by using medical tape to hold them in place. A loose band will be wrapped around the probe and limb in order to isolate the probe from external light sources, which could affect the measurements. This part of the experiment will take about 5 minutes.
2. Blood flow measurements will be taken before, during and after the various experimental conditions described below:
    a. Pressure of 100mmHg will be applied to the probe in order to compress the skin underneath the probe. This pressure will only be sustained for a maximum of 5 minutes.
    b. A blood pressure cuff will be placed around your thigh and inflated to a maximum of 200mmHg for a maximum of 2 minutes.
    c. A nitroglycerin patch (0.1mg/hr) will be placed on the skin of your leg in the same place where the probes will be taking measurements for 15 minutes.
3. The overall time duration of the experiment will be a maximum of 2 hours. This includes the required time to set-up and calibrate the instruments, as well as time taken to explain the experiment, answer any questions and obtain informed consent.

Participation in this study may involve some added risks or discomforts. These include:

1. Discomfort from the application of 100mmHg of pressure through the probe or from the inflation of the thigh pressure cuff to 200mmHg. Since the applied pressures are only sustained for a short period of time, there is no significant risk of long term damage to the muscle and skin tissue due to lack of blood supply. In the case of severe discomfort or pain,

the application of pressure can be ceased immediately. The subject will be asked to immediately report any pain or discomfort experienced during the experiment.

2. Nitroglycerin is a commonly used cardiac medication. There is a small risk of side effects from the nitroglycerin patch. The most common side effect is a headache. It is also possible that you may feel light-headed, dizziness or in some cases faint. However, these side effects are very uncommon. They are even less likely to occur since the patch is of a low dosage and it is only applied for 15 minutes; in contrast to an exposure of 12 hours, which would be a typical clinical prescription. If you have taken Viagra, Cialis or other similar medication in the past 24 hours, you should not participate in this part of the experiment. If you have an abnormally high or low blood pressure, you will not be allowed to participate in this part of the experiment.
3. Since we will be collecting information on any relevant medical conditions, there is the potential risk of loss of confidentiality.

Because this is a research study, there may be some unknown risks that are currently unforeseeable. You will be informed of any significant new findings.

There is no anticipated direct benefit to you from these procedures. However, knowledge gained through this study may have important clinical applications that could help patients suffering from numerous bone and cardiovascular pathologies. New findings will be available at your request and can be obtained by calling Dr. Hargens at (619) 543-6805.

Participation in this study is entirely voluntary. You may refuse to participate or withdraw at any time without penalty or loss of benefits to which you are entitled.

You may be withdrawn from the study if you do not follow the instructions given you by the study personnel.

You will be told if any important new information is found during the course of this study that may affect your wanting to continue.

Participation in this study is entirely voluntary and you will not be paid. There will be no cost to you for participating in this study.

If you are injured as a direct result of participation in this research, the University of California will provide any medical care you need to treat those injuries. The University will not provide any other form of compensation to you if you are injured. You may call the Human Research Protections Program Office at (858) 455-5050 for more information about this, to inquire about your rights as a research subject or to report research-related problems. If you have questions regarding your rights as a research subject or want to report research-related problems, you may also contact MIT's Committee on the Use of Humans as Experimental Subjects, at (617) 253-6787.

Research records will be kept confidential to the extent allowed by law. Any data from this study that may be published in scientific journals will be anonymous and will not reveal your identity. The collected data will be coded by replacing the subject's name with a numerical identifier, in order to protect the subject's identity and prevent loss of confidentiality. Written records will be kept inside a locked cabinet at the Clinical Physiology Lab, where the experiments will take place. Only the research staff involved in the project will have access to the records. Research records may be reviewed by the UCSD Institutional Review Board and federal regulatory agencies, as required.

Alan R. Hargens, PhD, and/or Jaime Mateus has explained this study to you and answered your questions. If you have other questions or research-related problems, you may reach Jaime Mateus at (617) 308-0652 or Alan Hargens at (619) 543-6805.

You have received a copy of this consent document and a copy of the "Experimental Subject's Bill of Rights" to keep.

You agree to participate.

_____	_____	_____
Subject's signature	Subject's printed name	Date
_____	_____	_____
Witness' signature	Witness' printed name	Date

UNIVERSITY OF CALIFORNIA, SAN DIEGO
CONSENT TO ACT AS A RESEARCH SUBJECT

BONE BLOOD FLOW RESPONSES TO CHANGES IN EXTERNAL PRESSURE

Alan R. Hargens, PhD and co-workers are conducting a research study to investigate the use of non-invasive blood flow measurement techniques to measure blood flow in bones during changes in externally applied pressure. This research project is being done at the University of California – San Diego, in collaboration with the Massachusetts Institute of Technology – Cambridge, MA. Adequate bone blood flow is important for maintaining bone health, and inadequate blood supply to the bones is associated with numerous bone diseases such as osteoporosis. The capability to non-invasively measure and affect bone blood flow may have important clinical applications in the assessment of bone health, and in facilitating bone blood flow research.

You have been asked to participate in this study because you are a healthy volunteer with an age of 18 or above. There will be approximately 20 subjects, both male and female, participating in the study. The purpose of this study is to investigate the effect of changes in external pressure on bone blood flow and oxygenation.

If you agree to be in this study, the following will happen to you:

1. The thickness of the skin on the front and inside part of your lower legs will be measured non-invasively using a skin fold thickness device. The skin fold thickness device is a mechanical device that measures the distance between the two tips of the instrument. In order to measure the skin thickness, the skin needs to be "pinched" so that a small section of the skin can be placed between the two tips of the instrument. This part of the experiment takes about 5 minutes.
2. Non-invasive skin and bone blood flow measurements will be taken using a photoplethysmography (PPG) probe. Tissue blood oxygenation will also be measured non-invasively using a near infrared spectroscopy instrument (NIRS). Both instruments are completely non-invasive, and do not cause any harm or discomfort. The PPG and NIRS probes rely on similar technology that uses a light source to illuminate the skin. The emitted light is absorbed, scattered, and a small part is reflected back onto the probe. The reflected light is sensed by a photodetector on the probe, which measures the intensity of the reflected light. Changes in the light intensity are directly related to the changes in blood volume and blood flow underneath the skin. The main difference between the PPG and NIRS probes is how the signal is processed by a computer. The PPG signal is minimally processed and gives us information on blood flow and volume. The NIRS probe has a more complex computer program to estimate the amount of oxygen being carried by the blood to your leg tissues. The probes will be placed flat along the surface of your skin. We will use medical tape and a loose band wrapped around your limb to secure the probes in place and to block room light from reaching the probes, as this could affect the measurements. Time for setting up the measurement equipment including calibrating the hardware takes about 10 minutes.

3. Blood flow measurements will be taken before, during and after exposure to different pressure levels. A single leg will be placed inside a pressure chamber that allows us to change the pressure around the limb while not affecting the pressure that the rest of your body is exposed to. A flexible seal around your thigh maintains the pressure difference between the inside and outside of the chamber. Measurements will be taken at various pressure levels in increments of 5 or 10 mmHg to a maximum pressure difference of 60mmHg either above or below room pressure. (A pressure difference of 60 mmHg is about half of what a normal blood pressure cuff would be inflated to when taking a blood pressure measurement on the arm). This part of the experiment takes approximately 1.5 hours.
4. The overall time duration of the experiment should not exceed 2 hours. This includes the time taken to explain the experiment, answer any questions and obtain informed consent as well as the time required to set-up the instruments and collect the data.

Participation in this study may involve some added risks or discomforts. These include:

1. Discomfort associated with pinching the skin in order to use the skin fold thickness device. This will be a momentary discomfort resulting in a similar sensation to pinching of the skin that will not cause any long-lasting sensation.
2. Exposure to some of the larger pressure differences may cause some mild discomfort. However, the magnitude and duration of the pressure exposures is not high enough to cause any significant problems such as severely impairing the blood flow to the limbs or a large reduction in blood pressure that could cause fainting. These conditions are only likely to occur with more extreme pressure exposures that are of a longer duration.
3. The pressure seal around the thigh is designed to be tight enough to maintain the pressure difference while not impeding venous blood flow or causing significant discomfort. The pressure seal may result in mild discomfort around the thigh.
4. Since we will be collecting information on your relevant medical conditions, there is the potential risk of loss of confidentiality.

Because this is a research study, there may be some unknown risks that are currently unforeseeable. You will be informed of any significant new findings.

There is no anticipated direct benefit to you from these procedures. However, knowledge gained through this study may have important clinical applications that could help patients suffering from bone and circulatory diseases. New findings will be available at your request and can be obtained by calling Dr. Hargens at (619) 543-6805.

Participation in this study is entirely voluntary. You may refuse to participate or withdraw at any time without penalty or loss of benefits to which you are entitled.

You may be withdrawn from the study if you do not follow the instructions given you by the study personnel.

You will be told if any important new information is found during the course of this study that may affect your wanting to continue.

Participation in this study is entirely voluntary and you will not be paid. There will be no cost to you for participating in this study.

If you are injured as a direct result of participation in this research, the University of California will provide any medical care you need to treat those injuries. The University will not provide any other form of compensation to you if you are injured. You may call the Human Research Protections Program Office at (858) 455-5050 for more information about this, to inquire about your rights as a research subject or to report research-related problems. If you have questions regarding your rights as a research subject or want to report research-related problems, you may also contact MIT's Committee on the Use of Humans as Experimental Subjects at (617) 253-6787.

Research records will be kept confidential to the extent allowed by law. Any data from this study that may be published in scientific journals will be anonymous and will not reveal your identity. The collected data will be coded by replacing the subject's name with a numerical identifier, in order to protect the subject's identity and prevent loss of confidentiality. Written records will be kept inside a locked cabinet at the Clinical Physiology Lab, where the experiments will take place. Only the research staff involved in the project will have access to the records. Research records may be reviewed by the UCSD Institutional Review Board and federal regulatory agencies, as required.

Alan R. Hargens, PhD, and/or Jaime Mateus has explained this study to you and answered your questions. If you have other questions or research-related problems, you may reach Jaime Mateus at (619) 543-7441 or Alan Hargens at (619) 543-6805.

You have received a copy of this consent document and a copy of the "Experimental Subject's Bill of Rights" to keep.

You agree to participate.

_____	_____	_____
Subject's signature	Subject's printed name	Date
_____	_____	_____
Witness' signature	Witness' printed name	Date

Appendix B: Tekscan® Pressure Seal Pilot Study

In any of the pressure chamber experiments an effective pressure seal is required to maintain the pressure difference between the inside and the outside of the chamber. A key design consideration is that the pressure seal has to be just tight enough to be able to maintain the pressure difference but, ideally, no tighter. If the pressure seal is too tight it will significantly interfere with the circulation to and from the limb and will become a confounding factor that limits our interpretation of the results. The purpose of the Tekscan® study was to measure the pressure transmitted to the skin by the pressure seal over the range of chamber operating pressures that we are concerned with.

In order to perform this study we placed a Tekscan® pressure sensor along the lateral side of the upper leg as can be seen in Figure 25, and in Figure 26 where the rest of the experimental set-up can also be seen. The sensor placement covered most of the length of the leg that was in contact with the pressure seal distally from just above the knee to proximally at the upper thigh.

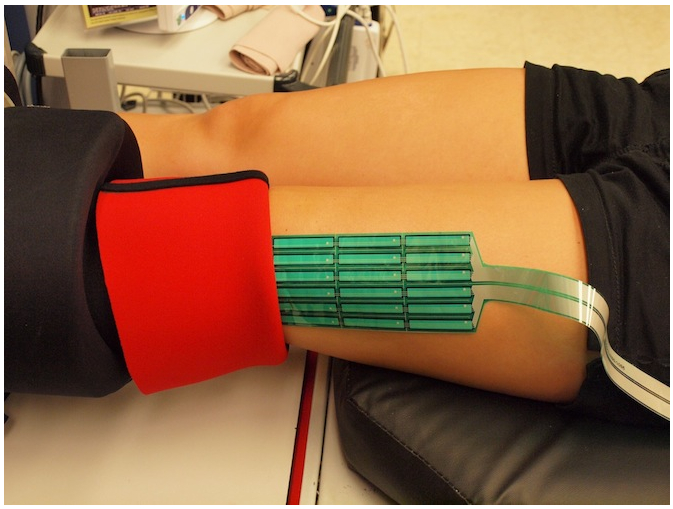

Figure 25 - Tekscan® pressure sensor placement with retracted pressure seal

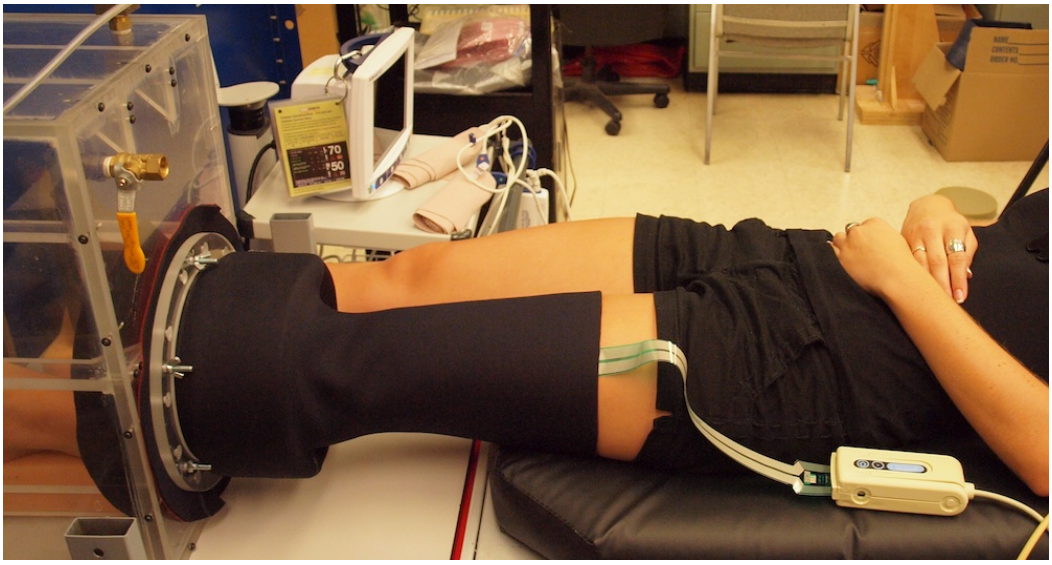

Figure 26 - Tekscan® pressure experiment set-up

Similarly to all the pressure chamber experiments, a wide pressure cuff was placed over the outside of the pressure seal and inflated to match the chamber pressure at all the positive pressure levels. The pressure cuff is not needed at the negative pressures since the friction of the pressure seal against the leg is enough to keep the pressure seal in place. As in all the pressure experiments, the subjects lay supine for the duration of this experiment. Subjects were exposed to pressures of 10, 20, 30, 40 and 50 mmHg above and below ambient. The subject was exposed to all the pressures sequentially from lowest to highest pressure differences for both negative and positive pressures. Subjects were randomly assigned to start with either the negative pressures or the positive pressures. The experiment started with a baseline recording at 0 mmHg and then proceeded sequentially to the higher pressure levels. A total of 6 subjects participated in this experiment.

Data was recorded for 20 frames using the Tekscan® software at each of the pressure levels. The Tekscan® software was used to process the data. First, any pressure cells that did not record any load were excluded from the calculations in order not to bias the data. (One of the pressure cells was damaged and did not record a load at any of the pressure levels). The 20-frame recording was averaged over time and saved as a single frame with average pressures over every cell. This data was input into an excel spreadsheet, which was used to calculate and average pressure for each subject at each

pressure level. From this data average and 95% confidence intervals for the pressure transmitted to the skin were computed, and these are presented in Figure 27 and Table 9.

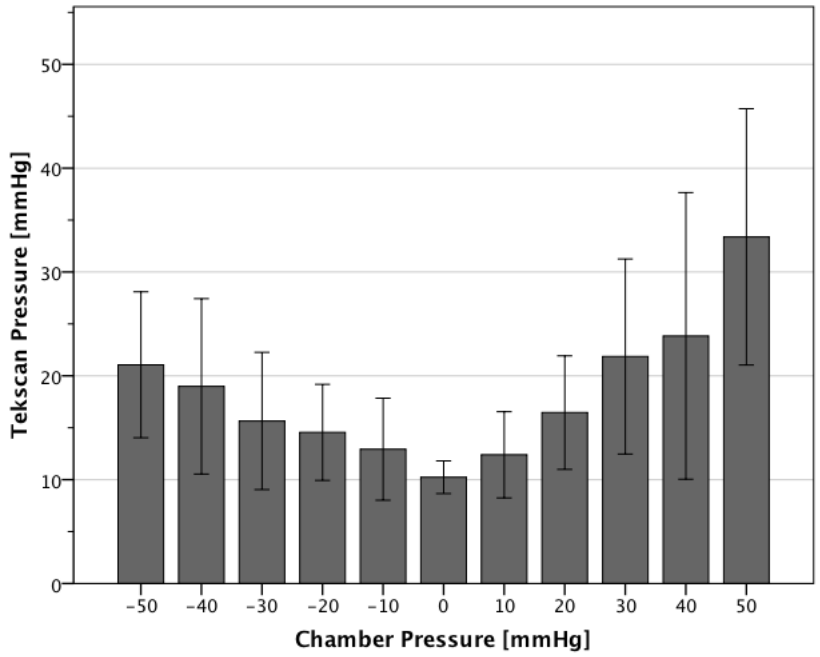

Figure 27 - Pressure transmitted to limb through pressure seal. Data expressed as means and 95% confidence intervals.

Note that the sample size is 12 for the 0 mmHg data point, since we averaged the baseline measurement from the positive and negative pressure sequences. We also had an outlier data point at +40mmHg for one subject, which was excluded from the calculations. This data point was anomalous because there was a lot of leakage through the pressure seal for this particular subject at that pressure (due to the subject having very skinny legs), therefore resulting in an abnormally low pressure value being recorded by the Tekscan® pressure sensor.

Table 9 - 95% confidence interval for seal pressures

Chamber Pressure [mmHg]	n	Average [mmHg]	95% confidence interval [mmHg]	
			lower	upper
-50	6	21.06	14	28
-40	6	18.99	11	27
-30	6	15.65	9	22
-20	6	14.55	10	19
-10	6	12.94	8	18
0	12	10.23	9	12
10	6	12.40	8	17
20	6	16.46	11	22
30	6	21.86	12	31
40	5	23.84	10	38
50	6	33.38	21	46

Appendix C: Normality Test Results from Validation Experiments

The Shapiro-Wilk test was used to test for normality in the various validation experiments. Tables with the outcome of these tests are given below for each of the validation experiments. The null hypothesis is that the data comes from a normal distribution, and the alternate hypothesis is that the data is not normally distributed. The Kolmogorov-Smirnov test (with Lilliefors significance correction) is also given alongside with the Shapiro-Wilk results. However, the Shapiro-Wilk test is more appropriate for situations with relatively small sample sizes with n<50, as is the case in all of our validation studies [181, 182]. Significance is set at 0.05 for all tests.

Arterial Occlusion Experiment

Table 10 - Normality tests for arterial occlusion experiment. [a]Lilliefors significance correction. *lower bound of the true significance

	Kolmogorov-Smirnov[a]			Shapiro-Wilk		
	Statistic	df	Sig.	Statistic	df	Sig.
AC_red_baseline	.162	9	.200*	.985	9	.986
AC_red_180	.246	9	.124	.824	9	.038
AC_red_recover	.179	9	.200*	.929	9	.468
AC_green_baseline	.251	9	.107	.856	9	.087
AC_green_180	.367	9	.001	.706	9	.002
AC_green_recover	.205	9	.200*	.895	9	.226

Cold Exposure and Control Experiments

Table 11 - Normality tests for cold exposure experiment. [a]Lilliefors significance correction. *lower bound of the true significance

	Kolmogorov-Smirnov[a]			Shapiro-Wilk		
	Statistic	df	Sig.	Statistic	df	Sig.
AC_red_baseline	.201	9	.200*	.925	9	.432
AC_red_cold	.268	9	.062	.843	9	.063
AC_red_recover	.160	9	.200*	.919	9	.381
AC_green_baseline	.173	9	.200*	.922	9	.413
AC_green_cold	.295	9	.023	.805	9	.023
AC_green_recover	.183	9	.200*	.911	9	.321

Table 12 - Normality tests for control experiment. [a]Lilliefors significance correction. *lower bound of the true significance

	Kolmogorov-Smirnov[a]			Shapiro-Wilk		
	Statistic	df	Sig.	Statistic	df	Sig.
AC_red_baseline	.203	9	.200*	.939	9	.573
AC_red_control	.136	9	.200*	.960	9	.798
AC_red_recover	.282	9	.037	.831	9	.046
AC_green_baseline	.184	9	.200*	.906	9	.286
AC_green_control	.299	9	.020	.809	9	.026
AC_green_recover	.238	9	.148	.785	9	.014

Nitroglycerin Experiment

Table 13 - Normality tests for nitroglycerin patch experiment. [a]Lilliefors significance correction. *lower bound of the true significance

	Kolmogorov-Smirnov[a]			Shapiro-Wilk		
	Statistic	df	Sig.	Statistic	df	Sig.
AC_red_baseline	.354	5	.040	.792	5	.069
AC_red_nitro	.323	5	.096	.816	5	.109
AC_green_baseline	.176	5	.200*	.964	5	.836
AC_green_nitro	.216	5	.200*	.935	5	.632

Skin Occlusion Experiment

Table 14 - Normality tests for skin occlusion experiment. [a]Lilliefors significance correction. *lower bound of the true significance

	Kolmogorov-Smirnov[a]			Shapiro-Wilk		
	Statistic	df	Sig.	Statistic	df	Sig.
AC_red_base	.381	6	.007	.635	6	.001
AC_red_occ	.410	6	.002	.654	6	.002
AC_red_rec	.387	6	.005	.747	6	.019
AC_green_base	.226	6	.200*	.939	6	.648
AC_green_occ	.186	6	.200*	.973	6	.910
AC_green_rec	.188	6	.200*	.978	6	.942

Appendix D: Paired T-Test Results from Validation Experiments

Two-tailed paired t-tests were used to compare all of the treatment levels to each other for each of the validation studies. T-tests were performed separately for the skin and bone signals. The detailed output for all the comparisons is given in the following tables for each of the experiments in the validation study. In all cases, the null hypothesis is that there is no difference between the sample means, and the alternate hypothesis is that there is a difference between the sample means. Significance is set at 0.05 for all comparisons.

Arterial Occlusion

Table 15 - Paired two-tailed t-test for arterial occlusion PPG AC data

		Paired Differences					t	df	p-value
					95% Confidence Interval of the Difference				
		Mean	Std. Deviation	Std. Error Mean	Lower	Upper			
Pair 1	AC_red_baseline - AC_red_180	1.38	.70	.23	.84	1.92	5.91	8	.000
Pair 2	AC_red_180 - AC_red_recover	-1.51	.72	.24	-2.06	-.95	-6.24	8	.000
Pair 3	AC_red_baseline - AC_red_recover	-.12	.54	.18	-.54	.29	-.68	8	.516
Pair 4	AC_green_baseline - AC_green_180	1.42	.80	.27	.80	2.03	5.29	8	.001
Pair 5	AC_green_180 - AC_green_recover	-1.53	.96	.32	-2.27	-.79	-4.79	8	.001
Pair 6	AC_green_baseline - AC_green_recover	-.12	.36	.12	-.39	.16	-.96	8	.367

Cold Exposure and Control Experiments

Table 16 - Paired two-tailed t-test for cold exposure PPG AC data

		Paired Differences					t	df	p-value
		Mean	Std. Deviation	Std. Error Mean	95% Confidence Interval of the Difference Lower	Upper			
Pair 1	AC_red_baseline – AC_red_cold	.578	.451	.150	.232	.925	3.850	8	.005
Pair 2	AC_red_cold – AC_red_recover	-.18	.510	.170	-.580	.203	-1.110	8	.299
Pair 3	AC_red_baseline – AC_red_recover	.390	.467	.156	.031	.749	2.502	8	.037
Pair 4	AC_green_baseline – AC_green_cold	.769	.533	.178	.359	1.179	4.323	8	.003
Pair 5	AC_green_cold – AC_green_recover	.038	.891	.297	-.647	.723	.128	8	.901
Pair 6	AC_green_baseline – AC_green_recover	.807	.803	.268	.190	1.424	3.016	8	.017

Table 17 - Paired two-tailed t-test for control experiment PPG AC data

		Paired Differences					t	df	p-value
		Mean	Std. Deviation	Std. Error Mean	95% Confidence Interval of the Difference Lower	Upper			
Pair 1	AC_red_baseline – AC_red_control	.172	.262	.087	-.030	.374	1.968	8	.085
Pair 2	AC_red_control – AC_red_recover	-.141	.369	.123	-.425	.142	-1.148	8	.284
Pair 3	AC_red_baseline – AC_red_recover	.031	.439	.146	-.307	.369	.210	8	.839
Pair 4	AC_green_baseline – AC_green_control	.327	.414	.138	.008	.645	2.367	8	.045
Pair 5	AC_green_control – AC_green_recover	-.151	.359	.120	-.427	.125	-1.263	8	.242
Pair 6	AC_green_baseline – AC_green_recover	.175	.528	.176	-.231	.582	.996	8	.348

Nitroglycerin Experiment

Table 18 - Paired two-tailed t-test for nitroglycerin patch experiment PPG AC data

		Paired Differences					t	df	p-value
		Mean	Std. Deviation	Std. Error Mean	95% Confidence Interval of the Difference Lower	Upper			
Pair 1	AC_red_baseline – AC_red_nitro	-.21	.904	.404	-1.335	.910	-.525	4	.627
Pair 2	AC_green_baseline – AC_green_nitro	-.87	.301	.135	-1.252	-.503	-6.50	4	.003

Skin Occlusion Experiment

Table 19 - Paired two-tailed t-test for skin occlusion experiment PPG AC data

		Paired Differences					t	df	p-value
		Mean	Std. Deviation	Std. Error Mean	95% Confidence Interval of the Difference Lower	Upper			
Pair 1	AC_red_base - AC_red_occ	.355	.529	.216	-.200	.910	1.645	5	.161
Pair 2	AC_red_occ - AC_red_rec	-.766	.654	.267	-1.453	-.079	-2.867	5	.035
Pair 3	AC_red_base - AC_red_rec	-.411	.429	.175	-.861	.039	-2.346	5	.066
Pair 4	AC_green_base - AC_green_occ	3.687	1.862	.760	1.733	5.642	4.849	5	.005
Pair 5	AC_green_occ - AC_green_rec	-3.84	1.535	.627	-5.454	-2.232	-6.132	5	.002
Pair 6	AC_green_base - AC_green_rec	-.156	.509	.208	-.690	.378	-.749	5	.487

Appendix E: PPG ANOVA Results from Pressure Experiment

For all the PPG data a repeated measures ANOVA was performed to test whether or not the chamber pressure affected the AC component of the bone and skin PPG data in both legs. Four separate ANOVAs were performed corresponding to both PPG signals on both limbs. Mauchly's test was used to test for sphericity. If the sphericity assumption was violated, the Greenhouse-Geisser correction was used when reporting the ANOVA omnibus F-test. Alternative approaches to correcting for sphericity include using a different procedure to adjust the degrees of freedom such as the Huynh-Feldt method, reporting the lower-bound corrections, or using the multivariate ANOVA (MANOVA) approach to repeated measures analysis. While we have chosen to use the Greenhouse-Geisser approach, all these alternative procedures are included in the tables below for comparison. Regardless of what approach we select, we arrive at the same conclusions with similar p-values in all approaches. In all cases significance is set at 0.05.

For each ANOVA model, plots of the residuals versus the predicted values are also given. These plots include a histogram of the residuals along the y-axis, allowing a visual inspection of their distribution. Homoscedasticity of the residuals is tested using the Brown-Forsythe test, and normality of the residuals can be visually inspected by looking at the accompanying histograms. We are only concerned with very large departures from the homoscedasticity assumption, since, for ANOVA models with equal sample sizes, the F test comparing the equality of factor level means is robust to departures from this assumption [119]. Significance for the Brown-Forsythe test is therefore set at 0.01. Significance for the normality tests is left as usual at 0.05.

PPG Bone Results for Leg Inside Chamber

Table 20 - MANOVA results for bone PPG signal for leg inside chamber

Multivariate Tests[b]

Effect		Value	F	Hypothesis df	Error df	Sig.
Pressure	Pillai's Trace	.926	8.955[a]	7.000	5.000	.014
	Wilks' Lambda	.074	8.955[a]	7.000	5.000	.014
	Hotelling's Trace	12.537	8.955[a]	7.000	5.000	.014
	Roy's Largest Root	12.537	8.955[a]	7.000	5.000	.014

a. Exact statistic

b. Design: Intercept
Within Subjects Design: Pressure

Table 21 - Sphericity test for bone PPG signal for leg inside chamber

Mauchly's Test of Sphericity[b]

Measure:Bone

Within Subjects Effect	Mauchly's W	Approx. Chi-Square	df	Sig.	Epsilon[a]		
					Greenhouse-Geisser	Huynh-Feldt	Lower-bound
Pressure	.000	70.890	27	.000	.364	.483	.143

Tests the null hypothesis that the error covariance matrix of the orthonormalized transformed dependent variables is proportional to an identity matrix.

a. May be used to adjust the degrees of freedom for the averaged tests of significance. Corrected tests are displayed in the Tests of Within-Subjects Effects table.

b. Design: Intercept
Within Subjects Design: Pressure

Table 22 - Effect of pressure on bone PPG signal for leg inside chamber

Tests of Within-Subjects Effects

Measure:Bone

Source		Type III Sum of Squares	df	Mean Square	F	Sig.
Pressure	Sphericity Assumed	259.248	7	37.035	21.730	.000
	Greenhouse-Geisser	259.248	2.548	101.729	21.730	.000
	Huynh-Feldt	259.248	3.382	76.661	21.730	.000
	Lower-bound	259.248	1.000	259.248	21.730	.001
Error(Pressure)	Sphericity Assumed	131.237	77	1.704		
	Greenhouse-Geisser	131.237	28.033	4.682		
	Huynh-Feldt	131.237	37.199	3.528		
	Lower-bound	131.237	11.000	11.931		

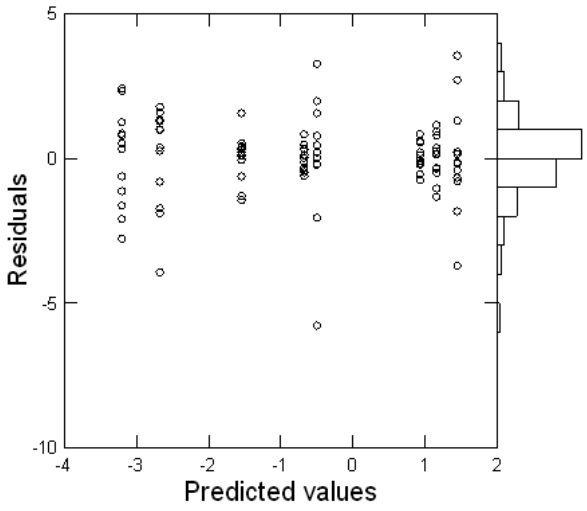

Figure 28 - Plot of residuals versus predicted values for bone PPG signal for the leg inside the chamber

Table 23 - Homoscedasticity test for bone PPG signal for leg inside the chamber

Test	Test statistic	df	p-value
Brown-Forsythe	2.514	7,88	0.021

PPG Skin Results for Leg Inside Chamber

Table 24 - MANOVA results for skin PPG signal for leg inside chamber

Multivariate Tests[b]

Effect		Value	F	Hypothesis df	Error df	Sig.
Pressure	Pillai's Trace	.964	19.082[a]	7.000	5.000	.003
	Wilks' Lambda	.036	19.082[a]	7.000	5.000	.003
	Hotelling's Trace	26.715	19.082[a]	7.000	5.000	.003
	Roy's Largest Root	26.715	19.082[a]	7.000	5.000	.003

a. Exact statistic

b. Design: Intercept
Within Subjects Design: Pressure

Table 25 - Sphericity test for skin PPG signal for leg inside chamber

Mauchly's Test of Sphericity[b]

Measure:Skin

Within Subjects Effect	Mauchly's W	Approx. Chi-Square	df	Sig.	Epsilon[a]		
					Greenhouse-Geisser	Huynh-Feldt	Lower-bound
Pressure	.002	53.414	27	.003	.424	.597	.143

Tests the null hypothesis that the error covariance matrix of the orthonormalized transformed dependent variables is proportional to an identity matrix.

a. May be used to adjust the degrees of freedom for the averaged tests of significance. Corrected tests are displayed in the Tests of Within-Subjects Effects table.

b. Design: Intercept
Within Subjects Design: Pressure

Table 26 - Effect of pressure on skin PPG signal for leg inside chamber

Tests of Within-Subjects Effects

Measure:Skin

Source		Type III Sum of Squares	df	Mean Square	F	Sig.
Pressure	Sphericity Assumed	213.138	7	30.448	37.350	.000
	Greenhouse-Geisser	213.138	2.965	71.889	37.350	.000
	Huynh-Feldt	213.138	4.179	51.004	37.350	.000
	Lower-bound	213.138	1.000	213.138	37.350	.000
Error(Pressure)	Sphericity Assumed	62.772	77	.815		
	Greenhouse-Geisser	62.772	32.613	1.925		
	Huynh-Feldt	62.772	45.967	1.366		
	Lower-bound	62.772	11.000	5.707		

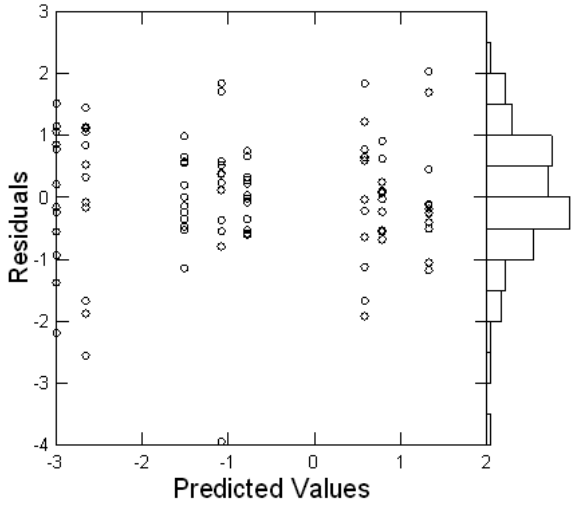

Figure 29 - Plot of residuals versus predicted values for skin PPG signal for the leg inside the chamber

Table 27 - Homoscedasticity test for skin PPG signal for leg inside the chamber

Test	Test statistic	df	p-value
Brown-Forsythe	1.859	7,88	0.086

PPG Bone Results for Leg Outside Chamber

Table 28 - MANOVA results for bone PPG signal for leg outside chamber

Multivariate Tests[b]

Effect		Value	F	Hypothesis df	Error df	Sig.
Pressure	Pillai's Trace	.636	1.246[a]	7.000	5.000	.418
	Wilks' Lambda	.364	1.246[a]	7.000	5.000	.418
	Hotelling's Trace	1.745	1.246[a]	7.000	5.000	.418
	Roy's Largest Root	1.745	1.246[a]	7.000	5.000	.418

a. Exact statistic

b. Design: Intercept
Within Subjects Design: Pressure

Table 29 - Sphericity test for bone PPG signal for leg outside chamber

Mauchly's Test of Sphericity[b]

Measure:Bone

Within Subjects Effect	Mauchly's W	Approx. Chi-Square	df	Sig.	Epsilon[a]		
					Greenhouse-Geisser	Huynh-Feldt	Lower-bound
Pressure	.002	51.136	27	.006	.396	.543	.143

Tests the null hypothesis that the error covariance matrix of the orthonormalized transformed dependent variables is proportional to an identity matrix.

a. May be used to adjust the degrees of freedom for the averaged tests of significance. Corrected tests are displayed in the Tests of Within-Subjects Effects table.

b. Design: Intercept
Within Subjects Design: Pressure

Table 30 - Effect of pressure on bone PPG signal for leg outside chamber

Tests of Within-Subjects Effects

Measure:Bone

Source		Type III Sum of Squares	df	Mean Square	F	Sig.
Pressure	Sphericity Assumed	2.079	7	.297	.961	.466
	Greenhouse-Geisser	2.079	2.773	.749	.961	.418
	Huynh-Feldt	2.079	3.802	.547	.961	.436
	Lower-bound	2.079	1.000	2.079	.961	.348
Error(Pressure)	Sphericity Assumed	23.803	77	.309		
	Greenhouse-Geisser	23.803	30.507	.780		
	Huynh-Feldt	23.803	41.826	.569		
	Lower-bound	23.803	11.000	2.164		

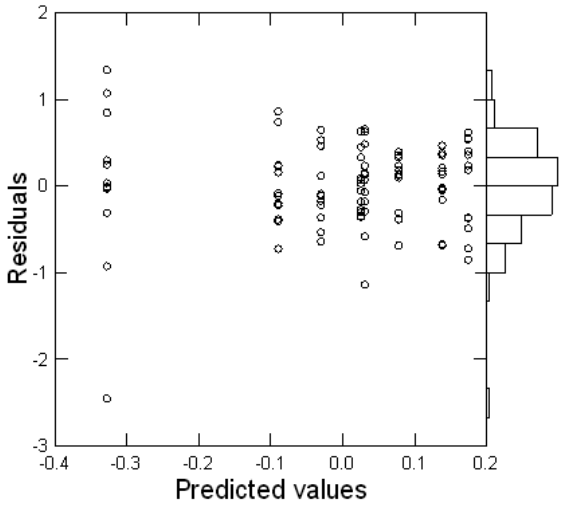

Figure 30 - Plot of residuals versus predicted values for bone PPG signal for the leg outside the chamber

Table 31 - Homoscedasticity test for bone PPG signal for leg outside the chamber

Test	Test statistic	df	**p-value**
Brown-Forsythe	1.326	7,88	0.248

PPG Skin Results for Leg Outside Chamber

Table 32 - MANOVA results for skin PPG signal for leg outside chamber

Multivariate Tests[b]

Effect		Value	F	Hypothesis df	Error df	Sig.
Pressure	Pillai's Trace	.339	.367[a]	7.000	5.000	.888
	Wilks' Lambda	.661	.367[a]	7.000	5.000	.888
	Hotelling's Trace	.514	.367[a]	7.000	5.000	.888
	Roy's Largest Root	.514	.367[a]	7.000	5.000	.888

a. Exact statistic

b. Design: Intercept
Within Subjects Design: Pressure

Table 33 - Sphericity test for skin PPG signal for leg outside chamber

Mauchly's Test of Sphericity[b]

Measure:Skin

Within Subjects Effect	Mauchly's W	Approx. Chi-Square	df	Sig.	Epsilon[a]		
					Greenhouse-Geisser	Huynh-Feldt	Lower-bound
Pressure	.007	42.407	27	.044	.424	.598	.143

Tests the null hypothesis that the error covariance matrix of the orthonormalized transformed dependent variables is proportional to an identity matrix.

a. May be used to adjust the degrees of freedom for the averaged tests of significance. Corrected tests are displayed in the Tests of Within-Subjects Effects table.

b. Design: Intercept
Within Subjects Design: Pressure

Table 34 - Effect of pressure on skin PPG signal for leg outside chamber

Tests of Within-Subjects Effects

Measure:Skin

Source		Type III Sum of Squares	df	Mean Square	F	Sig.
Pressure	Sphericity Assumed	.446	7	.064	.744	.635
	Greenhouse-Geisser	.446	2.968	.150	.744	.532
	Huynh-Feldt	.446	4.185	.107	.744	.572
	Lower-bound	.446	1.000	.446	.744	.407
Error(Pressure)	Sphericity Assumed	6.599	77	.086		
	Greenhouse-Geisser	6.599	32.649	.202		
	Huynh-Feldt	6.599	46.039	.143		
	Lower-bound	6.599	11.000	.600		

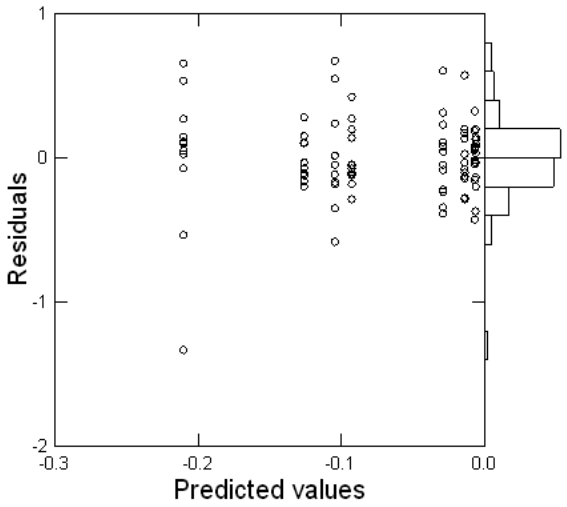

Figure 31 - Plot of residuals versus predicted values for skin PPG signal for the leg outside the chamber

Table 35 - Homoscedasticity test for skin PPG signal for leg outside the chamber

Test	Test statistic	df	**p-value**
Brown-Forsythe	1.247	7,88	0.286

Appendix F: HR and BP Results from Pressure Experiment

The Shapiro-Wilk test was used to test for normality for the BP and HR data at the extreme pressure levels of +50 and -50 mmHg. The outcome of these tests are shown in Table 36. The null hypothesis is that the data comes from a normal distribution, and the alternate hypothesis is that the data is not normally distributed. The Kolmogorov-Smirnov test (with Lilliefors significance correction) is also given alongside the Shapiro-Wilk results (which are more applicable for our small sample sizes). Significance is set at 0.05 for all comparisons.

Table 36 - Normality tests for BP and HR data. [a]Lilliefors significance correction. *lower bound of the true significance

	Kolmogorov-Smirnov[a]			Shapiro-Wilk		
	Statistic	df	Sig.	Statistic	df	Sig.
HR50_base	.235	12	.066	.880	12	.087
HR_50	.162	12	.200*	.934	12	.422
HR_n50_base	.182	12	.200*	.911	12	.221
HR_n50	.202	12	.190	.896	12	.143
BP_sys_50_base	.158	12	.200*	.932	12	.404
BP_sys_50	.119	12	.200*	.968	12	.885
BP_sys_n50_base	.152	12	.200*	.944	12	.550
BP_sys_n50	.184	12	.200*	.898	12	.148
BP_dia_50_base	.147	12	.200*	.961	12	.798
BP_dia_50	.236	12	.064	.911	12	.221
BP_dia_n50_base	.151	12	.200*	.948	12	.607
BP_dia_n50	.090	12	.200*	.982	12	.989

Table 37 - Paired two-tailed t-test for BP and HR data from pressure experiment

		Paired Differences					t	df	p-value
		Mean	Std. Deviation	Std. Error Mean	95% Confidence Interval of the Difference Lower	Upper			
Pair 1	HR50_base - HR_50	-1.427	5.361	1.548	-4.833	1.979	-.922	11	.376
Pair 2	HR_n50_base - HR_n50	-.719	2.892	.835	-2.556	1.119	-.861	11	.408
Pair 3	BP_sys_50_base - BP_sys_50	-3.583	3.728	1.076	-5.952	-1.214	-3.329	11	.007
Pair 4	BP_sys_n50_base - BP_sys_n50	-.417	4.441	1.282	-3.238	2.405	-.325	11	.751
Pair 5	BP_dia_50_base - BP_dia_50	-2.500	6.260	1.807	-6.477	1.477	-1.384	11	.194
Pair 6	BP_dia_n50_base - BP_dia_n50	-2.167	3.243	.936	-4.227	-.106	-2.315	11	.041

References

1. Ahearn, C., *Intermittent Negative Pressure Wound Therapy and Lower Negative Pressures - Exploring the Disparity between Science and Current Practice: A Review of the Literature.* Ostomy Wound Manage, 2009. **55**(6): p. 22-8.
2. Albertazzi, P., S.A. Steel, and M. Bottazzi, *Effect of intermittent compression therapy on bone mineral density in women with low bone mass.* Bone, 2005. **37**(5): p. 662-8.
3. Allen, J., *Photoplethysmography and its application in clinical physiological measurement.* Physiol Meas, 2007. **28**(3): p. R1-39.
4. Anderson, R.R. and J.A. Parrish, *The optics of human skin.* J Invest Dermatol, 1981. **77**(1): p. 13-9.
5. Anetzberger, H., et al., *Microspheres accurately predict regional bone blood flow.* Clin Orthop Relat Res, 2004(424): p. 253-65.
6. Aratow, M., et al., *Transcapillary fluid responses to lower body negative pressure.* J Appl Physiol, 1993. **74**(6): p. 2763-70.
7. Arbeille, P., et al., *Femoral flow response to lower body negative pressure: an orthostatic tolerance test.* Aviat Space Environ Med, 1995. **66**(2): p. 131-6.
8. Ardill, B.L., et al., *Some effects on the blood vessels of the human forearm of local exposure to pressures below atmospheric.* J Physiol, 1969. **203**(1): p. 31-43.
9. Bashkatov, A.N., et al., *Optical properties of human cranial bone in the spectral range from 800 to 2000 nm - art. no. 616310.* Saratov Fall Meeting 2005: Optical Technologies in Biophysics and Medicine VII, 2006. **6163**: p. 16310-16310.
10. Bayliss, W.M., *On the local reactions of the arterial wall to changes of internal pressure.* J Physiol, 1902. **28**(3): p. 220-31.
11. Bergstrand, S., et al., *Blood flow measurements at different depths using photoplethysmography and laser Doppler techniques.* Skin Res Technol, 2009. **15**(2): p. 139-47.
12. Bergula, A.P., W. Huang, and J.A. Frangos, *Femoral vein ligation increases bone mass in the hindlimb suspended rat.* Bone, 1999. **24**(3): p. 171-7.
13. Bevegard, S., J. Castenfors, and L.E. Lindblad, *Effect of changes in blood volume distribution on circulatory variables and plasma renin activity in man.* Acta Physiol Scand, 1977. **99**(2): p. 237-45.
14. Bier, A.K.G. and G.M. Blech, *Hyperemia as a therapeutic agent*. 1905, Chicago,: A. Robertson & co. 239 p.
15. Binzoni, T., et al., *Human tibia bone marrow blood perfusion by non-invasive near infrared spectroscopy: a new tool for studies on microgravity.* J Gravit Physiol, 2002. **9**(1): p. P183-4.
16. Binzoni, T., et al., *Human tibia bone marrow: defining a model for the study of haemodynamics as a function of age by near infrared spectroscopy.* J Physiol Anthropol Appl Human Sci, 2003. **22**(5): p. 211-8.
17. Binzoni, T., et al., *Blood volume and haemoglobin oxygen content changes in human bone marrow during orthostatic stress.* J Physiol Anthropol, 2006. **25**(1): p. 1-6.

18. Blair, D.A., et al., *The increase in tone in forearm resistance blood vessels exposed to increased transmural pressure.* J Physiol, 1959. **149**: p. 614-25.
19. Blecken, S.R., J.L. Villavicencio, and T.C. Kao, *Comparison of elastic versus nonelastic compression in bilateral venous ulcers: a randomized trial.* J Vasc Surg, 2005. **42**(6): p. 1150-5.
20. Bloomfield, S.A., *Does altered blood flow to bone in microgravity impact on mechanotransduction?* J Musculoskelet Neuronal Interact, 2006. **6**(4): p. 324-6.
21. Bloomfield, S.A., *Disuse osteopenia.* Curr Osteoporos Rep, 2010. **8**(2): p. 91-7.
22. Blume, P.A., et al., *Comparison of negative pressure wound therapy using vacuum-assisted closure with advanced moist wound therapy in the treatment of diabetic foot ulcers: a multicenter randomized controlled trial.* Diabetes Care, 2008. **31**(4): p. 631-6.
23. Bochmann, R.P., et al., *External compression increases forearm perfusion.* J Appl Physiol, 2005. **99**(6): p. 2337-44.
24. Boegehold, M.A. and P.C. Johnson, *Periarteriolar and tissue PO2 during sympathetic escape in skeletal muscle.* Am J Physiol, 1988. **254**(5 Pt 2): p. H929-36.
25. Boegehold, M.A. and P.C. Johnson, *Response of arteriolar network of skeletal muscle to sympathetic nerve stimulation.* Am J Physiol, 1988. **254**(5 Pt 2): p. H919-28.
26. Booth, E.A., et al., *Cerebral and somatic venous oximetry in adults and infants.* Surg Neurol Int, 2010. **1**: p. 75.
27. Bouskela, E. and C.A. Wiederhielm, *Microvascular myogenic reaction in the wing of the intact unanesthetized bat.* Am J Physiol, 1979. **237**(1): p. H59-65.
28. Breit, G.A., et al., *Regional cutaneous microvascular flow responses during gravitational and LBNP stresses.* Physiologist, 1993. **36**(1 Suppl): p. S110-1.
29. Brinker, M.R., et al., *Pharmacological regulation of the circulation of bone.* J Bone Joint Surg Am, 1990. **72**(7): p. 964-75.
30. Brookes, M., *Blood flow rates in compact and cancellous bone, and bone marrow.* J Anat, 1967. **101**(Pt 3): p. 533-41.
31. Brookes, M., *Approaches to non-invasive blood flow measurement in bone.* Biomed Eng, 1974. **9**(8): p. 342-7.
32. Brookes, M., et al., *A new concept of capillary circulation in bone cortex.* The Lancet, 1961. **I**: p. 1078-1081.
33. Brookes, M. and W.J. Revell, *Blood supply of bone : scientific aspects*. Rev. and updated ed. 1998, London ; New York: Springer. xx, 359 p.
34. Brown, B.G., et al., *The mechanisms of nitroglycerin action: stenosis vasodilatation as a major component of the drug response.* Circulation, 1981. **64**(6): p. 1089-97.
35. Brown, E., et al., *Filling and emptying of the low-pressure blood vessels of the human forearm.* J Appl Physiol, 1966. **21**(2): p. 573-82.
36. Brown, P., *Forensic Anthropology*, in *The Online Skeleton: www-personal.une.edu.au/~pbrown3/skeleton.pdf*.
37. Buckey, J.C., *Space physiology*. 2006, Oxford ; New York: Oxford University Press. xv, 283 p.

38. Burton, A.C. and S. Yamada, *Relation between blood pressure and flow in the human forearm.* J Appl Physiol, 1951. **4**(5): p. 329-39.
39. Caro, C.G., T.H. Foley, and M.F. Sudlow, *Early effects of abrupt reduction of local pressure on the forearm and its circulation.* J Physiol, 1968. **194**(3): p. 645-58.
40. Caro, C.G., et al., *Effect of venous pressure on forearm blood flow.* J Physiol, 1968. **198**(2): p. 96passim-97p.
41. Challoner, A.V.J., *Photoelectric plethysmography for estimating cutaneous blood flow*, in *Non-Invasive Physiological Measurements*, P. Rolfe, Editor. 1979, Academic Press: London. p. 127-151.
42. Challoner, A.V.J. and C.A. Ramsay, *A Photoelectric Plethysmograph for the Measurement of Cutaneous Blood Flow.* Phys Med Biol, 1974. **19**(3): p. 317-328.
43. Chan, R.C., et al., *Dynamic measurement of bone blood perfusion with modified laser Doppler imaging.* J Orthop Res, 1999. **17**(4): p. 578-81.
44. Chance, B., et al., *Time-resolved spectroscopy of hemoglobin and myoglobin in resting and ischemic muscle.* Anal Biochem, 1988. **174**(2): p. 698-707.
45. Coles, D.R., *Heat elimination from the toes during exposure of the foot to subatmospheric pressures.* J Physiol, 1957. **135**(1): p. 171-81.
46. Coles, D.R. and A.D. Greenfield, *The reactions of the blood vessels of the hand during increases in transmural pressure.* J Physiol, 1956. **131**(2): p. 277-89.
47. Coles, D.R. and B.S. Kidd, *Effect of small degrees of venous distension on the apparent inflow rate of blood to the human calf.* Circ Res, 1957. **5**(3): p. 223-5.
48. Coles, D.R., B.S. Kidd, and W. Moffat, *Distensibility of blood vessels of the human calf determined by local application of subatmospheric pressures.* J Appl Physiol, 1957. **10**(3): p. 461-8.
49. Coles, D.R., B.S. Kidd, and G.C. Patterson, *The reactions of the blood vessels of the human calf to increases in transmural pressure.* J Physiol, 1956. **134**(3): p. 665-74.
50. Coles, D.R. and G.C. Patterson, *The capacity and distensibility of the blood vessels of the human hand.* J Physiol, 1957. **135**(1): p. 163-70.
51. Colleran, P.N., et al., *Alterations in skeletal perfusion with simulated microgravity: a possible mechanism for bone remodeling.* J Appl Physiol, 2000. **89**(3): p. 1046-54.
52. Collins, T.C., et al., *Peripheral arterial disease is associated with higher rates of hip bone loss and increased fracture risk in older men.* Circulation, 2009. **119**(17): p. 2305-12.
53. Crock, H.V., *An atlas of vascular anatomy of the skeleton and spinal cord*. 1996, London: M. Dunitz. xvi,307p.
54. Crossley, R.J., et al., *The interrelation of thermoregulatory and baroreceptor reflexes in the control of the blood vessels in the human forearm.* J Physiol, 1966. **183**(3): p. 628-36.
55. Crowe, J.A. and D. Damianou, *The Wavelength Dependence of the Photoplethysmogram and Its Implication to Pulse Oximetry.* Proceedings of the Annual International Conference of the Ieee Engineering in Medicine and Biology Society, Vol 14, Pts 1-7, 1992. **14**: p. 2423-2424.

56. Cui, W., N. Wang, and B. Chance, *Study of photon migration depths with time-resolved spectroscopy.* Opt Lett, 1991. **16**(21): p. 1632-4.
57. Cutuk, A., et al., *Ambulation in simulated fractional gravity using lower body positive pressure: cardiovascular safety and gait analyses.* J Appl Physiol, 2006. **101**(3): p. 771-7.
58. Dai, G., J.P. Gertler, and R.D. Kamm, *The effects of external compression on venous blood flow and tissue deformation in the lower leg.* J Biomech Eng, 1999. **121**(6): p. 557-64.
59. Davis, M.J., *Control of bat wing capillary pressure and blood flow during reduced perfusion pressure.* Am J Physiol, 1988. **255**(5 Pt 2): p. H1114-29.
60. Dayan, L., et al., *SPECT/CT-plethysmography - non-invasive quantitation of bone and soft tissue blood flow.* J Orthop Surg, 2008. **3**: p. 36.
61. de Trafford, J. and K. Lafferty, *What does photoplethysmography measure?* Med Biol Eng Comput, 1984. **22**(5): p. 479-80.
62. Delis, K.T., et al., *Enhancing venous outflow in the lower limb with intermittent pneumatic compression. A comparative haemodynamic analysis on the effect of foot vs. calf vs. foot and calf compression.* Eur J Vasc Endovasc Surg, 2000. **19**(3): p. 250-60.
63. Dorlas, J.C. and J.A. Nijboer, *Photo-electric plethysmography as a monitoring device in anaesthesia. Application and interpretation.* Br J Anaesth, 1985. **57**(5): p. 524-30.
64. Driessens, M. and P.M. Vanhoutte, *Vascular reactivity of the isolated tibia of the dog.* Am J Physiol, 1979. **236**(6): p. H904-8.
65. Drinker, C.K. and K.R. Drinker, *A method for maintaining an artificial circulation through the tibia of the dog, with demonstration of the vasomotor control of the marrow vessels.* American Journal of Physiology, 1916. **40**(4): p. 514-521.
66. Dyke, J.P. and R.K. Aaron, *Noninvasive methods of measuring bone blood perfusion.* Ann N Y Acad Sci, 2010. **1192**(1): p. 95-102.
67. Eastlack, R.K., et al., *Lower body positive-pressure exercise after knee surgery.* Clin Orthop Relat Res, 2005(431): p. 213-9.
68. Eiken, O. and H. Bjurstedt, *Dynamic exercise in man as influenced by experimental restriction of blood flow in the working muscles.* Acta Physiol Scand, 1987. **131**(3): p. 339-45.
69. Feng, S., F.A. Zeng, and B. Chance, *Photon migration in the presence of a single defect: a perturbation analysis.* Appl Opt, 1995. **34**(19): p. 3826-37.
70. Fleming, J.T., et al., *Bone blood flow and vascular reactivity.* Cells Tissues Organs, 2001. **169**(3): p. 279-84.
71. Fortney, S.M., *Development of lower body negative pressure as a countermeasure for orthostatic intolerance.* J Clin Pharmacol, 1991. **31**(10): p. 888-92.
72. Fronek, A., *Photoplethysmography in the diagnosis of venous disease.* Dermatol Surg, 1995. **21**(1): p. 64-6.
73. Fronek, A., D.G. DiTomasso, and M. Allison, *Noninvasive assessment of endothelial activity in patients with peripheral arterial disease and cardiovascular risk factors.* Endothelium, 2007. **14**(4-5): p. 199-205.

74. Fu, Q., et al., *Effects of lower body positive pressure on muscle sympathetic nerve activity response to head-up tilt.* Am J Physiol Regul Integr Comp Physiol, 2001. **281**(3): p. R778-85.
75. Fu, Q., et al., *A comparison of autonomic responses in humans induced by two simulation models of weightlessness: lower body positive pressure and 6 degrees head-down tilt.* J Auton Nerv Syst, 2000. **80**(1-2): p. 101-7.
76. Fu, Q., et al., *Responses of muscle sympathetic nerve activity to lower body positive pressure.* Am J Physiol, 1998. **275**(4 Pt 2): p. H1254-9.
77. Gailite, L., J. Spigulis, and A. Lihachev, *Multilaser photoplethysmography technique.* Lasers Med Sci, 2008. **23**(2): p. 189-93.
78. Goodman, J.M., M.R. Freeman, and L.S. Goodman, *Left ventricular function during arm exercise: influence of leg cycling and lower body positive pressure.* J Appl Physiol, 2007. **102**(3): p. 904-12.
79. Gordy, E. and D.L. Drabkin, *Spectrophotometric studies. XVI. Determination of the oxygen saturation of blood by a simplified technique, applicable to standard equipment.* J Biol Chem, 1957. **227**(1): p. 285-99.
80. Goswami, N., et al., *The cardiovascular response to lower body negative pressure in humans depends on seal location.* Physiol Res, 2008.
81. Goswami, N., J.A. Loeppky, and H. Hinghofer-Szalkay, *LBNP: past protocols and technical considerations for experimental design.* Aviat Space Environ Med, 2008. **79**(5): p. 459-71.
82. Greenfield, A.D., *A simple water filled plethysmograph for the hand or forearm with temperature control.* J Physiol, 1954. **123**(3): p. 62P-64P.
83. Greenfield, A.D., *Blood Flow through the Human Forearm and Digits as Influenced by Subatmospheric Pressure and Venous Pressure.* Circ Res, 1964. **15**: p. SUPPL:70-5.
84. Greenfield, A.D., D.M. Kerslake, and G.C. Patterson, *Prolonged dilatation of the forearm blood vessels after a large increase in transmural pressure.* J Physiol, 1954. **125**(1): p. 40-1P.
85. Greenfield, A.D. and G.C. Patterson, *Reactions of the blood vessels of the human forearm to increases in transmural pressure.* J Physiol, 1954. **125**(3): p. 508-24.
86. Greenfield, A.D. and G.C. Patterson, *The effect of small degrees of venous distension on the apparent rate of blood inflow to the forearm.* J Physiol, 1954. **125**(3): p. 525-33.
87. Greenfield, A.D. and G.C. Patterson, *On the capacity and distensibility of the blood vessels of the human forearm.* J Physiol, 1956. **131**(2): p. 290-306.
88. Guyton, A.C. and J.E. Hall, *Textbook of medical physiology*. 11th ed. 2006, Philadelphia: Elsevier Saunders. xxxv, 1116 p.
89. Hachiya, T., A.P. Blaber, and M. Saito, *Near-infrared spectroscopy provides an index of blood flow and vasoconstriction in calf skeletal muscle during lower body negative pressure.* Acta Physiol (Oxf), 2008. **193**(2): p. 117-27.
90. Hagblad, J., et al., *A technique based on laser Doppler flowmetry and photoplethysmography for simultaneously monitoring blood flow at different tissue depths.* Med Biol Eng Comput, 2010.

91. Hales, J.R., et al., *Evidence for skin microvascular compartmentalization by laser-Doppler and photoplethysmographic techniques.* Int J Microcirc Clin Exp, 1993. **12**(1): p. 99-104.
92. Han, W.Q., et al., *Cerebral hemodynamics and brain functional activity during lower body negative pressure.* Aviat Space Environ Med, 2009. **80**(8): p. 698-702.
93. Hargens, A.R., et al., *The gravity of LBNP exercise: preliminary lessons learned from identical twins in bed for 30 days.* J Gravit Physiol, 2002. **9**(1): p. P59-62.
94. Hargens, A.R., et al. *New Limb Compression Device Increases Skin, Muscle, and Bone Microvascular Flows*. in *American Venous Forum - 19th Annual Meeting*. 2007. San Diego, CA.
95. Hargens, A.R., D.E. Watenpaugh, and G.A. Breit, *Control of circulatory function in altered gravitational fields.* Physiologist, 1992. **35**(1 Suppl): p. S80-3.
96. He, J.Y., L.S. Jiang, and L.Y. Dai, *The roles of the sympathetic nervous system in osteoporotic diseases: A review of experimental and clinical studies.* Ageing Res Rev, 2011.
97. Hertzman, A.B., *Photoelectric plethysmography of the fingers and toes in man.* Proceedings of the Society for Experimental Biology and Medicine, 1937. **37**(3): p. 529-534.
98. Hertzman, A.B., *The blood supply of various skin areas as estimated by the photoelectric plethysmograph.* American Journal of Physiology, 1938. **124**(2): p. 328-340.
99. Hertzman, A.B. and J.B. Dillon, *Applications of photoelectric plethysmography in peripheral vascular disease.* American Heart Journal, 1940. **20**: p. 750-761.
100. Hill, M.A., et al., *New technologies for dissecting the arteriolar myogenic response.* Trends Pharmacol Sci, 2007. **28**(7): p. 308-15.
101. Hillsley, M.V. and J.A. Frangos, *Bone tissue engineering: the role of interstitial fluid flow.* Biotechnol Bioeng, 1994. **43**(7): p. 573-81.
102. Hmamouchi, I., et al., *Low bone mineral density is related to atherosclerosis in postmenopausal Moroccan women.* BMC Public Health, 2009. **9**: p. 388.
103. Hohmann, E.L., et al., *Innervation of periosteum and bone by sympathetic vasoactive intestinal peptide-containing nerve fibers.* Science, 1986. **232**(4752): p. 868-71.
104. Iabichella, M.L., E. Melillo, and G. Mosti, *A review of microvascular measurements in wound healing.* Int J Low Extrem Wounds, 2006. **5**(3): p. 181-99.
105. Ibegbuna, V., et al., *Effect of elastic compression stockings on venous hemodynamics during walking.* J Vasc Surg, 2003. **37**(2): p. 420-5.
106. Imadojemu, V.A., et al., *Contribution of perfusion pressure to vascular resistance response during head-up tilt.* Am J Physiol Heart Circ Physiol, 2001. **281**(1): p. H371-5.
107. Intaglietta, M., P.C. Johnson, and R.M. Winslow, *Microvascular and tissue oxygen distribution.* Cardiovasc Res, 1996. **32**(4): p. 632-43.
108. Jacobsen, T.N., et al., *Subcutaneous and skeletal muscle vascular responses in human limbs to lower body negative pressure.* Acta Physiol Scand, 1992. **144**(3): p. 247-52.

109. Jamal, S.A., et al., *Effect of nitroglycerin ointment on bone density and strength in postmenopausal women: a randomized trial.* JAMA, 2011. **305**(8): p. 800-7.
110. Johnson, P.C., *The Myogenic Response.* News in Physiological Sciences, 1991. **6**: p. 41-43.
111. Jugdutt, B.I. and J.W. Warnica, *Intravenous nitroglycerin therapy to limit myocardial infarct size, expansion, and complications. Effect of timing, dosage, and infarct location.* Circulation, 1988. **78**(4): p. 906-19.
112. Junod, V.T., *Action de l'air rarefie ou condense sur la surface du corps.* Revue medicale Francaise et etrangere, 1834. **3**: p. 460-462.
113. Junod, V.T., *Recherches physiologiques et thérapeutiques sur les effets de la compression et de la rerefaction de l'air, tant sur le corps que sur les membres isoles.* Revue medicale Francaise et etrangere, 1834. **3**: p. 350-368.
114. Kalodiki, E., *Use of intermittent pneumatic compression in the treatment of venous ulcers.* Future Cardiol, 2007. **3**(2): p. 185-91.
115. Kamal, A.A., et al., *Skin photoplethysmography--a review.* Comput Methods Programs Biomed, 1989. **28**(4): p. 257-69.
116. Kavros, S.J., et al., *Improving limb salvage in critical ischemia with intermittent pneumatic compression: a controlled study with 18-month follow-up.* J Vasc Surg, 2008. **47**(3): p. 543-9.
117. Kirby, J.P., et al., *Novel uses of a negative-pressure wound care system.* Journal of Trauma-Injury Infection and Critical Care, 2002. **53**(1): p. 117-121.
118. Kline, C.N., et al., *Inelastic compression legging produces gradient compression and significantly higher skin surface pressures compared with an elastic compression stocking.* Vascular, 2008. **16**(1): p. 25-30.
119. Kutner, M.H., *Applied linear statistical models*. 5th ed. The McGraw-Hill/Irwin series operations and decision sciences. 2005, Boston: McGraw-Hill Irwin. xxviii, 1396 p.
120. Laroche, M., *Intraosseous circulation from physiology to disease.* Joint Bone Spine, 2002. **69**(3): p. 262-9.
121. Lathers, C.M. and J.B. Charles, *Use of lower body negative pressure to counter symptoms of orthostatic intolerance in patients, bed rest subjects, and astronauts.* J Clin Pharmacol, 1993. **33**(11): p. 1071-85.
122. LeBlanc, A., et al., *Bone mineral and lean tissue loss after long duration space flight.* J Musculoskelet Neuronal Interact, 2000. **1**(2): p. 157-60.
123. Lee, S.M., et al., *Supine LBNP exercise maintains exercise capacity in male twins during 30-d bed rest.* Med Sci Sports Exerc, 2007. **39**(8): p. 1315-26.
124. Lee, S.M., et al., *LBNP exercise protects aerobic capacity and sprint speed of female twins during 30 days of bed rest.* J Appl Physiol, 2009. **106**(3): p. 919-28.
125. Leftheriotis, G., et al., *Effects of lower body positive pressure on forearm vasculature.* Physiologist, 1990. **33**(1 Suppl): p. S52-3.
126. Li, W., et al., *Does blood pressure enhance solute transport in the bone lacunar-canalicular system?* Bone, 2010.
127. Lindberg, L.G. and P.A. Oberg, *Photoplethysmography. Part 2. Influence of light source wavelength.* Med Biol Eng Comput, 1991. **29**(1): p. 48-54.

128. Lindberg, L.G., T. Tamura, and P.A. Oberg, *Photoplethysmography. Part 1. Comparison with laser Doppler flowmetry.* Med Biol Eng Comput, 1991. **29**(1): p. 40-7.
129. Lopez-Curto, J.A., J.B. Bassingthwaighte, and P.J. Kelly, *Anatomy of the microvasculature of the tibial diaphysis of the adult dog.* J Bone Joint Surg Am, 1980. **62**(8): p. 1362-9.
130. Lott, M.E., M.D. Herr, and L.I. Sinoway, *Effects of transmural pressure on brachial artery mean blood velocity dynamics in humans.* J Appl Physiol, 2002. **93**(6): p. 2137-46.
131. Lott, M.E., et al., *Vasoconstrictor responses in the upper and lower limbs to increases in transmural pressure.* J Appl Physiol, 2009. **106**(1): p. 302-10.
132. Lott, M.E., et al., *Sex differences in limb vasoconstriction responses to increases in transmural pressures.* Am J Physiol Heart Circ Physiol, 2009. **296**(1): p. H186-94.
133. Lundvall, J. and T. Lanne, *Transmission of externally applied negative pressure to the underlying tissue. A study on the upper arm of man.* Acta Physiol Scand, 1989. **136**(3): p. 403-9.
134. Lundvall, J., S. Quittenbaum, and T. Lanne, *Application of external negative pressure to the extremities in man allows measurement of myogenic vascular reactions.* J Hypertens Suppl, 1989. **7**(4): p. S93-5.
135. Macias, B.R., et al., *LBNP treadmill exercise maintains spine function and muscle strength in identical twins during 28-day simulated microgravity.* J Appl Physiol, 2007. **102**(6): p. 2274-8.
136. Mangiafico, R.A., et al., *Increased prevalence of peripheral arterial disease in osteoporotic postmenopausal women.* J Bone Miner Metab, 2006. **24**(2): p. 125-31.
137. Marieb, E.N. and K. Hoehn, *Human anatomy & physiology*. 8th ed. 2010, San Francisco: Benjamin Cummings. xxxii, 1114, 28, 23, 3, 61 p.
138. Mayrovitz, H.N. and J.A. Leedham, *Laser-Doppler imaging of forearm skin: perfusion features and dependence of the biological zero on heat-induced hyperemia.* Microvasc Res, 2001. **62**(1): p. 74-8.
139. McCarthy, I., *The physiology of bone blood flow: a review.* J Bone Joint Surg Am, 2006. **88 Suppl 3**: p. 4-9.
140. McCarthy, I.D., *Investigation of the role of venous pressure in bone changes during prolonged weightlessness.* J Gravit Physiol, 1996. **3**(2): p. 33-6.
141. McCarthy, I.D., *Fluid shifts due to microgravity and their effects on bone: a review of current knowledge.* Ann Biomed Eng, 2005. **33**(1): p. 95-103.
142. Mendelson, Y., *Pulse Oximetry - Theory and Applications for Noninvasive Monitoring.* Clinical Chemistry, 1992. **38**(9): p. 1601-1607.
143. Montori, V.M., et al., *Intermittent compression pump for nonhealing wounds in patients with limb ischemia. The Mayo Clinic experience (1998-2000).* Int Angiol, 2002. **21**(4): p. 360-6.
144. Morris, M.A. and P.J. Kelly, *Use of tracer microspheres to measure bone blood flow in conscious dogs.* Calcif Tissue Int, 1980. **32**(1): p. 69-76.

145. Morris, R.J., et al., *The effect of intermittent pneumatic compression on the bone uptake of (99m)Tc-labelled methylene diphosphonate in the lower limb.* Arch Orthop Trauma Surg, 2005. **125**(5): p. 348-54.
146. Morris, R.J. and J.P. Woodcock, *Effects of supine intermittent compression on arterial inflow to the lower limb.* Arch Surg, 2002. **137**(11): p. 1269-73.
147. Murray, A. and D. Marjanovic, *Optical assessment of recovery of tissue blood supply after removal of externally applied pressure.* Med Biol Eng Comput, 1997(35): p. 425-427.
148. Musgrave, F.S., F.W. Zechman, and R.C. Mains, *Changes in total leg volume during lower body negative pressure.* Aerosp Med, 1969. **40**(6): p. 602-6.
149. Musgrave, F.S., F.W. Zechman, and R.C. Mains, *Comparison of the effects of 70 degrees tilt and several levels of lower body negative pressure on heart rate and blood pressure in man.* Aerosp Med, 1971. **42**(10): p. 1065-9.
150. Naslund, J., et al., *Non-invasive continuous estimation of blood flow changes in human patellar bone.* Med Biol Eng Comput, 2006. **44**(6): p. 501-9.
151. Nelson, G.E., Jr., et al., *Blood supply of the human tibia.* J Bone Joint Surg Am, 1960. **42-A**: p. 625-36.
152. Nielsen, H.V., *Transmural pressures and tissue perfusion in man.* Acta Physiol Scand Suppl, 1991. **603**: p. 85-92.
153. Nieveen, J., W.J. Reichert, and L.B. Van Der Slikke, *Photoelectric plethysmography using reflected light.* Cardiologia, 1956. **29**(3): p. 160-73.
154. Nilsson, G.E., T. Tenland, and P.A. Oberg, *Evaluation of a laser Doppler flowmeter for measurement of tissue blood flow.* IEEE Trans Biomed Eng, 1980. **27**(10): p. 597-604.
155. Nishiyasu, T., et al., *Effects of posture on peripheral vascular responses to lower body positive pressure.* Am J Physiol Heart Circ Physiol, 2007. **293**(1): p. H670-6.
156. Nishiyasu, T., et al., *Effects of posture on cardiovascular responses to lower body positive pressure at rest and during dynamic exercise.* J Appl Physiol, 1998. **85**(1): p. 160-7.
157. Nishiyasu, T., et al., *Near-infrared monitoring of tissue oxygenation during application of lower body pressure at rest and during dynamical exercise in humans.* Acta Physiol Scand, 1999. **166**(2): p. 123-30.
158. Obad, A., et al., *Antioxidant pretreatment and reduced arterial endothelial dysfunction after diving.* Aviat Space Environ Med, 2007. **78**(12): p. 1114-20.
159. Oganov, V., et al., *Results of Studies of the Efects of Sapce Flight Factors on Human Physiological Systems And Psychological Status, and Suggestions of Future Collaborative Activities Between the NSBRI and the IBMP*, V. Oganov, Editor. 2000, State Research Center of the Russian Federation - Institute for Biomedical Problems: Moscow.
160. Oni, O.O.A. and P.J. Gregg. *The routes of venous escape from the marrow of the diaphysis of long bones*. in *Bone circulation and bone necrosis; proceedings of the IVth International symposium on bone circulation*. 1987. Toulouse, France.
161. Park, S.H. and M. Silva, *Intermittent pneumatic soft tissue compression: Changes in periosteal and medullary canal blood flow.* J Orthop Res, 2008. **26**(4): p. 570-7.

162. Pifferi, A., et al., *Optical biopsy of bone tissue: a step toward the diagnosis of bone pathologies.* J Biomed Opt, 2004. **9**(3): p. 474-80.
163. Ping, P. and P.C. Johnson, *Mechanism of enhanced myogenic response in arterioles during sympathetic nerve stimulation.* Am J Physiol, 1992. **263**(4 Pt 2): p. H1185-9.
164. Ping, P. and P.C. Johnson, *Role of myogenic response in enhancing autoregulation of flow during sympathetic nerve stimulation.* Am J Physiol, 1992. **263**(4 Pt 2): p. H1177-84.
165. Pooley, J., J. Pooley, and R. Montgomery. *The central venous sinus of long bones - its role in relation to exercise*. in *Bone circulation and bone necrosis; proceedings of the IVth International symposium on bone circulation*. 1987. Toulouse, France.
166. Rea, R.F. and B.G. Wallin, *Sympathetic nerve activity in arm and leg muscles during lower body negative pressure in humans.* J Appl Physiol, 1989. **66**(6): p. 2778-81.
167. Rosales-Velderrain, A., et al. *Microvascular blood flow and foot sensation improve with mild external compression of the leg*. in *American Academy of Orthopaedic Surgeons Annual Meeting*. 2010. New Orleans, LA.
168. Rowell, L.B., et al., *Cardiovascular responses to graded reductions in leg perfusion in exercising humans.* Am J Physiol, 1991. **261**(5 Pt 2): p. H1545-53.
169. Rowell, L.B., C.R. Wyss, and G.L. Brengelmann, *Sustained human skin and muscle vasoconstriction with reduced baroreceptor activity.* J Appl Physiol, 1973. **34**(5): p. 639-43.
170. Ruckstuhl, H., et al., *Comparing two devices of suspended treadmill walking by varying body unloading and Froude number.* Gait Posture, 2009. **30**(4): p. 446-51.
171. Sandberg, M., et al., *Different patterns of blood flow response in the trapezius muscle following needle stimulation (acupuncture) between healthy subjects and patients with fibromyalgia and work-related trapezius myalgia.* Eur J Pain, 2005. **9**(5): p. 497-510.
172. Sandberg, M., L.G. Lindberg, and B. Gerdle, *Peripheral effects of needle stimulation (acupuncture) on skin and muscle blood flow in fibromyalgia.* Eur J Pain, 2004. **8**(2): p. 163-71.
173. Sandberg, M., et al., *Effects of acupuncture on skin and muscle blood flow in healthy subjects.* Eur J Appl Physiol, 2003. **90**(1-2): p. 114-9.
174. Sandberg, M., et al., *Non-invasive monitoring of muscle blood perfusion by photoplethysmography: evaluation of a new application.* Acta Physiol Scand, 2005. **183**(4): p. 335-43.
175. Schmedtje, J.F., Jr., J. Gutkowska, and A.A. Taylor, *Reciprocity of hemodynamic changes during lower body negative and positive pressure.* Aviat Space Environ Med, 1995. **66**(4): p. 346-52.
176. Schonberger, R.B., et al., *Topical non-iontophoretic application of acetylcholine and nitroglycerin via a translucent patch: a new means for assessing microvascular reactivity.* Yale J Biol Med, 2006. **79**(1): p. 1-7.
177. Schubert, R. and M.J. Mulvany, *The myogenic response: established facts and attractive hypotheses.* Clin Sci (Lond), 1999. **96**(4): p. 313-26.

178. Semb, H., *Effect of vasoactive drugs on the bone marrow blood flow.* Acta Orthop Scand, 1971. **42**(1): p. 10-7.
179. Seo, S.K., *Bone mineral density, arterial stiffness, and coronary atherosclerosis in healthy postmenopausal women.* Menopause: The Journal of The American Menopause Society, 2009. **16**(5): p. 937-943.
180. Serre, C.M., et al., *Evidence for a dense and intimate innervation of the bone tissue, including glutamate-containing fibers.* Bone, 1999. **25**(6): p. 623-9.
181. Shapiro, S.S. and M.B. Wilk, *An Analysis of Variance Test for Normality (Complete Samples).* Biometrika, 1965. **52**: p. 591-&.
182. Shapiro, S.S., M.B. Wilk, and H.J. Chen, *A Comparative Study of Various Tests for Normality.* Journal of the American Statistical Association, 1968. **63**(324): p. 1343-&.
183. Shelley, K. and S. Shelley, *Pulse oximeter waveform: photoelectric plethysmography*, in *Clinical monitoring: practical applications for anesthesia and critical care*, C.L. Lake, R.L. Hines, and C.D. Blitt, Editors. 2001, Saunders. p. 420-428.
184. Shelley, K.H., *Photoplethysmography: beyond the calculation of arterial oxygen saturation and heart rate.* Anesth Analg, 2007. **105**(6 Suppl): p. S31-6, tables of contents.
185. Shelley, K.H., et al., *The use of joint time frequency analysis to quantify the effect of ventilation on the pulse oximeter waveform.* J Clin Monit Comput, 2006. **20**(2): p. 81-7.
186. Shelley, K.H., B. Stout, and D. Silverman. *The pulse oximeter waveform compared to the laser Doppler waveform*. in *Annual meeting of the society for technology in anesthesia*. 1999. San Diego, CA: Journal of Clinical Monitoring and Computing.
187. Shi, X., C.G. Crandall, and P.B. Raven, *Hemodynamic responses to graded lower body positive pressure.* Am J Physiol, 1993. **265**(1 Pt 2): p. H69-73.
188. Shim, S.S., *Physiology of blood circulation of bone.* J Bone Joint Surg Am, 1968. **50**(4): p. 812-24.
189. Shim, S.S., D.H. Copp, and F.P. Patterson, *Bone blood flow in the limb following complete sciatic nerve section.* Surg Gynecol Obstet, 1966. **123**(2): p. 333-5.
190. Shoemaker, J.K., Z.I. Pozeg, and R.L. Hughson, *Forearm blood flow by Doppler ultrasound during test and exercise: tests of day-to-day repeatability.* Med Sci Sports Exerc, 1996. **28**(9): p. 1144-9.
191. Shymkiw, R.C., et al., *Evaluation of laser-Doppler perfusion imaging for measurement of blood flow in cortical bone.* J Appl Physiol, 2001. **90**(4): p. 1314-8.
192. Sim, F.H. and P.J. Kelly, *Relationship of bone remodeling, oxygen consumption, and blood flow in bone.* J Bone Joint Surg Am, 1970. **52**(7): p. 1377-89.
193. Smith, S.M., et al., *Evaluation of treadmill exercise in a lower body negative pressure chamber as a countermeasure for weightlessness-induced bone loss: a bed rest study with identical twins.* J Bone Miner Res, 2003. **18**(12): p. 2223-30.
194. Smith, S.M., et al., *WISE-2005: supine treadmill exercise within lower body negative pressure and flywheel resistive exercise as a countermeasure to bed rest-*

induced bone loss in women during 60-day simulated microgravity. Bone, 2008. **42**(3): p. 572-81.
195. Spigulis, J., et al., *Simultaneous recording of skin blood pulsations at different vascular depths by multiwavelength photoplethysmography.* Appl Opt, 2007. **46**(10): p. 1754-9.
196. Stevens, H.Y., D.R. Meays, and J.A. Frangos, *Pressure gradients and transport in the murine femur upon hindlimb suspension.* Bone, 2006. **39**(3): p. 565-72.
197. Sundberg, S. and M. Castren, *Drug- and temperature-induced changes in peripheral circulation measured by laser-Doppler flowmetry and digital-pulse plethysmography.* Scand J Clin Lab Invest, 1986. **46**(4): p. 359-65.
198. Tanaka, K., et al., *Skin microvascular flow during hypobaric exposure with and without a mechanical counter-pressure space suit glove.* Aviat Space Environ Med, 2002. **73**(11): p. 1074-8.
199. Tu, Y.K., et al., *Statistical power for analyses of changes in randomized controlled trials.* J Dent Res, 2005. **84**(3): p. 283-7.
200. Tuchin, V.V., *Handbook of optical biomedical diagnostics*. 2002, Bellingham, Wash.: SPIE Press. xv, 1093 p.
201. Ugnell, H. and P.A. Oberg, *The time-variable photoplethysmographic signal; dependence of the heart synchronous signal on wavelength and sample volume.* Med Eng Phys, 1995. **17**(8): p. 571-8.
202. Ugryumova, N., S.J. Matcher, and D.P. Attenburrow, *Measurement of bone mineral density via light scattering.* Phys Med Biol, 2004. **49**(3): p. 469-83.
203. Vickers, A.J., *The use of percentage change from baseline as an outcome in a controlled trial is statistically inefficient: a simulation study.* BMC Med Res Methodol, 2001. **1**: p. 6.
204. Villringer, A. and B. Chance, *Non-invasive optical spectroscopy and imaging of human brain function.* Trends Neurosci, 1997. **20**(10): p. 435-42.
205. Vogt, M.T., et al., *Bone mineral density and blood flow to the lower extremities: the study of osteoporotic fractures.* J Bone Miner Res, 1997. **12**(2): p. 283-9.
206. Wallace, A.L., et al., *The effect of devascularisation upon early bone healing in dynamic external fixation.* J Bone Joint Surg Br, 1991. **73**(5): p. 819-25.
207. Warburton, D.E., et al., *Cardiovascular disease and osteoporosis: balancing risk management.* Vasc Health Risk Manag, 2007. **3**(5): p. 673-89.
208. Watenpaugh, D.E., et al., *Human cutaneous vascular responses to whole-body tilting, Gz centrifugation, and LBNP.* J Appl Physiol, 2004. **96**(6): p. 2153-60.
209. Weinman, J. and M. Manoach, *A photoelectric approach to the study of peripheral circulation.* Am Heart J, 1962. **63**: p. 219-31.
210. Weiss, L., *The blood cells and hematopoietic tissues*. 2nd ed. 1984, New York: Elsevier. vii, 573 p.
211. Whiteside, L.A., D.J. Simmons, and P.A. Lesker, *Comparison of regional bone blood flow in areas with differing osteoblastic activity in the rabbit tibia.* Clin Orthop Relat Res, 1977(124): p. 267-70.
212. Williamson, J.W., et al., *Blood pressure responses to dynamic exercise with lower-body positive pressure.* Med Sci Sports Exerc, 1994. **26**(6): p. 701-8.
213. Wolthuis, R.A., S.A. Bergman, and A.E. Nicogossian, *Physiological effects of locally applied reduced pressure in man.* Physiol Rev, 1974. **54**(3): p. 566-95.

214. Zamir, M., et al., *Myogenic activity in autoregulation during low frequency oscillations.* Auton Neurosci, 2011. **159**(1-2): p. 104-10.
215. Zhang, L.F., *Vascular adaptation to microgravity: what have we learned?* J Appl Physiol, 2001. **91**(6): p. 2415-30.
216. Zhang, Q., et al., *Muscle blood flow in response to concentric muscular activity vs passive venous compression.* Acta Physiol Scand, 2004. **180**(1): p. 57-62.
217. Zhang, Q. and J. Styf, *Abnormally elevated intramuscular pressure impairs muscle blood flow at rest after exercise.* Scand J Med Sci Sports, 2004. **14**(4): p. 215-20.
218. Zhang, Q.X., K. Ericson, and J. Styf, *Blood flow in the tibialis anterior muscle by photoplethysmography during foot-transmitted vibration.* European Journal of Applied Physiology, 2003. **90**(5-6): p. 464-469.
219. Zhang, Q.X., et al., *A non-invasive measure of changes in blood flow in the human anterior tibial muscle.* European Journal of Applied Physiology, 2001. **84**(5): p. 448-452.
220. Zhang, Q.X., J. Styf, and L.G. Lindberg, *Effects of limb elevation and increased intramuscular pressure on human tibialis anterior muscle blood flow.* European Journal of Applied Physiology, 2001. **85**(6): p. 567-571.
221. Zoller, R.P., et al., *The role of low pressure baroreceptors in reflex vasoconstrictor responses in man.* J Clin Invest, 1972. **51**(11): p. 2967-72.
222. Zweifler, A.J., G. Cushing, and J. Conway, *The relationship between pulse volume and blood flow in the finger.* Angiology, 1967. **18**(10): p. 591-8.